

SYNTHESES OF FLUORINE-18 LABELLED COMPOUNDS AND
RADIOPHARMACEUTICALS BY ELECTROPHILIC FLUORINATION

By

NEIL VASDEV, B.Sc., B.A.

A Thesis

Submitted to the School of Graduate Studies

in Partial Fulfilment of the Requirements

for the Degree

Doctor of Philosophy

McMaster University

©Copyright by Neil Vasdev, March 2003

**SYNTHESES OF FLUORINE-18 LABELLED COMPOUNDS AND
RADIOPHARMACEUTICALS BY ELECTROPHILIC FLUORINATION**

Dedicated in the memory of my father, Sudhir Kumar Vasdev

DOCTOR OF PHILOSOPHY (2003)

McMaster University

(Chemistry)

Hamilton, Ontario

TITLE: Syntheses of Fluorine-18 Labelled Compounds and
Radiopharmaceuticals by Electrophilic Fluorination

AUTHOR: Neil Vasdev, B.Sc., B.A.

SUPERVISORS: Professor. R. V. Chirakal and Professor G. J. Schrobilgen

NUMBER OF PAGES: xvii, 168

ABSTRACT

Previously, the fate of 5-fluoro-L-DOPA in the human brain was unknown because an efficient method for the synthesis of [^{18}F]5-fluoro-L-DOPA in mCi quantities was not available. In the present work, a method for the synthesis of [^{18}F]5-fluoro-L-DOPA in mCi quantities was developed by studying the reactivity and selectivity of fluorine during the electrophilic fluorination of L-DOPA in acidic solvents. As a result of this work, the present study has reported the first clinical study, using positron emission tomography (PET), that compared the *in vivo* behaviour of [^{18}F]2-, [^{18}F]5- and [^{18}F]6-fluoro-L-DOPA, in the living human brain.

The site-specific fluorination method developed in the present work was extended to develop a high-yield synthesis of [^{18}F]3-fluoro-L- α -methyltyrosine, which is a tumour imaging agent. Direct fluorination of L- α -methyltyrosine with [^{18}F]F₂ in HF solvent produced the 3-fluoro isomer as the major product in 30% radiochemical yield (RCY) with respect to [^{18}F]F₂, the highest RCY to date. These studies also revealed that a previous report had incorrectly characterized [^{18}F]3,5-difluoro-L- α -methyltyrosine as [^{18}F]2-fluoro-L- α -methyltyrosine. This methodology was further extended to develop a new PET tracer, [^{18}F]5-fluoro-3-nitro-L-tyrosine, in order to trace "reactive nitrogen species", which are responsible for tissue damage *in vivo*.

A recent study has claimed that XeF₂ exchanges with [2,2,2-crypt-M][^{18}F] (M = K or Cs) to produce [^{18}F]XeF₂ at room temperature in CH₂Cl₂ solvent and that exchange between F⁻ and XeF₂ cannot occur in CH₃CN solvent. Contrary to the previous work, the present study

showed that both XeF_2 and F^- react with CH_2Cl_2 at room temperature and that XeF_2 fluorinates 2,2,2-crypt under rigorously anhydrous conditions. The major products resulting from these reactions include several hydrochlorofluorocarbons and large amounts of HF and HF_2^- . Thus, the exchange between XeF_2 and $^{18}\text{F}^-$ reported in the prior work arises from exchange between XeF_2 and HF/ HF_2^- , and does not involve fluoride ion. Furthermore, two-dimensional EXSY and single selective inversion NMR spectroscopic studies in the present work have shown that anhydrous $[\text{N}(\text{CH}_3)_4][\text{F}]$ exchanges with XeF_2 in CH_3CN solvent. The exchange between XeF_2 and F^- is postulated to proceed by the formation of the trifluoroxenate(II) anion, XeF_3^- , a novel VSEPR system (i.e., the first AX_3E_3 arrangement), as the exchange intermediate.

ACKNOWLEDGEMENTS

My most sincere thanks must be extended to my supervisors: Dr. Raman Chirakal and Dr. Gary Schrobilgen for their exceptional training, guidance and constant encouragement. I thank them both for always making time for me despite their hectic schedules and for their continued support and friendship.

I would also like to thank the other member of my supervisory committee, Dr. Russell Bell, for his interest in my research and for helpful suggestions. I wish to take the opportunity to thank the past and present Chiefs of Nuclear Medicine at Hamilton Health Sciences, Dr. Geoff Coates and Dr. Karen Gulenchyn, for making hospital facilities available for this research.

To my past and present colleagues in Nuclear Medicine and in Dr. Schrobilgen's laboratory group, I would also like to extend my gratitude, with special thanks to Dr. H el ene Mercier, Dr. Michael Gerken, Bernard Pointner, John Lehmann, Matt Moran and Rezwan Ashique. To Bernie and John I especially owe a great deal for their involvement in my scientific and personal life during both my undergraduate and graduate years at McMaster.

I also would like to thank Dr. Claude Nahmias for assistance with the PET study, Dr. Reijo Suontamo for conducting the theoretical calculations and Dr. Alex Bain and Dr. Don Hughes for their help with NMR spectroscopic studies.

I acknowledge financial support from the Natural Sciences and Engineering Research Council (NSERC) of Canada for a postgraduate scholarship, The Christie Group for the E.S. Garnett Bursary in Medical Imaging and McMaster University for the James A. Morrison Memorial Scholarship.

Finally, I would like to thank my family and my friends who have become the most important part of my life. I thank my Mom, Dad and Shawn for always believing in me and for their constant love, support and patience throughout the years of my studies.

“Nothing in life is to be feared, it is only to be understood”

-Marie Curie

LIST OF ABBREVIATIONS AND SYMBOLS

General

DFT	density functional theory
ELF	electron localization function
FEP	perfluoroethylene/perfluoropropylene copolymer
HPLC	high performance liquid chromatography
i.d.	inner diameter
IR	infrared
Kel-F	chlorotrifluoroethylene polymer
MP2	Møller Plesset, second order
NMR	nuclear magnetic resonance
o.d.	outer diameter
PFA	perfluoroalkoxy
PTFE	tetrafluoroethylene copolymer
UV	ultraviolet
VSEPR	valence shell electron pair repulsion

Nuclear Magnetic Resonance

δ	chemical shift
I	nuclear spin quantum number
J	nuclear spin-spin coupling constant
EXSY	exchange spectroscopy
FID	free induction decay
HSQC	heteronuclear single quantum coherence
NOESY	nuclear Overhauser enhancement spectroscopy
ROESY	rotating frame Overhauser enhancement spectroscopy
SF	spectrometer frequency
SW	spectral width
NS	number of scans
ppm	parts per million
T ₁	spin-lattice relaxation time
$\Delta\nu_{1/2}$	line width at half height

Radiochemistry

eV	electron volt
n.c.a.	no-carrier-added
PET	positron emission tomography
RCY	radiochemical yield
SPECT	single photon emission computed tomography
$t_{1/2}$	half-life

TABLE OF CONTENTS

	Page
CHAPTER 1: INTRODUCTION	
1.1 Medical Applications of Fluorine.....	1
1.2 Isotopes of Fluorine and Use of Fluorine-18.....	2
1.3 Production of Fluorine-18.....	4
1.4 Application of Fluorine-18 in Positron Emission Tomography.....	7
1.5 Chemical Aspects in the Development of PET Radiopharmaceuticals.....	10
1.6 Organofluorine Chemistry.....	12
1.6.1 Radiofluorination of Aromatic Compounds.....	13
1.7 Electrophilic Fluorinating Agents.....	16
1.8 Fluorine-18 in Inorganic Chemistry.....	20
1.9 Purpose and Scope of the Present Work.....	26
CHAPTER 2: EXPERIMENTAL SECTION	
2.1 Non-labelled Experiments.....	28
2.1.2 Standard Techniques.....	28
2.1.2 Materials.....	30
2.1.3 Attempted Syntheses of Salts Containing the XeF_3^- Anion.....	32
2.2 Experiments Using Fluorine-18 Labelled Fluoride.....	34
2.2.1 Standard Techniques.....	34
2.2.2 Production of No-Carrier-Added $^{18}\text{F}^-$	34
2.2.3 Materials.....	34
2.2.4 Attempted Syntheses of $[^{18}\text{F}]\text{XeF}_2$	34

2.3 Experiments Involving [^{18}F]F ₂ or [^{18}F]CH ₃ COOF.....	35
2.3.1 General Fluorination of Aromatic Amino Acids with [^{18}F]F ₂	35
2.4 Separations and Purifications By Use of HPLC.....	36
2.4.1 Materials.....	38
2.4.2 Preparation, Separation and Purification of [^{18}F]Fluoro-L-DOPA, [^{18}F]Fluoro-L-tyrosine and [^{18}F]Fluoro-L- α -methyltyrosine Derivatives.....	38
2.4.3 Preparation and Separation of [^{18}F]Fluoro-nitro-tyrosine Derivatives.....	44
2.4 Dose Preparation and Quality Control.....	48
2.5 Nuclear Magnetic Resonance Spectroscopy.....	50
2.6.1 2-D HSQC.....	52
2.6.2 2-D ROESY.....	52
2.6.3 2-D EXSY.....	52
2.6.4 Single Selective Inversion.....	53
2.7 Raman Spectroscopy.....	53
2.8 Computational Methods.....	53
2.9 PET Scanning Protocol.....	54

CHAPTER 3: RADIOCHEMICAL AND NMR SPECTROSCOPIC INVESTIGATION OF THE SOLVENT EFFECT ON THE ELECTROPHILIC ELEMENTAL FLUORINATION OF L-DOPA: SYNTHESIS OF [^{18}F]5-FLUORO-L-DOPA

3.1 Introduction.....	55
3.2 Results and Discussion.....	57
3.2.1 Identification of 5-fluoro-L-DOPA.....	57
3.2.2 ^1H and ^{13}C NMR Spectroscopic Studies of Solvent Effects on the Fluorination of L-DOPA.....	58
3.2.3 Radiochemical Yield of [^{18}F]Fluoro-L-DOPA.....	62
3.2.4 Solvent Effect on the Orientation of Aromatic Fluorine Substitution in DOPA.....	65

3.2.5	Direct Fluorination Using Acetyl Hypofluorite.....	68
3.3	Conclusions.....	71
CHAPTER 4: THE EFFECT OF AROMATIC FLUORINE SUBSTITUTION IN L-DOPA ON THE <i>IN VIVO</i> BEHAVIOUR OF [¹⁸F]2-, [¹⁸F]5- AND [¹⁸F]6-FLUORO-L-DOPA IN THE HUMAN BRAIN		
4.1	Introduction.....	72
4.2	Results and Discussion.....	73
4.3	Concluding Remarks.....	80
CHAPTER 5: SELECTIVITY OF ELEMENTAL FLUORINE TOWARDS L-TYROSINE AND L-α-METHYLTYROSINE IN ACIDIC MEDIA AND THE SYNTHESSES OF THEIR [¹⁸F]3-FLUORO AND [¹⁸F]3,5-DIFLUORO DERIVATIVES		
5.1	Introduction.....	81
5.2	Results and Discussion.....	82
5.2.1	Identification of 3-F- α -MT.....	82
5.2.2	Identification of 3,5-Difluoro Isomers.....	83
5.2.3	Proton and ¹³ C NMR Spectra of L- α -MT in Various Solvents.....	89
5.2.4	Influence of Solvent Acidity on Radiochemical Yield of Fluoro-tyrosine Derivatives.....	90
5.2.5	Radiochemical Yields of [¹⁸ F]3-Fluoro-L-tyrosine and 3-F- α -MT.....	93
5.2.6	Orientation of Fluorination and the Formation of [¹⁸ F]3,5-Difluoro Derivatives of L-Tyrosine and L- α -MT.....	94
5.2.7	Proton and ¹³ C NMR Spectroscopic Studies of the Solvent Effect on the Radiochemical Yield of 3-F- α -MT.....	96
5.3	Conclusion.....	98
CHAPTER 6: SYNTHESSES OF [¹⁸F]5-FLUORO-3-NITRO-L-TYROSINE		
6.1	Introduction.....	99
6.2	Results and Discussion.....	100

6.2.1	Nitration of 3-Fluoro-DL-tyrosine and [¹⁸ F]3-Fluoro-L-tyrosine.....	101
6.2.2	Fluorination of 3-Nitro-L-tyrosine.....	103
6.2.3	One-Pot Nitration and Fluorination of L-Tyrosine.....	103
6.2.4	Relative Reactivity of [¹⁸ F]F ₂ Towards L-Tyrosine and 3-Nitro-L-tyrosine.....	104
6.2.5	Comparison of the Synthetic Routes to [¹⁸ F]FNT.....	107
6.3	Conclusion.....	107

CHAPTER 7: ON THE PREPARATION OF FLUORINE-18 LABELLED XeF₂ AND CHEMICAL EXCHANGE BETWEEN FLUORIDE ION AND XeF₂

7.1	Introduction.....	109
7.2	Results and Discussion.....	112
7.2.1	Reaction of XeF ₂ with 2,2,2-Crypt and KF in CH ₂ Cl ₂ Solvent.....	112
7.2.2	Stability of XeF ₂ and 2,2,2-crypt in CH ₂ Cl ₂ Solvent	113
7.2.3	Reaction of [N(CH ₃) ₄][F] and XeF ₂ in CH ₂ Cl ₂ Solvent.....	116
7.2.4	Reactions of [2,2,2-crypt-K][F] with CH ₃ CN and CH ₂ Cl ₂ Solvents.....	116
7.2.5	Fluoride Ion and HF Exchange with XeF ₂	119
7.2.6	On the Influence of Solvent and Vessel upon the Reactions of XeF ₂ with Organic Substrates.....	121
7.2.7	The Synthesis of [¹⁸ F]XeF ₂ by ¹⁸ F ⁻ Exchange with XeF ₂ in CH ₂ Cl ₂ ...	123
7.3	Conclusions.....	125

CHAPTER 8: AN NMR SPECTROSCOPIC STUDY OF XeF₂/F⁻ EXCHANGE, ATTEMPTED SYNTHESSES OF SALTS CONTAINING THE XeF₃⁻ ANION AND THEORETICAL STUDIES OF THE XeF₃⁻ ANION

8.1	Introduction.....	127
8.2	Results and Discussion.....	130
8.2.1	Energy Minimized Geometry of the XeF ₃ ⁻ Anion.....	132
8.2.2	Attempted Syntheses of Salts Containing the XeF ₃ ⁻ Anion.....	135

8.2.3	Intermolecular Exchange Between Fluoride Ion and XeF ₂	140
8.3	Conclusions.....	144
CHAPTER 9: CONCLUSIONS AND DIRECTIONS FOR FUTURE WORK		
9.1	Conclusions.....	145
9.2	Directions for Future Work.....	148
REFERENCES.....		152

LIST OF TABLES

Table	Page
1.1 Isotopes of Fluorine.....	3
1.2 Production Methods of Fluorine-18 for Medical Use.....	5
2.1 Typical NMR Spectroscopic Parameters for ^1H , ^{13}C , ^{19}F and ^{129}Xe NMR Spectroscopy.....	51
3.1 Radiochemical Yield and Orientation of Electrophilic Elemental Fluorination of L-DOPA in Acidic Solvents.....	59
3.2 ^1H NMR Chemical Shifts (ppm) of L-DOPA in Acidic Solvents.....	60
3.3 ^{13}C NMR Chemical Shifts (ppm) of L-DOPA in Acidic Solvents.....	61
3.4 Radiochemical Yield and Isomeric Distribution of Fluoro-DOPA After the Fluorination of L-DOPA Using Acetyl Hypofluorite.....	70
5.1 ^1H and ^{13}C NMR Parameters for L- α -MT and 3-F- α -MT.....	84
5.2 ^{13}C and ^1H NMR Chemical Shifts for L- α -Methyltyrosine in Various Solvents.....	91
5.3 Radiochemical Yields for Fluorinated Tyrosine Derivatives Resulting from the Direct Fluorination of Substrate in Acidic Media with $[^{18}\text{F}]\text{F}_2$	92
6.1 Proton, ^{13}C and ^{19}F NMR Parameters for FNT.....	102
8.1 Vibrational Frequencies Calculated ^a at the DFT level of Theory (SVWN/DZVP).....	137
8.2 Gas Phase Fluoride Ion Affinities at 0 K. Calculated at the DFT level of Theory (SVWN/DZVP).....	139

LIST OF FIGURES

Figure	Page
1.1	Schematic showing (a) a positron-electron annihilation to form two 511 keV photons (b) the photons detected by two coincidence detectors.....9
2.1	Experimental apparatus used for the radiofluorination of aromatic amino acids.....37
2.2	Radiochromatogram of (a) the reaction mixture after radiofluorination of L-DOPA in BF ₃ /HF, (b) [¹⁸ F]2-fluoro-L-DOPA after final purification and (c) [¹⁸ F]6-fluoro-L-DOPA after final purification.....42
2.3	Radiochromatogram of (a) the reaction mixture after radiofluorination of L-DOPA in glacial acetic acid containing 10% TFA, showing [¹⁸ F]2- and [¹⁸ F]5-fluoro-L-DOPA, and (b) [¹⁸ F]5-fluoro-L-DOPA after final purification.....43
2.4	HPLC chromatogram of the reaction mixture obtained from the fluorination of L-α-MT in aHF with [¹⁸ F]F ₂ ; (a) UV trace for absorption at 275 nm and (b) [¹⁸ F]-radioactivity trace.....45
2.5	HPLC chromatogram of the reaction mixture obtained from the fluorination of L-α-methyltyrosine in 0.13 M BF ₃ /HF with [¹⁸ F]F ₂ ; (a) UV trace for absorption at 275 nm and (b) [¹⁸ F]-radioactivity trace.....46
2.6	HPLC trace of the reaction mixture after the nitration of [¹⁸ F]3-fluoro-L-tyrosine using NaNO ₃ in TFA solvent at 4 °C for 5 min to produce [¹⁸ F]FNT (a) UV, λ = 275 nm and (b) [¹⁸ F]-radioactivity trace.....49
3.1	Radiochromatogram of the Reaction Mixture After the Radiofluorination of L-DOPA in (A) TFA (B) 10% TFA in CH ₃ COOH and (C) HCOOH.....64
4.1	Distribution of [¹⁸ F]2-, [¹⁸ F]5- and [¹⁸ F]6-fluoro-L-DOPA in Subject 1, 60 to 120 minutes after injection of the tracer.....75
4.2	Time course of radioactivity in the striata (solid symbols) and the cerebellum after an intravenous injection of [¹⁸ F]2-, [¹⁸ F]5- and [¹⁸ F]6-fluoro-L-DOPA.....76
5.1	Experimental and simulated ¹⁹ F NMR spectrum of 3,5-difluoro-L-α-MT.....86
5.2	¹⁹ F { ¹ H; 6.81 ppm} NMR spectrum and ¹ H { ¹⁹ F; -132.2 ppm} NMR spectrum of [¹⁸ F]3,5-difluoro-L-α-methyltyrosine.....87
5.3	A 2-D ROESY NMR spectrum showing the aromatic and side-chain protons of 3,5-difluoro-L-α-MT, in an unpurified mixture.....88

6.1	HPLC trace showing the relative reactivity of [¹⁸ F]F ₂ towards three-fold molar excesses of both L-tyrosine and 3-nitro-L-tyrosine in TFA solvent at 4 °C.....	106
7.1	2-D ¹⁹ F- ¹⁹ F EXSY spectrum of an equimolar sample of XeF ₂ and [N(CH ₃) ₄][F] in CH ₃ CN solvent, acquired at 15 °C using a mixing time of 400 ms.....	120
7.2	Variable-temperature ¹²⁹ Xe NMR spectra of a sample of XeF ₂ in HF.....	122
8.1	Diagonal relationships within the periodic table suggesting that XeF ₃ ⁻ may be stable.....	129
8.2	Geometries of the XeF ₃ ⁻ anion depicting octahedral arrangements of bond-pairs and lone-pairs, for the meridinal (a) and the facial (b) arrangements, respectively.....	131
8.3	The fully optimized geometry (SVWN/DZVP) for the XeF ₃ ⁻ anion.....	133
8.4	ELF calculations of (a) XeF ₂ and (b) the XeF ₃ ⁻ anion. Contours are drawn at the 0.60 localization.....	134
8.5	A comparison of the XeF ₃ ⁻ anion geometry with that of the XeF ₅ ⁻ anion.....	136
8.6	Results of a selective inversion experiment conducted on a sample containing quantities of XeF ₂ and [N(CH ₃) ₄][F] in CH ₃ CN solvent (0.2 M) acquired at -15 °C.....	142
8.7	Eyring Plot of the rate data for the intermolecular ¹⁹ F-exchange between XeF ₂ and [N(CH ₃) ₄][F] in CH ₃ CN solvent (0.2 M) acquired at temperatures between -40 to 0 °C.....	143

CHAPTER 1

INTRODUCTION

1.1 Medical Applications of Fluorine

Selectively fluorinated biomolecules have a long and successful history in medicinal chemistry.^{1,2,3} The replacement of fluorine for hydrogen in biologically active molecules usually has the effect of increasing the lipophilicity of the molecule and enhances the rates of *in vivo* transport and absorption.⁴ However, several physical and chemical properties are altered, and changes in biological activity occur when fluorine is the substituent in a bioactive compound.⁵ Kirk⁶ has reviewed the pharmacological effects of several selectively ring fluorinated catecholamines and has shown that the specific site of aromatic fluorine substitution can cause dramatic differences in pharmacological properties. This phenomenon has been termed the *fluorine effect*.^{7,8}

The extensive chemistry of ^{19}F in biological molecules has paved the way for use of biomolecules labelled with the radioisotope ^{18}F for applications in medical imaging, for example, in the detection of Parkinson's disease and Parkinsonian syndromes. The latter comprises the largest category of movement disorders, which is estimated to affect two percent of the population over sixty years of age.⁹ It is known that the clinical features of Parkinson's disease, muscular rigidity, akinesia and tremor, are associated with marked deficiencies of striatal dopamine.¹⁰ These observations have led to the use of

L-DOPA to alleviate the symptoms of Parkinson's disease. Garnett, *et al.*¹¹ pioneered the use of [^{18}F]6-fluoro-L-DOPA, in conjunction with positron emission tomography (PET) (see Chapter 3, section 3.1), to visualize the spatial distribution of intracerebral dopamine in the human brain during life. Subsequently, [^{18}F]6-fluoro-L-DOPA was also used to show that the accumulation of ^{18}F was reduced in the contralateral putamen of patients suffering from hemiparkinsonism.¹² These findings were the first demonstration, during life, that a disturbance of intrastriatal dopamine metabolism occurs in association with Parkinson's disease.

1.2 Isotopes of Fluorine and Use of Fluorine-18

Fluorine-19 is the only stable isotope of fluorine and is 100% naturally abundant. Although naturally occurring fluorine is monoisotopic, there are six known radioactive isotopes of fluorine with half-lives greater than 1 s (Table 1). Of the six radioisotopes of fluorine, ^{18}F has the longest half-life (109.7 min). Experimental work with ^{18}F must be carried out within one working day of its production. Although the half-life of fluorine-18 is relatively short from the point of view of a synthetic chemist, there are several advantages associated with the use of this isotope. The short half-life of ^{18}F eliminates problems relating to the storage and handling of radioactive waste. In addition, the short half-life and easy detection of the 511 keV gamma rays from the annihilation of its positron decay (see section 1.4) make ^{18}F -labelled compounds ideal as radiopharmaceuticals.

Table 1.1 Isotopes of Fluorine.¹³

Isotope	Half-Life	Decay Mode	Product
¹⁷ F	64.7 s	β^+	¹⁷ O
¹⁸ F	109.7 min	β^+	¹⁸ O
¹⁹ F ^a	Stable		
²⁰ F	11.0 s	β^-	²⁰ Ne
²¹ F	4.3 s	β^-	²¹ Ne
²² F	4.2 s	β^-	²² Ne
²³ F	2.2 s	β^-	²³ Ne

^aThis 100% naturally abundant isotope of fluorine has a nuclear spin, $I = \frac{1}{2}$ and a high NMR receptivity relative to that of the proton, 0.834,¹⁴ making it ideally suited for NMR spectroscopy.

Fluorine-18 has also been used in inorganic chemistry¹⁵ to probe chemical reaction mechanisms and to deduce information about molecular structure. Many technological advances in the field of fundamental inorganic fluorine chemistry have been transferred and applied to the syntheses and structural characterizations of ¹⁸F-labelled compounds and radiopharmaceuticals.

1.3 Production of Fluorine-18

Fluorine-18 can be prepared for medical applications by a number of nuclear reactions,^{16,17,18} however, an accelerator, cyclotron or a nuclear reactor is required. Methods for the production of fluorine-18 are listed in Table 1.2. The ¹⁸O(p,n)¹⁸F nuclear reaction is most commonly used because of the relatively wide availability of proton cyclotrons, which use moderate beam energies and currents to provide useful yields. Several other less common methods for the production of fluorine-18 are known and have also been reviewed.¹⁹

Ruth and Wolf²⁵ have determined the excitation function (the dependence of the cross section, σ , a measure of the probability of occurrence of a nuclear reaction, on the incident energy) for the ¹⁸O(p,n)¹⁸F reaction using an [¹⁸O]O₂ target for proton energies ranging from 2.3 to 14.7 MeV. The cross section for this reaction has a threshold energy of 2.3 MeV and a maximum at 5.1 MeV, and the saturation theoretical thick target yield, a measure of rate of formation of an isotope, is 147 to 167 mCi/ μ A for 10 MeV protons. This study²⁵ showed that the ¹⁸O(p,n)¹⁸F nuclear reaction is two to four times more

Table 1.2 Production Methods of Fluorine-18.

Source	Nuclear Reaction(s)	Target Material	Fluorinating Agent	Reference
1	$^{16}\text{O}(t^a, n)^{18}\text{F}$	$^6\text{Li}_2\text{CO}_3$	H^{18}F	20
2	$^{16}\text{O}(\alpha, 2n)^{18}\text{Ne}; ^{18}\text{Ne} - ^{18}\text{F}$ (E.C.) ^b	O_2	$[\text{}^{18}\text{F}]\text{HF}$	21
	$^{16}\text{O}(^3\text{He}, n)^{18}\text{Ne}, ^{18}\text{Ne} - ^{18}\text{F}$ (E.C.) ^b			
2	$^{16}\text{O}(\alpha, d)^{18}\text{F}$ and $^{16}\text{O}(\alpha, pn)^{18}\text{F}$	H_2O (aq)	$^{18}\text{F}^-$	22
2	$^{16}\text{O}(^3\text{He}, p)^{18}\text{F}$	H_2O (aq)	$^{18}\text{F}^-$	23
2	$^{16}\text{O}(^3\text{He}, p)^{18}\text{F}$	O_2	$[\text{}^{18}\text{F}]\text{F}_2$	24
2	$^{18}\text{O}(p, n)^{18}\text{F}$	$^{18}\text{O}_2$	$[\text{}^{18}\text{F}]\text{F}_2$	25,26
2	$^{18}\text{O}(p, n)^{18}\text{F}$	H_2^{18}O (aq)	$^{18}\text{F}^-$	27
2	$^{18}\text{O}(p, n)^{18}\text{F}$	H_2^{18}O (s)	$^{18}\text{F}^-$	28
2	$^{18}\text{O}(p, n)^{18}\text{F}$	CO^{18}O (s)	$^{18}\text{F}^-$	29
1	$^{19}\text{F}(n, 2n)^{18}\text{F}$	$[\text{NH}_4][\text{HF}_2]$	$[\text{}^{18}\text{F}]\text{HF}$	30
2,3	$^{20}\text{Ne}(d, \alpha)^{18}\text{F}$	Ne	$[\text{}^{18}\text{F}]\text{F}_2;$ $\text{H}^{18}\text{F}; ^{18}\text{F}^-$	31,32
2	$^{20}\text{Ne}(p, 2pn)^{18}\text{F}$	Ne	$[\text{}^{18}\text{F}]\text{F}_2$	33
2	$^{20}\text{Ne}(^3\text{He}, \alpha n)^{18}\text{Ne}, ^{18}\text{Ne} - ^{18}\text{F}$ (E.C.) ^b	Ne	H^{18}F	34

^aTritium was produced by the $^6\text{Li}(n, \alpha)^3\text{H}$ nuclear reaction.

^bTransformation from $^{18}\text{Ne} - ^{18}\text{F}$ occurs by electron capture ($t_{1/2} = 1.67$ s).

(1) Nuclear reactor, (2) cyclotron, (3) accelerator.

efficient for the production of ^{18}F than the $^{20}\text{Ne}(\text{d},\alpha)^{18}\text{F}$ nuclear reaction with 7 to 14 MeV deuterons.³¹

The $^{18}\text{O}(\text{p},\text{n})^{18}\text{F}$ reaction is convenient for use with a proton cyclotron and is mainly applied to prepare ^{18}F -fluoride and $[^{18}\text{F}]\text{F}_2$ (Table 1.2) by irradiation of enriched $[^{18}\text{O}]\text{H}_2\text{O}$ and $[^{18}\text{O}]\text{O}_2$, respectively. Fluorine-18 labelled fluoride and $[^{18}\text{O}]\text{H}_2\text{O}$ are extracted from the target directly (no-carrier-added, n.c.a.), and $[^{18}\text{F}]\text{F}_2$ is extracted by use of carrier-added F_2 . It should be noted that carrier-added syntheses result in lower specific activities (radioactivity/mass or radioactivity/mole) when compared with n.c.a. syntheses. All experiments described in this work that have involved the use of ^{18}F made use of the $^{18}\text{O}(\text{p},\text{n})^{18}\text{F}$ nuclear reaction using a Siemens 11 MeV proton-only cyclotron (RDS 112) at the Department of Nuclear Medicine, Hamilton Health Sciences.

The production of $[^{18}\text{F}]\text{F}_2$ by the $^{18}\text{O}(\text{p},\text{n})^{18}\text{F}$ nuclear reaction involves a two-step, "double-shoot" technique.²⁶ The first bombardment of isotopically enriched $[^{18}\text{O}]\text{O}_2$ produces ^{18}F activity, which binds to the metal target surface and remains behind when the $[^{18}\text{O}]\text{O}_2$ is cryogenically retrieved. A second bombardment of an F_2 carrier mixture, diluted with He, Ne or Ar, induces fluorine exchange and results in useful levels of $[^{18}\text{F}]\text{F}_2$. The factor limiting the more widespread use of $[^{18}\text{F}]\text{F}_2$ has been the relatively low specific activity available through radionuclide production from gas target materials (typically $^{18}\text{O}_2$ or ^{20}Ne). The amount of carrier fluorine increases the total yield of $[^{18}\text{F}]\text{F}_2$ and lowers the specific activity, however this increase in yield eventually reaches a plateau. Fluorine-18 labelled F_2 is produced at Hamilton Health Sciences (see Chapter 2, section 2.3) with a specific activity of 35 Ci/mmol,³⁵ whereas, n.c.a. $^{18}\text{F}^-$ is produced with

a specific activity of *ca.* 150 Ci/ μ mol in similar cyclotrons.¹⁸ It should be noted that the theoretical maximum specific activity of ^{18}F is 1.71×10^3 Ci/ μ mol.

Methods to increase the specific activity of [^{18}F]F₂ gas include an exchange reaction between n.c.a. H ^{18}F and F₂, converted to [^{18}F]F₂ by a microwave discharge.³⁶ Bergman and Solin³⁷ have also developed a method for the synthesis of relatively high specific activity [^{18}F]F₂ (1.5 Ci/ μ mol) by reaction of CH₃ ^{18}F (synthesized from n.c.a. $^{18}\text{F}^-$) with carrier F₂ in an inert Ne matrix followed by atomizing the contents in an electric discharge to initiate exchange between ^{18}F and ^{19}F .

Although enriched [^{18}O]H₂O targets have been reliably used to synthesize high specific activity $^{18}\text{F}^-$, efforts are ongoing to further increase the specific activity of $^{18}\text{F}^-$. Ruth *et al.*³⁸ and Satyamurthy³⁹ have developed methods that utilize gas targets and the $^{18}\text{O}(\text{p},\text{n})^{18}\text{F}$ nuclear reaction, which can be conducted at higher beam currents (>100 μA), compared with those used in water targets (<50 μA). This is accomplished by an initial irradiation, as conducted in the “double-shoot” method (*vide supra*), however, instead of performing a second irradiation, the target is washed out with water, followed by trapping $^{18}\text{F}^-$ on an ion exchange column. The specific activity of $^{18}\text{F}^-$ generated in these reactions is 10 Ci/ μ mol, determined by use of an ion selective electrode.³⁹

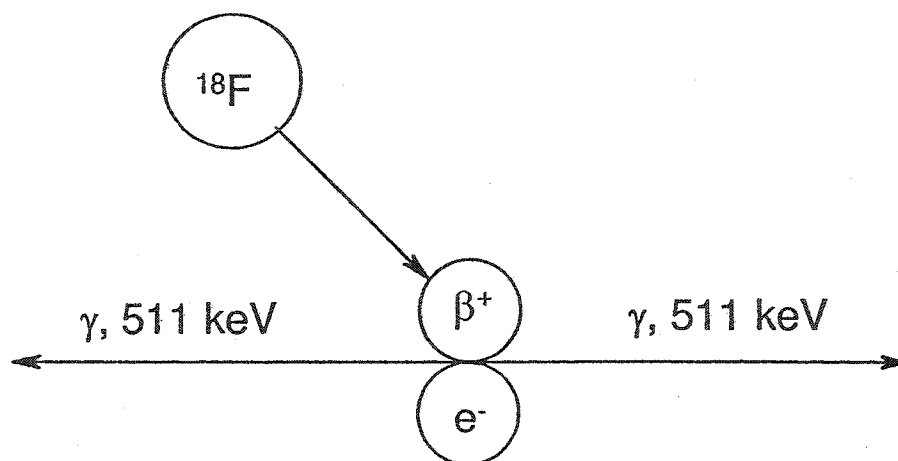
1.4 Application of Fluorine-18 in Positron Emission Tomography

The process of reconstructing tomographic images of the radioactivity distribution of a gamma-emitting radionuclide is known as single photon emission computerized

tomography (SPECT). There are, however, many advantages in determining the distribution of radioactivity when the gamma-photons are derived from positrons.⁴⁰ When radiotracers labelled with positron-emitting radionuclides are introduced into the body, the positron emitted from the radionuclide travels several micrometers in tissue, during which time it loses kinetic energy through ionization and excitation interactions. After a positron has lost most of its energy, it will undergo an annihilation reaction with its anti-matter particle, the electron, can result in the creation of two annihilation photons (gamma rays). The annihilation photons have energies of 511 keV each and are emitted at 180° to each other. The coincident detection of the annihilation photons enables the determination of the line along which the positron annihilation event occurred.⁴⁰ Positron emission tomography is accomplished through the coincident detection of the 511 keV photons arising from the annihilation of positrons in the material, and is illustrated in Figure 1.1.⁹

Common radioisotopes used in PET, other than ^{18}F , include ^{11}C ($t_{1/2}$, 20.3 min), ^{13}N ($t_{1/2}$, 10.0 min) and ^{15}O ($t_{1/2}$, 2.1 min) can also be efficiently produced in a proton cyclotron by the $^{14}\text{N}(p,\alpha)^{11}\text{C}$, $^{16}\text{O}(p,\alpha)^{13}\text{N}$ and $^{15}\text{N}(p,n)^{15}\text{O}$ nuclear reactions, respectively. Because carbon, nitrogen and oxygen are constituents of organic molecules, these radioisotopes can be substituted into a biomolecule without changing its biological properties. Among the disadvantages of these positron-emitting radioisotopes are the need to synthesize and characterize their radiopharmaceuticals on much shorter timescales and the added problem that the labelled compounds may not have sufficient time to accumulate in the desired tissues.

(a)



(b)

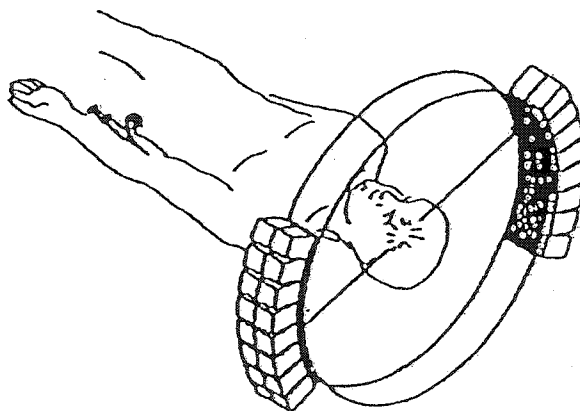


Figure 1.1. (a) A schematic showing a positron-electron annihilation to give two 511 keV photons, emitted at 180° to each other. (b) A schematic showing the two photons detected by coincidence detectors, connected in series. Each coincidence line is used to localize the radioactive source *in vivo*.⁹

1.5 Chemical Aspects in the Development of PET Radiopharmaceuticals

Many practical aspects must be considered when developing synthetic routes on a nanomolar scale for short-lived PET radiopharmaceuticals and many constraints arise that are unknown in traditional (non-tracer) synthetic chemistry.⁴¹ Once a particular labelled compound has been targeted for *in vivo* use with PET, the synthetic protocol and quality control regimes must take several factors into consideration,⁴² including, radiochemical yield, chemical, radionuclidic and radiochemical purities, specific activity, shelf-life, sterility and apyrogenicity.

The radiochemical yield is the amount of radionuclide incorporated into the radiopharmaceutical in the desired form and is the most practical criterion when seeking to develop radiopharmaceuticals for routine clinical use in PET. The measure of radiochemical yield dictates the efficiency of the chemical synthesis, however, lower radiochemical yields for reactions can be tolerated in the interest of total synthesis time. Chemical purity is the fraction of compound present in the formulated radiopharmaceutical that is in the desired molecular form. Efforts should be made to thoroughly characterize as many products of a chemical reaction as possible in order to identify and minimize, or eliminate, the undesirable products. Radionuclidic purity must also be monitored in order to assure that contaminating radionuclides are not present in the sample for injection. Radiochemical purity is defined as the fraction of a specific radionuclide incorporated into the desired molecule. In the case of ^{18}F , the ability of the fluorinating agent to produce predominantly one regioisomer is extremely important because the site of fluorine substitution often determines the biological activity of a

molecule. Furthermore, the use of a selective fluorinating agent that produces predominantly a monofluorinated product and minimizes competitive reaction pathways can increase radiochemical purity. Similarly, the enantiomeric purity of a molecule is often critical in dictating the biological activity. It is imperative that racemic mixtures with different biological properties are separated so that these compounds do not increase the background in the images and unnecessarily expose patients to radiation.

Specific activity is the measure of the amount of labelled compound compared with the total amount of labelled and unlabelled compound in the final product (*vide supra*). The specific activity should be as high as possible so that the labelled compound behaves as a tracer and the quantities of the labelled and unlabelled species do not interfere with the biochemical pathways being studied. For example, high specific activity radiopharmaceuticals are particularly important in measuring receptor densities in which the concentration of receptors is in the nanomolar range. The specific activity of a radiopharmaceutical has a direct impact on the shelf-life, the time during which the radiopharmaceutical can be used effectively, because specific activity continually decreases with time according to equation 1.1, where A_0 is the radioactivity at time, $t = 0$, and A is the radioactivity at any subsequent time t .

$$A = A_0 e^{-\left(\frac{\ln 2}{t_{1/2}}\right) t} \quad (1.1)$$

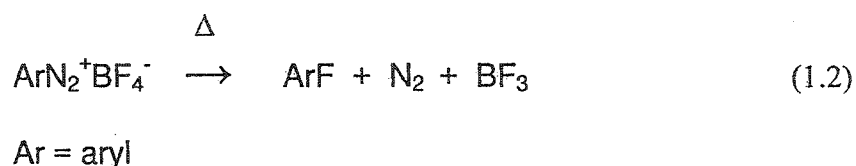
With short-lived radiopharmaceuticals, the half-life limits the shelf-life, however, decomposition and/or contaminant levels must be determined. Addition of stabilizers and pH control are among the methods used to increase the shelf-life. Prior to injection, efforts must be undertaken to ensure that the product is sterile, free from bacteria and organisms, and free of pyrogens, substances that cause fever.

1.6 Organofluorine Chemistry

With few exceptions, the vast ranges of molecules containing carbon-fluorine bonds are man-made.³ Therefore, many methods for the introduction of fluorine into organic molecules and approaches using various fluorinating agents have been developed and continue to be a significant synthetic challenge in modern fluorine chemistry. Reactions of fluorine with organic substrates were often regarded as being highly unselective and exothermic, often resulting in the production of tars and occasionally explosions. The high reactivity of fluorine with organic substrates is principally the result of the relative weakness of the fluorine-fluorine bond, which has a bond dissociation energy (BDE) of $157.7 \text{ kJ mol}^{-1}$, compared with the BDE of carbon-fluorine bonds ($452\text{-}531 \text{ kJ mol}^{-1}$) that form on reaction of elemental fluorine with hydrocarbons.⁴³

Aromatic fluorine chemistry has a remarkably long history dating back to 1870 when the first aryl C-F bond was made.⁴⁴ These syntheses were a direct consequence of the earlier discovery of aromatic diazo compounds which opened the door to many aryl derivatives, including fluoroaromatics. One of the most notable developments for the syntheses of fluoroaromatics was the discovery of the Balz-Schiemann reaction in the

early part of the 20th century.⁴⁵ The Balz-Schiemann reaction, and related reactions,⁴⁶ are among the most important and simplest reactions used for the laboratory scale preparation of fluoroaromatics and are particularly attractive because specialized equipment and precautions traditionally associated with the use of elemental fluorine are not required. The Balz-Schiemann reaction typically involves thermal decomposition of an aryldiazonium fluoride, yielding a fluoroaromatic compound, nitrogen and boron trifluoride (eq. 1.2).



The Balz-Schiemann reaction does, however, have a number of significant disadvantages from a synthetic point of view. For example, yields are often not reproducible and side reactions during decomposition may reduce yields and product purity. These reactions are not well suited for work with ¹⁸F because products with very high specific activity cannot be produced, as exchange of ¹⁸F with the ¹⁹F of BF₄⁻ results in extensive dilution of activity and low radiochemical yields (see section 3.1).

1.6.1 Radiofluorination of Aromatic Compounds

Nucleophilic fluorination methods currently offer the only n.c.a. method for reactions with ¹⁸F and must be used when labelled compounds are required with relatively

high specific activity. There are several applications of nucleophilic fluorination methodologies that have been developed from the wide variety of leaving groups, substrates and reaction conditions which can be used.⁴⁷ There are, however, drawbacks associated with nucleophilic fluorination methods. For example, high temperatures are often required and tend to produce low yields of the desired product. Another drawback is that the low solubilities of fluorides in traditional organic solvents tends to reduce their reactivities. From a radiochemical viewpoint, the presence of metallic ions (commonly an impurity from the target material used in isotope synthesis) may also reduce the nucleophilicity of the fluoride ion, resulting in lower radiochemical yields.

Electrophilic aromatic fluorinations can be achieved by direct fluorination using F_2 or an intermediate fluorinating reagent, such as, CH_3COOF . In attempts to improve the regioselectivities of fluorination reactions, fluorodemetalation reactions have been developed. Fluorodemetalation reactions involve cleavage of aryl mercury or Group 14 metal (Si, Ge, Sn) bonds, by use of a fluorinating agent.⁴⁸ Demetallation reactions offer an advantage over direct fluorination methods because these reactions do not require separation of fluoro-isomers after the introduction of fluorine.

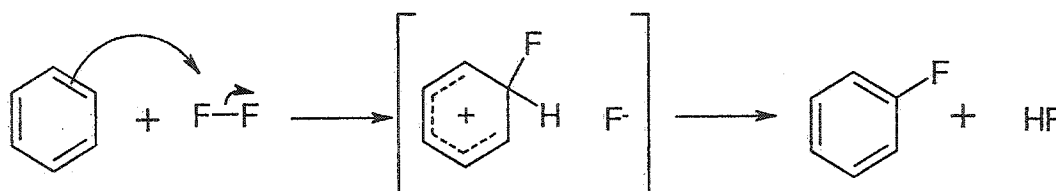
Despite advantages associated with increased regioselectivity, demetallation reactions have limitations. One such issue arises because the precursors often have their functional groups protected in order to survive the fluorination process. Protecting group synthesis can be a laborious process and additional time is expended to remove the protecting groups. Furthermore, preparative HPLC fractionation of the product mixtures is often also required for final purification.⁴ It should be noted that mercury precursors

were commonly used for selective fluorination of aromatics, however, traces of mercury had to be unerringly removed from the final product. Other drawbacks are noted when using mercury precursors, such as, the reactions tend to fail when a strong electron withdrawing group is present *ortho* to the mercury function⁴ and the reaction is rather ineffective when acetyl hypofluorite replaces F₂ as the fluorinating agent.⁴⁹

Fluorine gas is the original electrophilic fluorinating agent and nearly all electrophilic fluorinating agents are derived from elemental fluorine. From a radiochemical standpoint, the highest radiochemical yields resulting from electrophilic fluorination should be attainable when using [¹⁸F]F₂ directly. Electrophilic fluorination of aromatic compounds using F₂ gas has been perceived to be a poor and non-selective method because fluorine is a powerful oxidizing agent which may cause highly exothermic reactions and can result in multiple by-products and tars. To minimize such side reactions, it was found that the reactivity of F₂ could be moderated and controlled at low temperatures using F₂ diluted with an inert gas.^{50,51} Wolf and co-workers⁵² demonstrated that F₂/neon mixtures (0.1 - 0.5% F₂ in neon) are well suited for the production of ¹⁸F and the subsequent electrophilic fluorinations of biologically active compounds. Elemental fluorine has since become regarded as a selective fluorinating agent for monofluorination of organic molecules.⁵³

Recently, Chambers *et al.*⁵⁴ showed that protic solvents promote electrophilic fluorination of aromatic compounds and that the reactivity of fluorine as an electrophile varied significantly with the acidity of the medium. In a subsequent publication,⁵⁵ the same group suggested that the mechanism for direct fluorination of aromatic compounds

proceeds by a two-electron transfer (S_N2 -type process) when the acidic medium interacts with fluorine, thereby making fluorine more susceptible to nucleophilic attack (Scheme 1.1). Previous work has shown that elemental fluorination in acidic media is an efficient method for the production of ^{18}F -labelled aromatic amino acids.^{56,57,58}



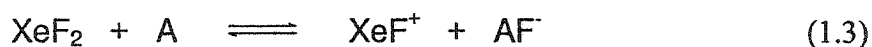
Scheme 1.1 Mechanism for the direct fluorination of aromatic compounds.⁵⁵

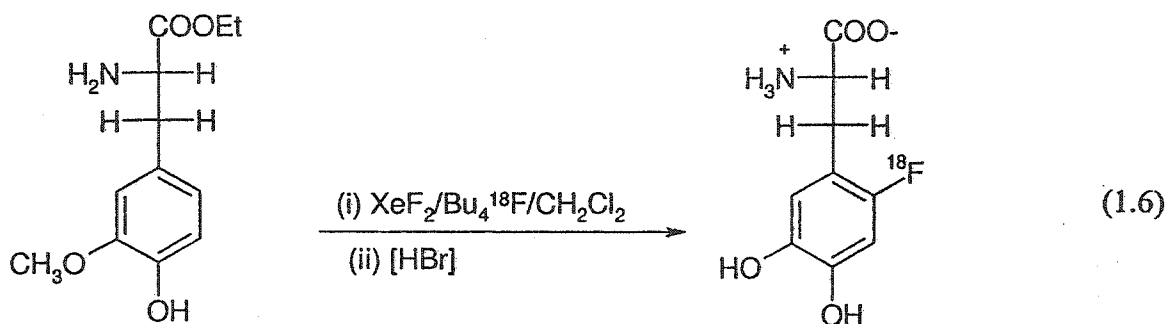
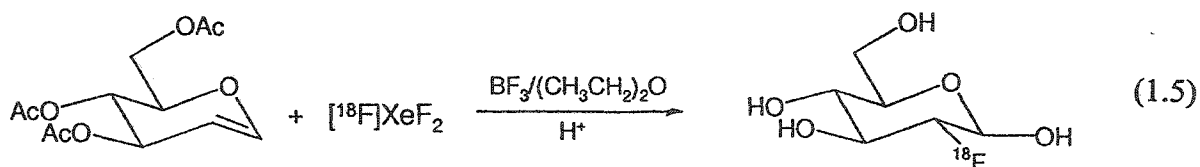
1.7 Electrophilic Fluorinating Agents

The perceived difficulties associated with direct fluorination have stimulated the development of alternative sources of electrophilic fluorine sources for use in organofluorine chemistry. Barton and coworkers⁵⁹ were the first to introduce the term electrophilic fluorination when reacting fluoromethyl hypofluorite (CF_3OF) with organic compounds. Rozen⁶⁰ has reviewed the use of CF_3OF and other hypofluorites and their use as selective fluorination reagents. Rozen⁶⁰ noted that the development of acetyl hypofluorite (CH_3COOF) as a selective fluorinating agent for organic compounds was driven by its rapid preparation, making it suitable for the syntheses of ^{18}F -labelled PET

radiopharmaceuticals.

Xenon difluoride is a versatile electrophilic fluorinating agent and has been used for selective fluorination of a wide variety of organic compounds.⁶¹ Fluorine-18 labelled XeF₂ was first prepared in our laboratories⁶² by treating SO₂ClF solutions of XeF₂ with [¹⁸F]HF, [¹⁸F]SiF₄ or [¹⁸F]AsF₅. The exchanges are attributed to the Lewis acid properties of the labelled fluorides, which presumably act as weak acceptors towards XeF₂ and promote exchange according to the equilibria shown in equations 1.3 and 1.4. Our laboratories have since shown that [¹⁸F]XeF₂ can also be synthesized by the thermochemical reaction of carrier-added [¹⁸F]F₂ and excess Xe in a high pressure nickel vessel at 390 °C for 40 min.⁶³ The first regiospecific syntheses of the positron-emitting medical imaging agents [¹⁸F]2-fluoro-2-deoxy-D-glucose⁶⁴ (eq. 1.5) and [¹⁸F]6-fluoro-L-DOPA⁶⁵ (eq. 1.6) were accomplished by use of [¹⁸F]XeF₂ as the fluorinating agent.

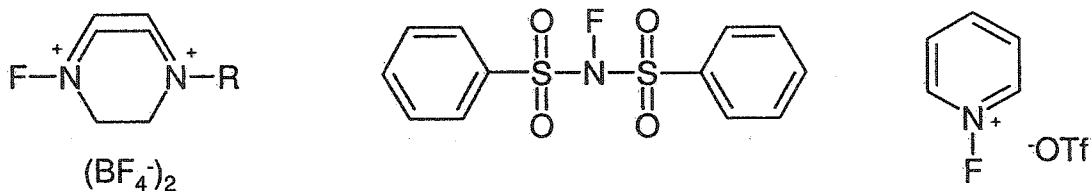




A recent study by Pike *et al.*⁶⁶ reports that n.c.a. ¹⁸F-labelled KF and CsF, sequestered by 2,2,2-crypt (1,10-diaza-4,7,13,16,21,24-hexaoxabicyclo[8.8.8]hexacosane), undergo fluorine exchange with XeF₂ at room temperature in CH₂Cl₂ and CHCl₃ solvents. However, the present work has proven many aspects of this work to be erroneous and the method is not suitable for the syntheses of PET radiopharmaceuticals (see Chapter 7).⁶⁷

Many recent reports that have arisen in the field of electrophilic fluorination have originated from the development of electrophilic N-F fluorinating agents.^{68,69} Electrophilic N-F reagents have the advantages over other selective fluorinating agents of being stable, easy to handle and generally safer to use. Taylor and co-workers⁶⁹ have

attributed the ease of preparation and commercial availability of many N-F reagents, such as, 1-chloromethyl-4-fluoro-1,4-diazoniabicyclo[2.2.2]octane bis(tetrafluoroborate), also known as Selectfluor® (compound 1 a), 1-methyl-4-fluoro-1,4-diazoniabicyclo[2.2.2]octane bis(tetrafluoroborate), also known as Selectfluor (II),⁷⁰ N-fluorobenzylsulfonamide, also known as NSFI (compound 2), N-fluoropyridinium triflate (compound 3) and others, to many recent advances in the field of organofluorine chemistry. The use of ¹⁸F-labelled N-F fluorinating agents may prove to have applications in PET radiopharmaceutical and inorganic syntheses provided they can be rapidly synthesized with minimal isotopic dilution.



(a) R = CH₂Cl (Selectfluor (I))

(b) R = CH₃ (Selectfluor (II))

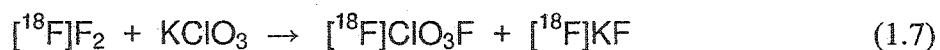
1

2

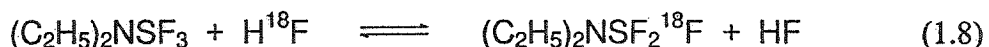
3

Fluorine-18 labelled perchlorylfluoride, [¹⁸F]ClO₃F, has been prepared by reaction of potassium chlorate and [¹⁸F]F₂ (eq. 1.7) in 23% radiochemical yield, with respect to [¹⁸F]F₂.⁷¹ The [¹⁸F]ClO₃F was successfully used to prepare fluoroaromatics with lithiated precursors. The yields of the fluoroaromatics varied between 3 and 30%, with respect to [¹⁸F]ClO₃F. This fluorinating agent was suggested for use in the preparation of ¹⁸F-

labelled radiopharmaceuticals, however, toxic residues of ClO_3^- , and the relatively low radiochemical yields have limited its use in radiopharmaceutical development.



It is noteworthy that fluorine-18 labelled diethylaminosulfur trifluoride (DAST) has been prepared by reaction with H^{18}F , $[^{18}\text{F}]\text{F}_2$ or $[^{18}\text{F}]\text{SF}_4$.⁷² Labelling accomplished with n.c.a. H^{18}F (eq. 1.8) resulted in the production of >80% of the radioactivity to be incorporated into DAST. Fluorine-18 labelled DAST was shown to have potential in labelling biological molecules, and is particularly well suited for reactions involving the displacement of hydroxyl groups with ^{18}F . However, because only one of three fluorine atoms in DAST is labelled, only one-third of the available ^{18}F is incorporated into the final product, therefore the maximum theoretical yield can only be 25%.

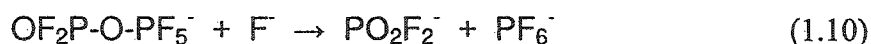


1.8 Fluorine-18 in Inorganic Chemistry

Winfield has reviewed the preparation and uses of fluorine-18 in inorganic chemistry.¹⁵ Tracer studies with ^{18}F were shown to be useful for studying the mechanisms of chemical reactions and deducing structural information that would be difficult or impossible to obtain using standard physical methods.

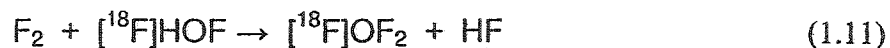
Fluorine-18 has been useful in studying fluorine exchange reactions. For example, early studies used ^{18}F to detect exchange between gaseous HF and F_2 at high

temperatures.⁷³ Furthermore, Azeem and Gillespie⁷⁴ prepared ¹⁸F-labelled BF₃, POF₃, PF₅, AsF₅, SF₄, SOF₂ and SeF₄ by an exchange reaction, which involved passing these volatile compounds over heated Li¹⁸F. Fluorine-18 labelled LiF was prepared by irradiation of lithium carbonate with thermal neutrons (*vide supra*). This study claimed to have provided the first evidence for the POF₄⁻ anion, by the observation of fluorine exchange between POF₃ and Li¹⁸F at 200 °C. More recently the POF₄⁻ anion was formed by reaction of [N(CH₃)₄][F] and POF₃ in CHF₃ solvent at -140 °C and was characterized for the first time at this temperature by ¹⁹F and ³¹P NMR spectroscopy.⁷⁵ The POF₄⁻ anion was shown to react with POF₃ between -140 to -100 °C, forming the OF₂P-O-PF₅⁻ anion (eq. 1.9), which, at higher temperatures, reacts with F⁻ to form the PO₂F₂⁻ and PF₆⁻ (eq. 1.10), providing a low activation energy barrier pathway for the highly exothermic disproportionation reaction of the POF₄⁻ anion. The thermal instability of the POF₄⁻ anion at low temperatures demonstrates the unlikelihood of this anion as an exchange intermediate in the reaction of POF₃ and Li¹⁸F at 200 °C.⁷⁴

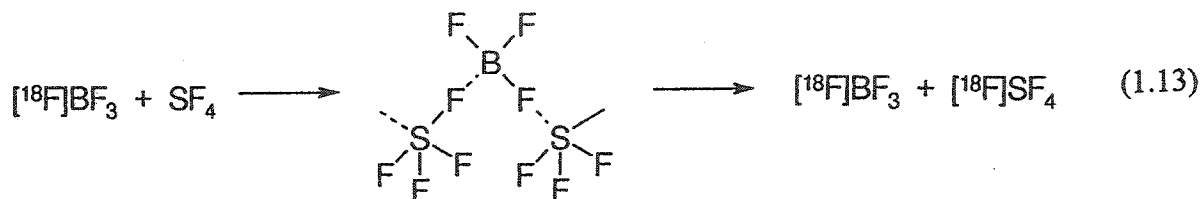
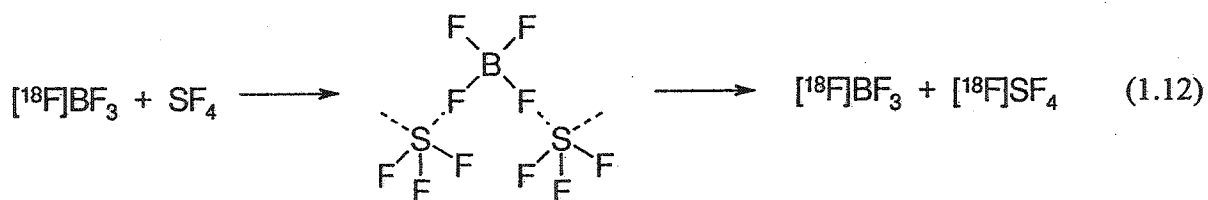


Appelman and Jache⁷⁶ showed that the reaction of F₂ with ice produced mixtures of OF₂, HOF, O₂ and H₂O₂. These authors⁷⁶ used ¹⁸F-labelling experiments to determine

the reaction stoichiometry of [^{18}F]HOF with F_2 , and they were able to conclude that the OF_2 produced contained one fluorine atom from HOF and one from F_2 (eq. 1.11).

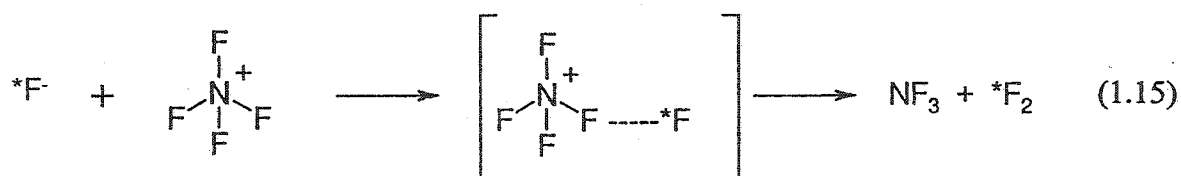
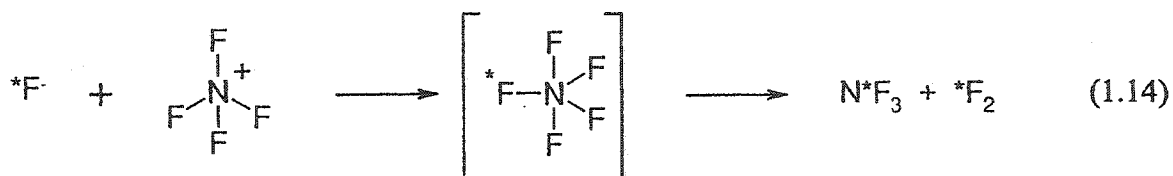


Fluorine-18 labelling has also been used to deduce structural information. For example, the Lewis acid-base adduct [^{18}F]BF $_3$ ·SF $_4$ was shown to have a symmetrical bridging fluorine between the boron and sulfur atoms (eq. 1.12), as opposed to unsymmetrical fluorine bridge bonds (eq. 1.13), by determination of the relative distribution of ^{18}F radioactivity in BF $_3$ (83%) and SF $_4$ (17%) after the decomposition of the ^{18}F -labelled BF $_3$ ·SF $_4$ adduct.⁷⁷



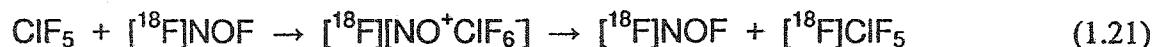
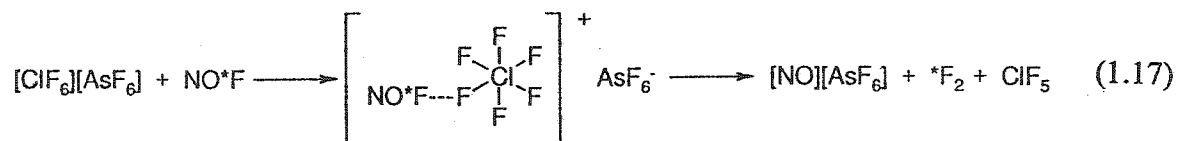
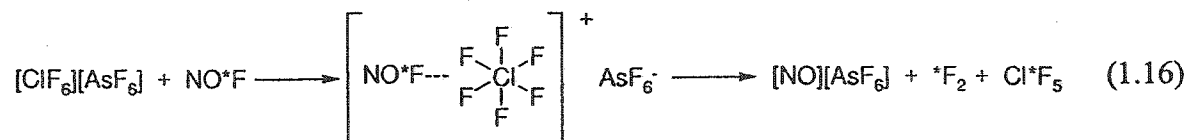
More recently ^{18}F has been employed as a radiotracer to probe inorganic reaction mechanisms in which so-called “hypervalent” species of nitrogen⁷⁸ and chlorine⁷⁹ are

possible intermediates. Whereas experimental data indicates the existence of hypervalent carbon⁸⁰ and boron,⁸¹ convincing evidence for penta-coordinated nitrogen compounds had not been presented. On the question of the existence of NF_5 , the reaction of $[\text{}^{18}\text{F}]\text{CsHF}_2$ with NF_4PF_6 was carried out at room temperature in HF solvent to form $[\text{}^{18}\text{F}]\text{NF}_4\text{HF}_2$.⁷⁸ Upon thermal decomposition at 100 °C, the ^{18}F -activity would be scrambled among NF_3 , HF and F_2 . There are two possible mechanisms which can lead to ^{18}F scrambling among these species: (1) the nucleophilic attack of $[\text{}^{18}\text{F}]\text{F}^-$ on nitrogen would cause isotopic scrambling among the five fluorines and therefore 60% of the original ^{18}F -activity should be found as $[\text{}^{18}\text{F}]\text{NF}_3$ and 40% should be found as $[\text{}^{18}\text{F}]\text{F}_2$ (eq. 1.14), (2) if the $[\text{}^{18}\text{F}]\text{F}^-$ attacks a fluorine of NF_4^+ , then $[\text{}^{18}\text{F}]\text{NF}_3$ will not form and all of the radioactivity would be found as $[\text{}^{18}\text{F}]\text{F}_2$ (eq. 1.15). Following the decomposition of $[\text{}^{18}\text{F}]\text{NF}_4\text{HF}_2$, essentially no ^{18}F -activity was detected on NF_3 , providing conclusive proof that the attack of $[\text{}^{18}\text{F}]\text{HF}_2^-$ on NF_4^+ occurred exclusively on the fluorine and not on the nitrogen, therefore NF_5 is not an intermediate in this reaction.



Although ^{18}F -labelling was used to show the non-existence of a hypervalent nitrogen species, the existence of a hypervalent chlorine species was conclusively shown by use of ^{18}F -labelling experiments, in conjunction with ^{19}F NMR and vibrational spectroscopic studies.⁷⁹ This work considered the existence of ClF_7 by reaction of $\text{ClF}_6^+\text{AsF}_6^-$ with $[^{18}\text{F}]\text{NOF}$. Two modes of attack by F^- on ClF_6^+ were possible, fluoride attack at the chlorine center (eq. 1.16) and fluoride attack at a fluorine ligand (eq. 1.17). The existence of ClF_7 as an intermediate would be indicated by the presence of $[^{18}\text{F}]\text{ClF}_5$ in the products. These experiments did reveal the presence of $[^{18}\text{F}]\text{ClF}_5$, but other exchange pathways that could transfer ^{18}F to ClF_5 could not be ruled out (eq. 1.18 – 1.20).⁸² Another experiment conducted between ClF_5 and $[^{18}\text{F}]\text{NOF}$ showed complete

randomization of ^{18}F -distribution between the two molecules. This reaction required the ClF_6^- anion as the intermediate (eq. 1.21).



Although the above-mentioned examples have shown the enormous potential of ^{18}F -labelling in inorganic fluorine chemistry, Winfield's¹⁵ conclusion in 1980 that fluorine-18 has been underused in inorganic chemistry still applies today. Although clinical applications of ^{18}F have increased dramatically in the past two decades, and greater use of ^{18}F in medical work has made facilities for its production more widely available, the application of ^{18}F in inorganic fluorine chemistry is still relatively

unexplored and remains underused to date. The limited use of ^{18}F in inorganic chemistry can be attributed to the short-half life of ^{18}F , which restricts the chemical techniques that can be employed in synthetic work, as well the limited number of inorganic fluorine chemistry groups working in collaboration with a cyclotron or accelerator center in close proximity.

1.9 Purpose and Scope of the Present Work

The purpose of this research is to study the electrophilic reactivity of fluorine-18 labelled electrophilic fluorinating agents towards biological molecules for use in PET. This work includes the direct fluorination of aromatic amino acids with electrophilic fluorine sources and the development of site-specific aromatic fluorination procedures.

One goal of the present research includes the synthesis and characterization of [^{18}F]5-fluoro-L-DOPA, the only ring fluoro-isomer of L-DOPA not synthesized in clinically useful quantities for human studies. Because [^{18}F]5-fluoro-L-DOPA was not developed as a PET radiopharmaceutical, its fate in the human brain had yet to be determined. The present work also focuses on applying methods of site-specific fluorination to L- α -methyltyrosine (L- α -MT). Iodine-123 labelled L- α -MT is the most frequently used amino acid tracer for SPECT, and its uptake mechanisms and clinical applications have been recently reviewed.⁸³ Preliminary results of the PET analog, [^{18}F]3-fluoro-L- α -MT, have affirmed the need for a more efficient synthesis of this radiopharmaceutical. Therefore, another goal of the present work is to extend site-specific fluorination methodology improving the radiochemical yield of [^{18}F]3-fluoro-L-

α -MT.

Recent controversies involving the processes of *in vivo* nitration, and the use of 3-nitro-L-tyrosine as a biomarker for reactive nitrogen species *in vivo* would render a radiolabelled 3-nitro-L-tyrosine an interesting radioprobe. Therefore, another goal of the present work is the development of general synthetic routes to ^{18}F -labelled nitrofluoroaromatic derivatives.

Another facet of the present research is to reconsider the use of $[^{18}\text{F}]\text{XeF}_2$ as an electrophilic fluorinating agent for the synthesis of PET radiopharmaceuticals. Recent reports claim that n.c.a. $^{18}\text{F}^-$ can be efficiently exchanged with XeF_2 in chlorinated solvents at room temperature to produce $[^{18}\text{F}]\text{XeF}_2$. The present work aims to reinvestigate the use of $[^{18}\text{F}]\text{XeF}_2$ synthesized by exchange of XeF_2 and $^{18}\text{F}^-$ and considers the likelihood that the hitherto unknown trifluoroxenate(II) anion, XeF_3^- , is an exchange intermediate in these reactions. Because XeF_2 has not been shown to exhibit fluoride acceptor properties, the syntheses of salts containing the XeF_3^- anion, in addition to NMR exchange studies between fluoride ion and XeF_2 would contribute significantly to the fields of inorganic fluorine chemistry, noble-gas chemistry and radiochemistry. The geometry of the XeF_3^- anion is also interesting because it would represent the first AX_3E_3 valence shell electron pair repulsion (VSEPR) arrangement.

CHAPTER 2

EXPERIMENTAL SECTION

2.1 Non-labelled Experiments

2.1.1 Standard Techniques

The compounds used in non-labelled experiments were moisture-sensitive, consequently, all manipulations were carried on glass and metal vacuum line systems or in the moisture-free (< 0.1%) nitrogen atmosphere of a Vacuum Atmospheres Model DLX drybox as previously described.⁸⁴ In instances where low-temperature sample preparations were required, samples were cooled inside the drybox by placing the FEP sample tubes inside a metal Dewar filled with 4.5 mm copper plated steel spheres previously cooled to ca. -140 °C inside the glass cryowell of the drybox.

Anhydrous CH_3CN and CH_2Cl_2 solvents were manipulated using a Pyrex glass vacuum line equipped with grease-free 6-mm J. Young glass stopcocks equipped with PTFE barrels. Pressures inside the vacuum manifold were monitored using a mercury manometer. Fluorine and anhydrous HF were handled on a metal vacuum line constructed from nickel and 316 stainless steel, and equipped with 316 stainless steel valves and fittings (Autoclave Engineers, Inc.). Vessels were attached to vacuum lines through ¼-in. o.d. FEP tubing and ¼-in. PTFE Swagelok connectors by means of PTFE

compression fittings or ¼-in. stainless steel Cajon Ultra-Torr connectors fitted with Viton rubber O-rings. Pressures were measured at ambient temperature using an MKS Model PDR-5B power supply and digital readout in conjunction with pressure transducers (effective range 0 - 1000 Torr) having inert wetted surfaces constructed of Inconel.

CAUTION: Precautionary measures should be established prior to repeating aspects of this work, particularly when $^{18}\text{F}^-$ is employed. Rapid outgassing and/or detonation can result from the oxidation of 2,2,2-crypt by XeF_2 in CH_2Cl_2 if the reaction temperature is not properly moderated. Before beginning work with anhydrous HF, first-aid treatment procedures^{85,86,87} should be available and known to all laboratory personnel. Disposal of samples containing XeF_2 or HF were carried out by freezing the heat-sealed FEP sample tube in liquid nitrogen, followed by cutting off the tube top and inverting the open tube end in a mixture of ice and aqueous base solution inside a fumehood.

All preparative work was carried out in 4-mm o.d. FEP tubes. One end of the tube was heat sealed by pushing it into the end of a 5-mm o.d. glass NMR tube previously heated in a Bunsen flame. The other end was fused to ca. 5-cm of ¼-in. o.d. FEP tubing, which was heat flared and fitted with a Kel-F valve. The FEP sample tubes were dried under dynamic vacuum for ca. 12 h on a glass vacuum line prior to transfer to a metal vacuum line where they were passivated with ca. 1 atm of F_2 for ca. 12 h. Samples were prepared in the drybox prior to addition of solvent (ca. 0.5 mL) and contained ca. 0.2 mmol of $[\text{N}(\text{CH}_3)_4][\text{F}]$, KF and/or 2,2,2-crypt, and the molar ratio of XeF_2 to the aforementioned reagent was adjusted. The equimolar samples of $[\text{N}(\text{CH}_3)_4][\text{F}]$ and XeF_2 in CH_3CN solvent used for single selective inversion NMR spectroscopy were prepared

in concentrations of ca. 0.18 M and 0.36 M. The sample containing a 33-fold molar excess of XeF_2 to 2,2,2-crypt contained 0.942 mmol and 0.0289 mmol, respectively.

Samples of L-DOPA or L- α -MT for low-temperature ^1H and ^{13}C NMR spectroscopy were prepared in 20 cm-lengths of AWG 9 (ca. 4 mm o.d., 0.8 mm wall) FEP plastic tubing heat sealed at one end with the other end joined by sealing to a ¼-in. o.d. thick-walled FEP tube and connected with a compression fitting to a Kel-F valve, which was connected to a stainless steel vacuum line. The assembly was pumped on overnight under dynamic vacuum prior to use. Fifty μmol of L-DOPA or L- α -MT were loaded into the FEP tube and approximately 0.7 mL of HF or BF_3/HF (ca. 0.13 M to maintain the same concentration used for the fluorination) was condensed into the FEP tube at -196°C .

The sample tubes used for recording the NMR spectra were sealed under vacuum at -196°C using a miniature nichrome wire resistance furnace. The sealed samples were stored submerged in liquid nitrogen. For NMR measurements, the 4-mm FEP tube was equilibrated to the required temperature and inserted into standard 5-mm precision Wilmad NMR tube before insertion into the NMR probe.

2.1.2 Materials

Fluorine (Air Products) was used without further purification. Anhydrous hydrogen fluoride (Harshaw Chemical Co.) was purified as described previously⁸⁸ and stored in a Kel-F storage vessel equipped with a Kel-F valve until used. Hydrogen fluoride was transferred into reaction vessels by vacuum distillation on a stainless steel vacuum line through a submanifold fabricated from FEP and Kel-F. Literature methods

were used for the synthesis of xenon difluoride,⁸⁹ krypton difluoride,^{90,91,92} the naked fluoride ion source, anhydrous $[\text{N}(\text{CH}_3)_4][\text{F}]$,⁹³ for the drying of anhydrous potassium fluoride (J.T. Baker Chemical Company, 99.6%)⁹⁴ and 2,2,2-crypt (1,10-diaza-4,7,13,16,21,24-hexaoxabicyclo[8.8.8]hexacosane) (Merck, 99%).⁹⁵ The CsF (ICN-KCK Laboratories Inc., 99.9%) was dried by fusion in a platinum crucible, followed by transfer of the red hot clinker to the drybox port where it was immediately evacuated. Upon transferring to the dry nitrogen atmosphere of the glovebox, the sample was ground to a fine powder and stored in the drybox until used.

Acetonitrile (HPLC Grade, Caledon) was purified to electrochemical standards according to the literature procedure.⁹⁶ Dichloromethane (Reagent Grade, Caledon) was dried over CaH_2 powder (BDH Chemicals, 99.5%) for several days and vacuum distilled onto Davison Type 3A molecular sieves (Fisher Scientific) and stored in a dry glass bulb equipped with a 4-mm glass J. Young glass stopcock equipped with a PTFE barrel until used. Molecular sieves were dried under dynamic vacuum for 24 h at ca. 250 °C prior to use as a drying agent. Dried CH_2Cl_2 (^1H chemical shift, 5.34 ppm) did not show water in the ^1H NMR spectrum under high gain conditions (the ^1H chemical shift of water in CH_2Cl_2 was determined from a spiked sample to be 1.58 ppm). Fluoroform, CHF_3 (Canadian Liquid Air, 98%) was transferred through a metal vacuum line. Before entering the vacuum manifold, CHF_3 gas was passed through a copper coil cooled to -78 °C in solid dry ice.

2.1.3 Attempted Syntheses of Salts Containing the XeF_3^- Anion

Inside the drybox, $[\text{N}(\text{CH}_3)_4][\text{F}]$ (0.03079 g, 0.3306 mmol) and XeF_2 (0.10775 g,

0.6365 mmol) were loaded into a thick wall "h" shaped glass reaction vessel (9 mm o.d., 2,5 mm i.d.). The reaction vessel was attached to a stainless steel vacuum line and anhydrous CHF₃ was condensed into the vessel by passing CHF₃ through a previously cooled vacuum dried helix made of ¼-in. copper tubing and packed in solid dry ice. Once the reaction vessel was flame sealed it was placed in a Dewar containing 95% ethanol/liquid nitrogen slush at ca. -110 °C. The reaction mixture was then agitated over a period of 30 min while warming to 0 °C and allowed to stand for 12 h. The sample was mixed again and a Raman spectrum was recorded at -160 °C directly on the thick walled glass reaction vessel containing the solid sample. The CHF₃ was distilled into one arm of the reaction vessel and was flame-sealed off. A white crystalline powder was obtained and Raman spectra were recorded at -155 °C directly on the sealed off portion of the thick wall glass reaction vessel containing the solid sample, at the lower, middle and uppermost regions of the powder.

Equimolar amounts of [N(CH₃)₄][F] (0.01620 g, 0.1739 mmol) and XeF₂ (0.02960 g, 0.1749 mmol) were added into a ¼-in. glass tube fused to a 5-mm o.d. thick wall glass NMR tube, inside the drybox. The reaction vessel was attached to a stainless steel vacuum line and anhydrous CHF₃ was condensed into the vessel (*vide supra*) to a height of ca. 5 cm and the tube was flame-sealed under vacuum. The reaction vessel was warmed in stages up to room temperature and stored at 0 °C for 12 h. A white crystalline powder was obtained and Raman spectra were recorded at -160 °C directly on the upper and lower regions of the sealed off portion of the thick wall glass reaction vessel containing the solid sample.

Equimolar amounts of $[\text{N}(\text{CH}_3)_4][\text{F}]$ (0.01474 g, 0.1582 mmol) and XeF_2 (0.02394 g, 0.1414 mmol) were added to a 4-mm o.d. FEP tube. Dry acetonitrile solvent was then added to the sample and reacted for ca. 1 h at $-30\text{ }^\circ\text{C}$. The solvent was then pumped off at $-30\text{ }^\circ\text{C}$ and a Raman spectrum was recorded at $-160\text{ }^\circ\text{C}$ on the non-volatile residue.

Cesium fluoride (0.08105 g, 0.5336 mmol) and XeF_2 (0.38827 g, 2.294 mmol) were loaded into a 4-mm o.d. FEP tube. The tube was then heat sealed under ca. 0.5 atm N_2 , and then immersed in an oil bath and heated to $145\text{ }^\circ\text{C}$. A Raman spectrum recorded at $-155\text{ }^\circ\text{C}$. In all of the aforementioned attempts to synthesize salts containing the XeF_3^- anion, Raman spectra in all cases revealed strong bands at 480 cm^{-1} , assigned to the symmetric stretch of unreacted XeF_2 , in addition to the characteristic lines of the unreacted $\text{N}(\text{CH}_3)_4^+$ cation.⁹⁷ No new lines arising from the XeF_3^- anion were observed (see Chapter 8, Table 8.1).

A sample of $[\text{N}(\text{CH}_3)_4][\text{F}]$ (0.02076 g, 0.0223 mol) and XeF_2 (0.23772 g, 1.404 mmol) was similarly prepared. The sample was immersed in an oil bath and detonated violently at the melting point of XeF_2 ($129\text{ }^\circ\text{C}$).

2.2 Experiments Using Fluorine-18 Labelled Fluoride

2.2.1 Standard Techniques

The use of radioactive isotopes was carried out in a safe and effective manner in compliance with all requirements of the Canadian Nuclear Safety Commission (CNSC) and Radioisotope Protection Committee (RPC) or Hamilton Health Sciences.

2.2.2 Production of No-Carrier-Added $^{18}\text{F}^-$

No-carrier-added ^{18}F -fluoride was produced using a Siemens 11 MeV proton-only cyclotron (RDS 112) by means of the $^{18}\text{O}(\text{p},\text{n})^{18}\text{F}$ nuclear reaction at the Department of Nuclear Medicine, Hamilton Health Sciences. The $[\text{}^{18}\text{O}]\text{H}_2\text{O}$ was separated from the $^{18}\text{F}^-$ by passing the bolus through an anion exchange column (Bio-Rad, AG 11 A8 resin, 50 – 100 mesh, converted to HCO_3^- form). The $^{18}\text{F}^-$ was subsequently eluted from the column using 1 mL $\text{CH}_3\text{CN}/\text{H}_2\text{O}$ (95/5, v/v) solution containing 8 mg of 2,2,2-crypt and 2 mg of KHCO_3 and the $\text{CH}_3\text{CN}/\text{H}_2\text{O}$ was evaporated at 120 °C. The residue was redissolved in 1 mL of anhydrous CH_3CN and redried.

2.2.3 Materials

Anhydrous CH_3CN (Aldrich, 99.8%), anhydrous CH_2Cl_2 (Aldrich, 99.8%), Kryptofix[®] 222 (Aldrich, 98%), KHCO_3 (British Drug Houses, 99.5%) and $[\text{}^{18}\text{O}]\text{H}_2\text{O}$ (Isotec, Ohio, USA, 98 atom %) were used without further purification. Xenon difluoride was prepared as described previously (vide supra).

2.2.4 Attempted Syntheses of $[\text{}^{18}\text{F}]\text{XeF}_2$

The dry ^{18}F -containing residue was redissolved in anhydrous CH_3CN or anhydrous CH_2Cl_2 diluted to 10 mCi mL^{-1} and 1 mL was transferred to a covered Teflon

or glass vessel containing 10 to 50 mg of XeF₂ (XeF₂ had been transferred in a glove bag purged with dry nitrogen). Aliquots of the resulting reaction mixtures were analyzed at various time intervals between 5 and 90 min on a reverse phase HPLC column (Phenomenex, Hypersil C18, 5 μm, 25 x 0.46 cm) eluted with 60% CH₃CN (HPLC Grade, Caledon) in water, at a flow rate of 1.0 mL/min. The eluates from the column were passed through a Waters 490E programmable multiwavelength detector (255 nm) and a Beckman radioisotope detector (Model 170). Both detectors were connected to a Waters Millennium Chromatography Manager.

2.3 Experiments Involving [¹⁸F]F₂ or [¹⁸F]CH₃COOF

2.3.1 General Fluorination of Aromatic Amino Acids with [¹⁸F]F₂

Fluorine-18 labelled F₂ was produced by the ¹⁸O(p,n)¹⁸F nuclear reaction using a Siemens RDS 112 proton cyclotron operating at 11 MeV by the “double shoot” method²⁶ at the Department of Nuclear Medicine, Hamilton Health Sciences, as previously described.³⁵

Fluorine-18 labelled F₂ (15 - 20 μmol) in neon was bubbled through a 0.5 - 1.1 mL solution of aromatic amino acid (ca. 50 μmol), at -65 °C for the reactions involving anhydrous HF or BF₃/HF, and at +4 to +10 °C for all other solvents, in a ⁵/₁₆-in. o.d. x ⁵/₃₂-in. i.d. FEP tube attached to a Kel-F Y-piece. One arm of the Y-piece was attached to a PFA outlet valve and the other arm was attached to a ¹/₁₆-in. o.d. x ¹/₃₂-in. i.d. Teflon tube for bubbling dilute [¹⁸F]F₂ gas through the precursor in solution. The outlet gas from

the reaction vessel was passed through a 0.1 M solution of NaOH (same geometry as the reaction vessel) before it was vented out through the hot cell. The amount of [^{18}F]F₂ consumed during the reaction was determined by measuring the radioactivity in the reaction mixture after all of the target gas had passed through. Fluorine-18 labelled acetyl hypofluorite was produced by passing dilute [^{18}F]F₂ through a 2-in. x ¼-in. o.d. x ⅛-in i.d. FEP column packed with KOAc·2HOAc.⁹⁶ A schematic diagram of the experimental set-up used in our laboratory is shown in Figure 2.1

In reactions involving anhydrous HF or BF₃/HF, the solvent was condensed into an FEP U-tube under dynamic vacuum at -196 °C. In reactions where other solvents were used, the reaction mixture was transferred to a rotary evaporator and the solvent was removed. The residue was dissolved in 5 mL 0.1% HOAc and evaporated and the process was repeated. The final residue was dissolved in 2 mL of 0.1% HOAc and filtered through a 0.22 µm filter prior to HPLC analysis.

2.4 Separations and Purifications By Use of HPLC

In all preparative separations, the eluate from the column was monitored using a fixed wavelength UV detector (280 nm) and a Geiger-Müller counter (Bicron SWGM B980C) coupled to a rate meter (Bicron Erik-Tech™). In all analytical separations, the eluate from the column was passed through a Waters 490E Programmable Multiwavelength detector (275 nm for fluoro-tyrosine derivatives and 280 nm for fluoro-

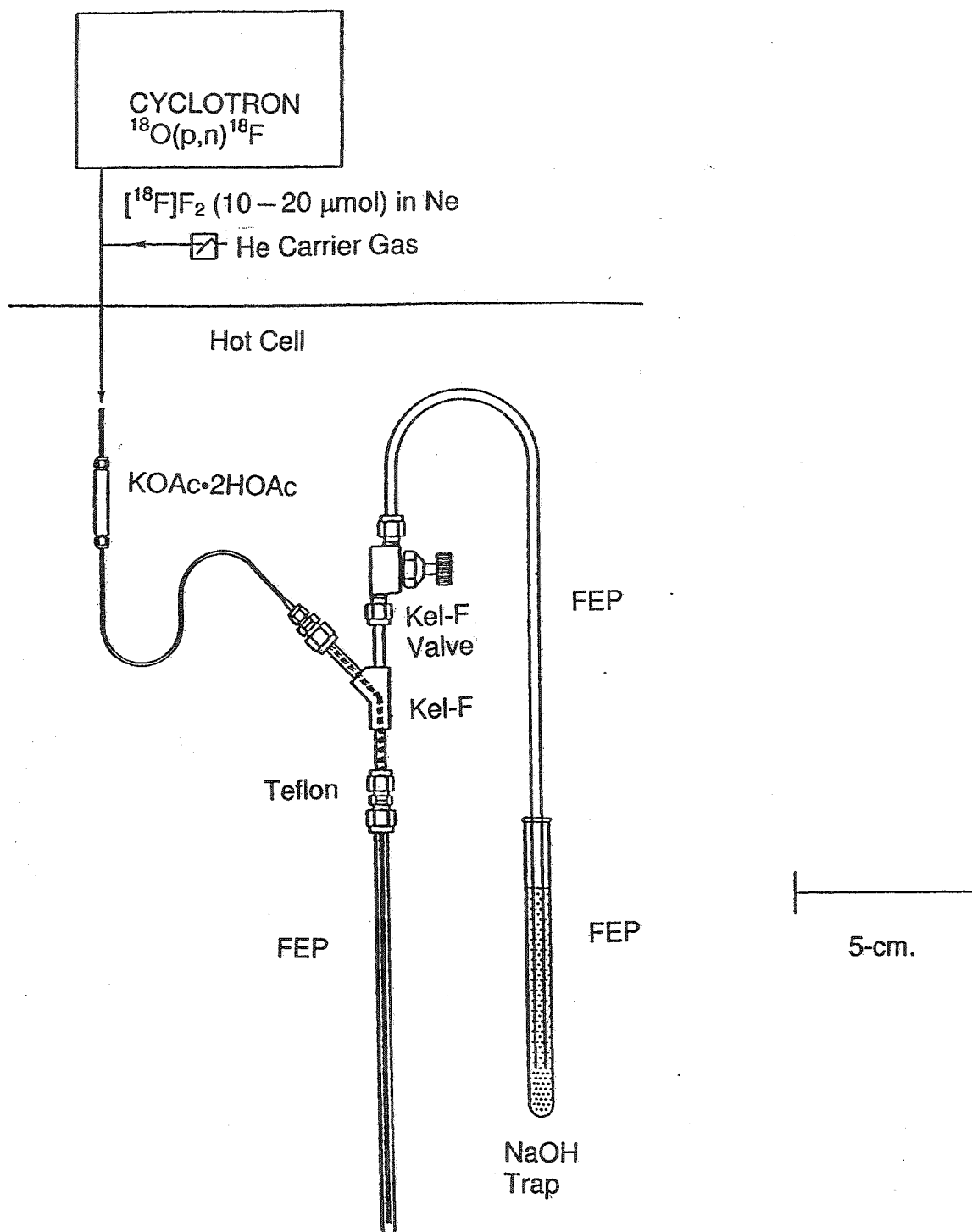


Figure 2.1 Experimental apparatus used for the radiofluorination of aromatic amino acids.

DOPA studies) and Beckman Radioisotope Detector (Model 170). Both detectors were connected to a Waters Millennium Chromatography Manager.

2.4.1 Materials

Enriched [^{18}O]O₂ (95.87 atom %, Eurisotop, Saint Aubin, France, or min 98 atom %, Isotec, Ohio, USA), neon (99.999%, Air Products), anhydrous hydrogen fluoride (Air Products), 1% F₂ in neon (Canadian Liquid Air), boron trifluoride (Matheson), helium (99.9999%, Matheson), potassium dihydrogenphosphate (Aldrich), potassium acetate (British Drug Houses), β -3,4-dihydroxyphenyl-L-alanine (Sigma), 3,4-dihydroxyphenyl-acetic acid (Sigma), L-tyrosine (Fisher), 3-fluoro-DL-tyrosine (Aldrich), L- α -methyl-*p*-tyrosine (Research Biochemicals International), 3-nitro-L-tyrosine (Aldrich), sodium nitrate (Caledon), trifluoroacetic acid (Caledon), glacial acetic acid (British Drug Houses), formic acid (98 to 100%; British Drug Houses), *o*-phosphoric acid (85%, Fisher) and HPLC grade acetonitrile (Caledon) were used without further purification.

2.4.2 Preparation, Separation and Purification of [^{18}F]Fluoro-L-DOPA,

[^{18}F]Fluoro-L-tyrosine and [^{18}F]Fluoro-L- α -methyltyrosine Derivatives

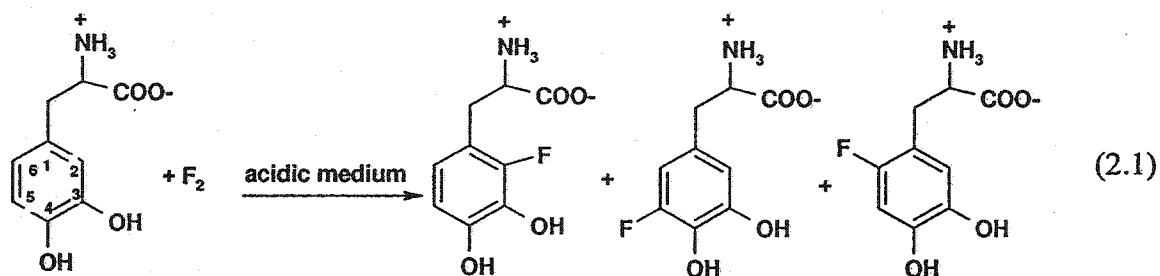
Fluorine-18 labelled [^{18}F]fluoro-L-DOPA (FDOPA), [^{18}F]fluoro-L-tyrosine and [^{18}F]fluoro-L- α -methyltyrosine (F- α -MT) and the respective precursors were separated from the reaction mixture after fluorination of the aromatic amino acid in acidic media using a reverse-phase HPLC column (Phenomenex M9 Partisil 10/50, ODS-3) with an aqueous solution of 0.01 M (for F- α -MT) or 0.02 M (for FDOPA and fluoro-L-tyrosine)

KH_2PO_4 (pH adjusted to 3.0 - 3.5 with 85% H_3PO_4), containing 5% CH_3CN (v/v) as the mobile phase, using flow rates of 3.5 mL/min for FDOPA and fluoro-L-tyrosine studies and 4.0 mL/min for the F- α -MT studies. HPLC analysis of the reaction mixture typically showed one broad UV peak having the same retention time as L-aromatic amino acid. The radiochromatograms showed the fluoro-isomers eluting after the precursor.

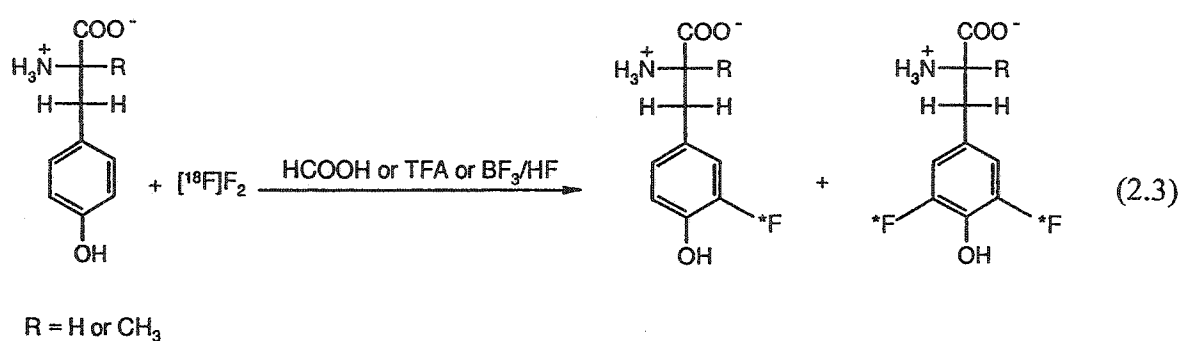
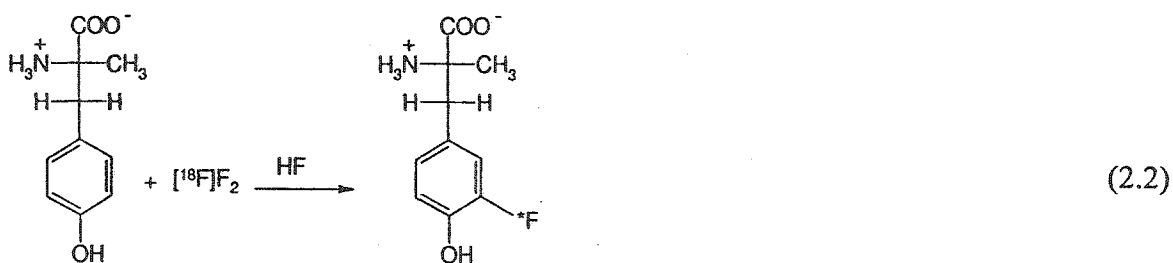
The peaks of interest were collected and evaporated to dryness. The dry residue was re-dissolved in 0.5 mL of water and the process repeated prior to further purification using a second reverse-phase HPLC column (Vydac C_{18} , 0.9 x 25 cm) and 0.1% acetic acid in water as the mobile phase using flow rates of 2.5 to 3.5 mL min^{-1} . The entire syntheses and purifications were completed in 65 min. The syntheses were repeated 3 times and the samples were combined for characterization by ^1H , ^{13}C and ^{19}F NMR spectroscopy and mass spectrometry. It has been shown that electrophilic fluorination of the aromatic ring using F_2 ,⁹⁹ XeF_2 ,⁶⁵ or acetyl hypofluorite¹⁰⁰ do not affect the chiral center of the side chain, therefore, chirality was assumed to be that of the precursor.

Preparative HPLC analysis of the FDOPA reaction mixture showed one broad UV peak having the same retention time as L-DOPA at 14 min. In cases where 5-fluoro-L-DOPA was synthesized (solvent was 10% TFA in HOAc or formic acid), the radiochromatogram of the reaction mixtures showed peaks at 8, 9, 12, 15, 16 and 21 min. The peaks eluting at 15 and 16 min contained 26.5 and 28.3%, respectively, of the injected radioactivity. Based on the ^{18}F activity in the two peaks and the ratio of ^{19}F NMR signals at -139.6 and -134.7 ppm, the two peaks have been identified as 2- and 5-fluoro-DOPA, respectively. The peak eluting at 16 min and the peak eluting at 12 min

contained 98% of the radioactivity and it was collected. The radiochemical purity of [^{18}F]5-fluoro-DOPA was 98%, consistent with integration of the ^{19}F NMR spectrum. Synthesis of 5-fluoro-DOPA was repeated four times and samples were combined for identification and characterization of the product using mass spectrometry and ^1H and ^{19}F NMR spectroscopy. The concentration of the sample was too low for characterization by ^{13}C NMR spectroscopy. The radiochromatogram of all other samples showed two major radioactive peaks having retention times between 14 and 17 min. Their identification has been described before.⁵⁸ The radioactive peak eluting at 12 to 13 min corresponded to [^{18}F]2-, 5- or 6-FDOPA and was collected for dose preparation.



Analysis of the reaction mixture, by use of HPLC, after fluorination of L- α -MT (eq. 2.2) showed one broad UV peak having the same retention time as L- α -MT at 17 min and a minor peak at 20 min. The radiochromatogram of the same sample showed peaks at 6.5, 9, 12.5 and 20 min (and an additional peak at 25 min when formic acid, TFA or BF_3/HF was the solvent, eq. 2.3). The peaks eluting at 20 (and 25 min where applicable) contained the majority of the radioactivity and were collected, evaporated to dryness and re-dissolved in 0.5 mL of water; the evaporation/dissolution process was repeated. The same HPLC system was used for reactions involving L-tyrosine and 3-fluoro-DL-tyrosine.



An aliquot of the reaction mixture and an aliquot of the purified product were each analyzed on an analytical reverse phase HPLC column. For the FDOPA study, a Vydac C₁₈ column was used (0.9 x 25 cm) with a mobile phase of 0.1% TFA in water containing 5 % CH₃CN at 2.5 mL/min. Analytical HPLC analysis of the reaction mixtures after the fluorination of L-DOPA (eq. 2.1) are shown in Figures 2.2 and 2.3 respectively.

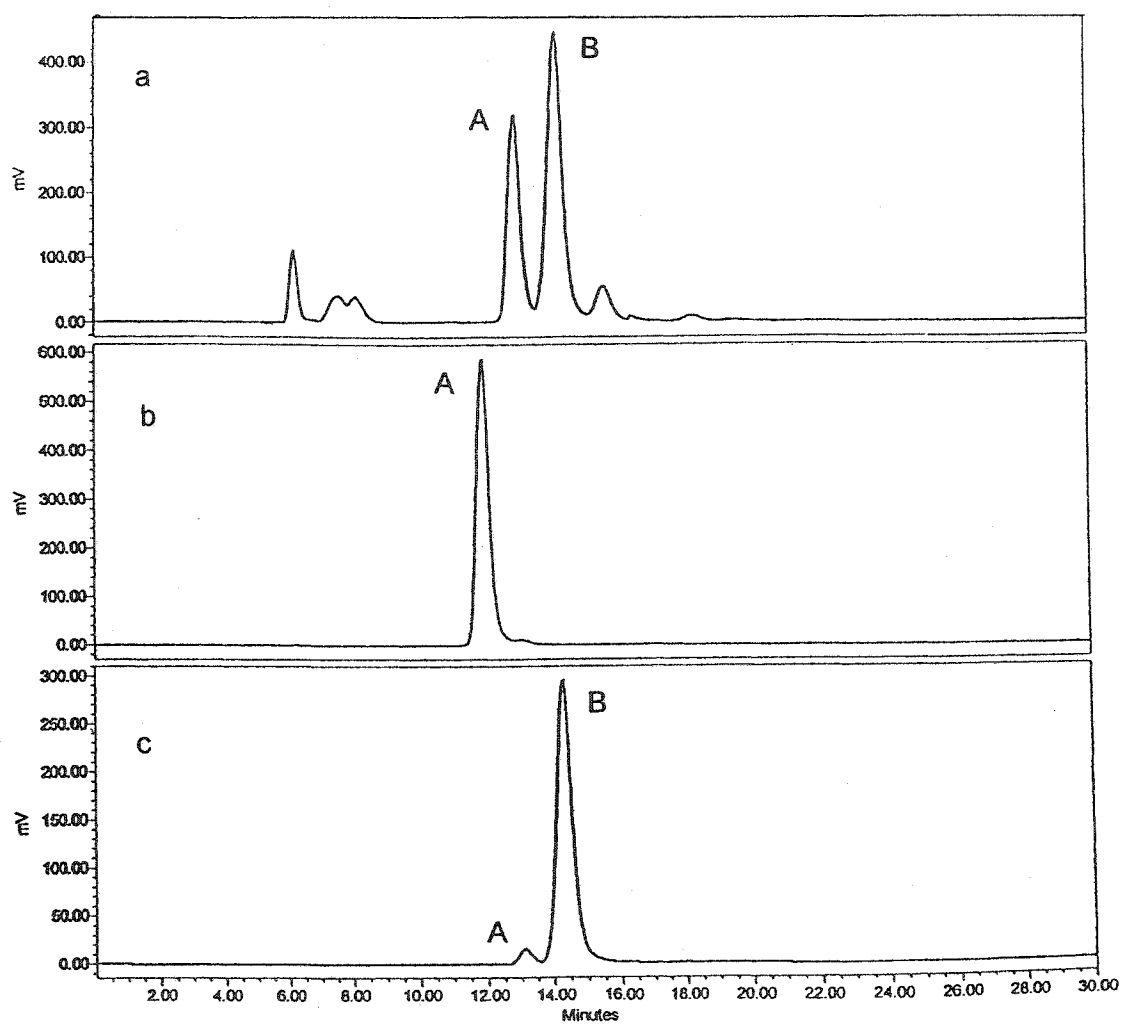


Figure 2.2. Radiochromatogram of (a) the reaction mixture after radiofluorination of L-DOPA in BF_3/HF , (b) $[^{18}\text{F}]2$ -fluoro-L-DOPA (A) after final purification and (c) $[^{18}\text{F}]6$ -fluoro-L-DOPA (B) after final purification. Unlabelled peaks are unknown fluorine-containing species.

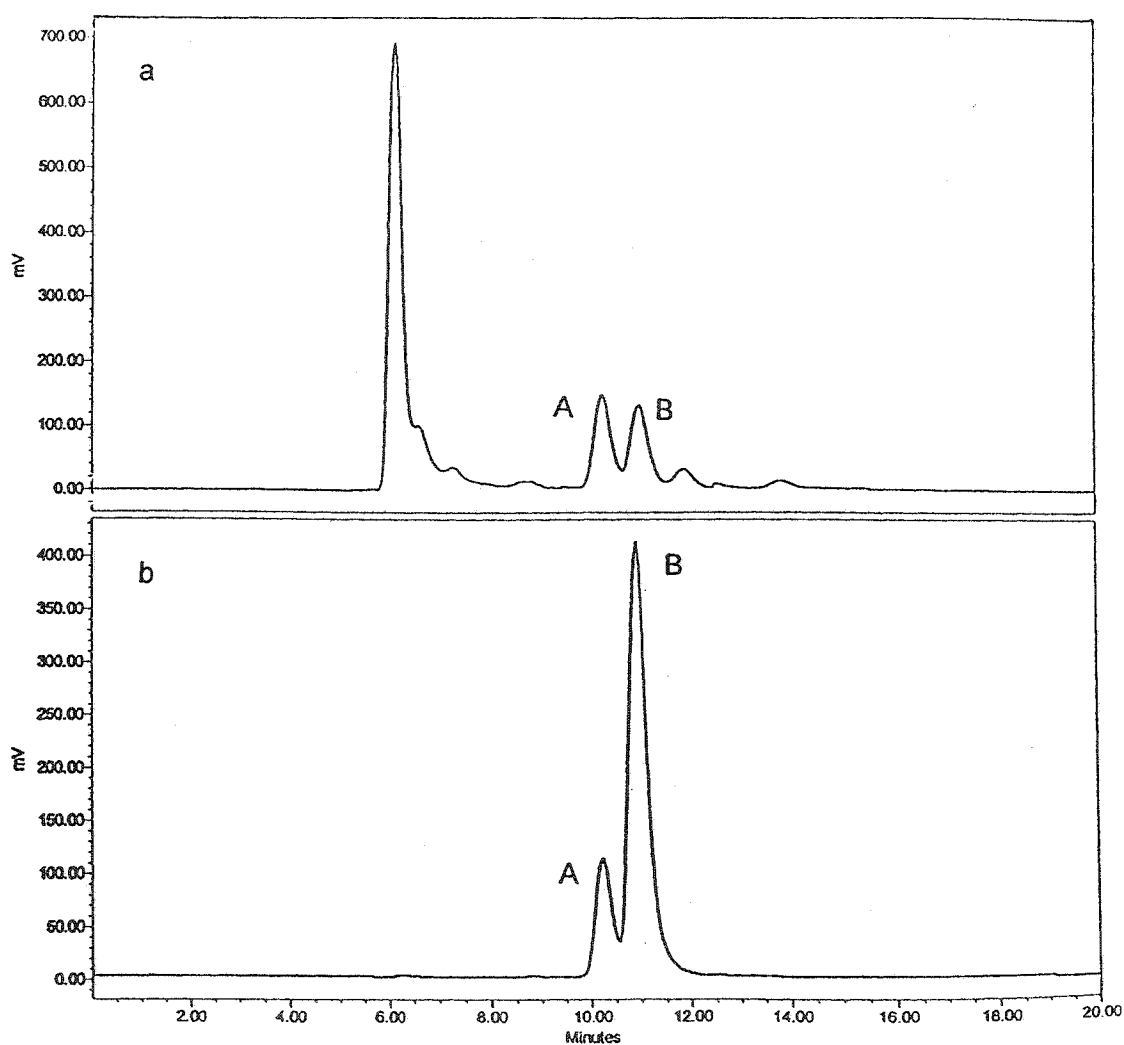
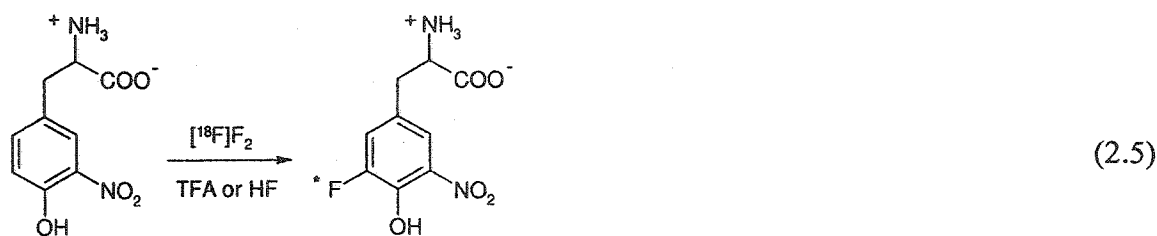
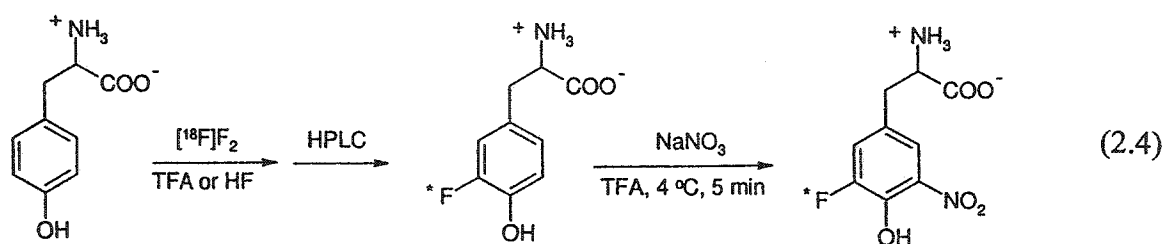


Figure 2.3. Radiochromatogram of (a) the reaction mixture after radiofluorination of L-DOPA in glacial acetic acid containing 10% TFA, showing [^{18}F]2- (A) and [^{18}F]5- (B) fluoro-L-DOPA, and (b) [^{18}F]5-fluoro-L-DOPA after final purification. Unlabelled peaks are unknown fluorine-containing species.

For the F- α -MT study a Phenomenex ODS-2 column was used (0.9 x 25 cm) with a mobile phase of 0.1% TFA in water containing 10 % CH₃CN using a flow rate of 4.0 mL/min. Analytical HPLC analysis of the reaction mixtures after the fluorination of L- α -MT in HF (eq. 2.2) and in 0.13 M BF₃/HF (eq. 2.3) are shown in Figures 2.4 and 2.5 respectively.

2.4.2 Preparation and Separation of [¹⁸F]Fluoro-nitro-L-tyrosine Derivatives

Three methods were developed for the syntheses of [¹⁸F]5-fluoro-3-nitro-L-tyrosine: nitration of [¹⁸F]3-fluoro-L-tyrosine (eq. 2.4), direct fluorination of 3-nitro-L-tyrosine (eq. 2.5), and a one-pot nitration followed by fluorination of L-tyrosine (eq. 2.6).



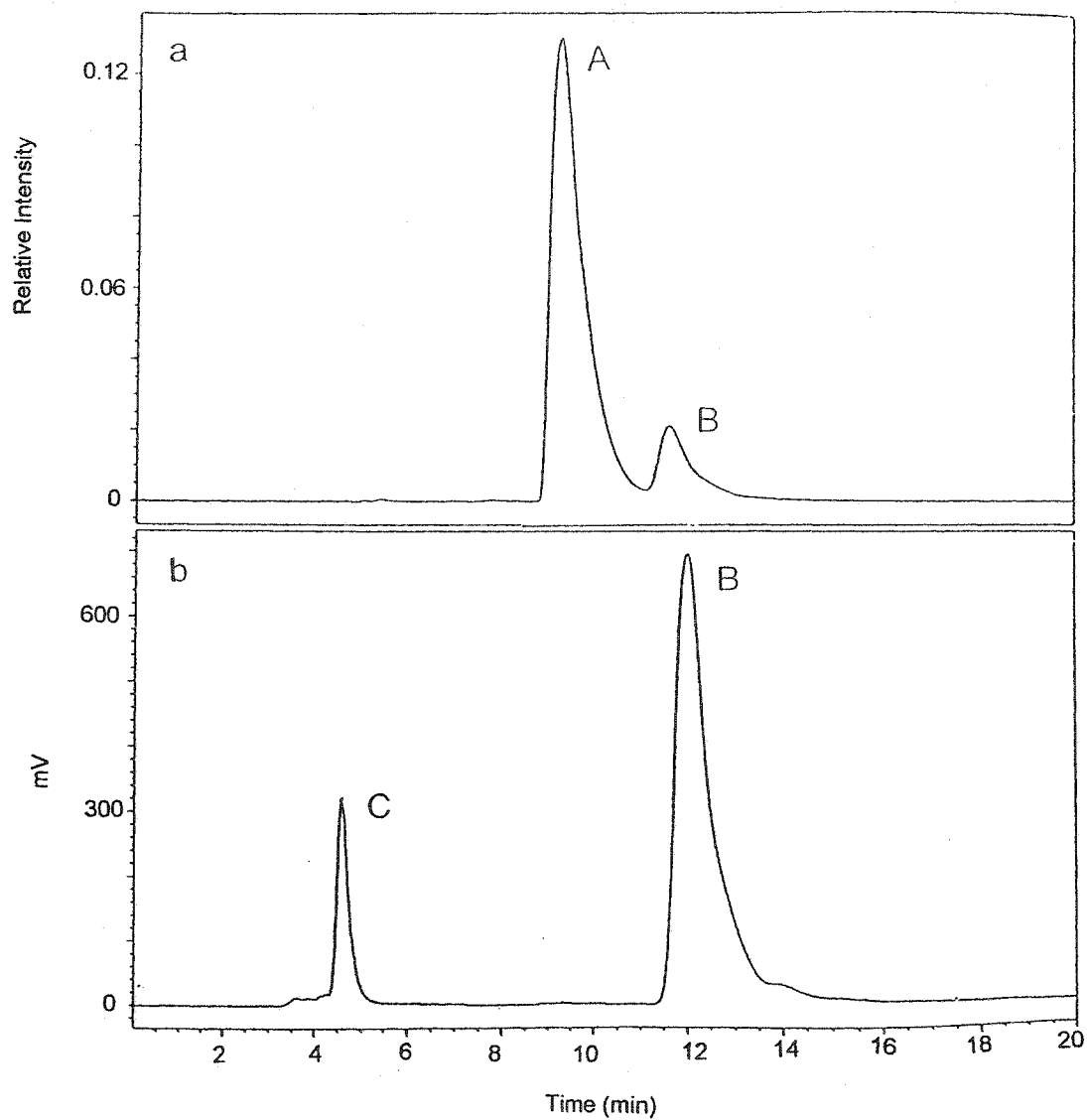


Figure 2.4. HPLC chromatogram of the reaction mixture obtained from the fluorination of L- α -MT in aHF with [^{18}F]F $_2$; (a) UV trace for absorption at 275 nm and (b) [^{18}F]-radioactivity trace. The labels A, B and C correspond to L- α -MT, 3-F- α -MT and an unknown fluorine-containing species, respectively.

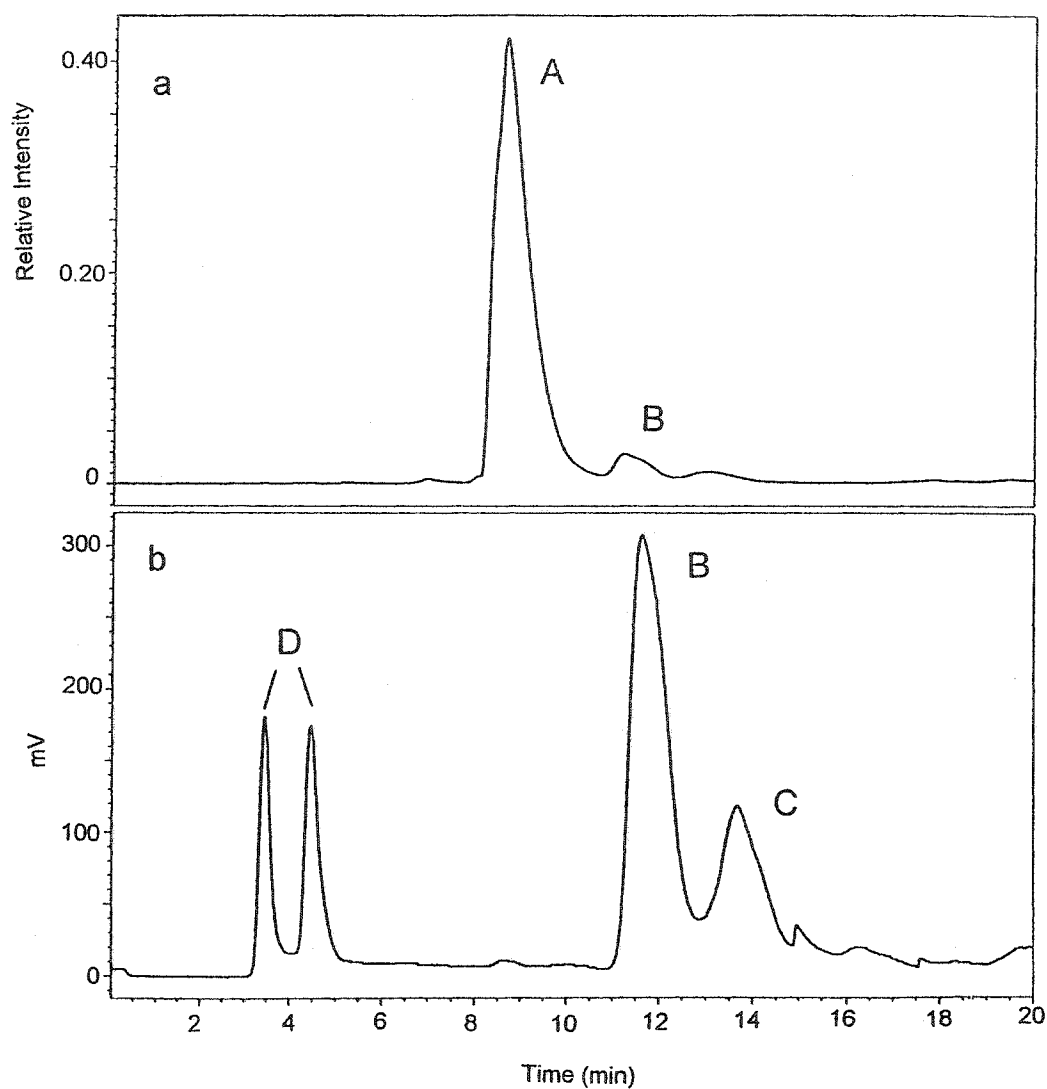
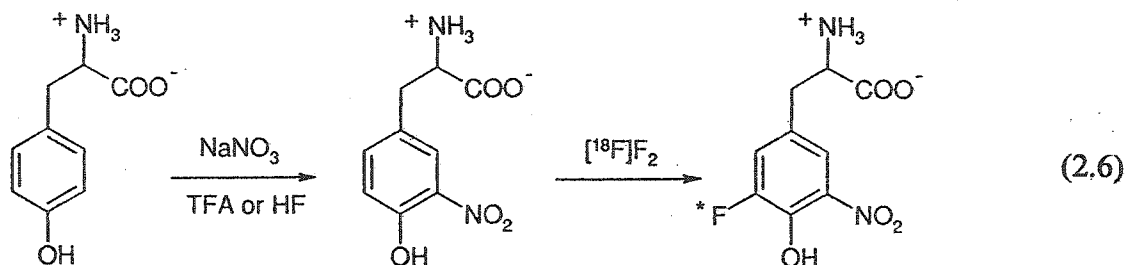


Figure 2.5. HPLC chromatogram of the reaction mixture obtained from the fluorination of L- α -methyltyrosine in 0.13 M BF_3/HF with ^{18}F ; F_2 ; (a) UV trace for absorption at 275 nm and (b) ^{18}F -radioactivity trace. The labels A, B, C and D correspond to L- α -MT, 3-F- α -MT, 3,5-difluoro-L- α -MT and unknown fluorine containing species, respectively.



Separation of L-tyrosine from [^{18}F]3-fluoro-L-tyrosine by preparative HPLC was carried out using a reverse-phase column (Phenomenex M9 Partisil 10/50, ODS-3) and an aqueous solution of 5% CH_3CN with 0.1% TFA (v/v) as the mobile phase and a flow rate of 3.0 mL min^{-1} . Preparative HPLC analysis of the reaction mixture (eq. 2.4) showed one major UV peak having the same retention time as L-tyrosine at 13.5 min and another major peak at 16 min. The radiochromatogram of the same sample showed peaks at 8, 9.5, 11, 13 and 16 min. The peak eluting at 16 min contained the majority of the radioactivity and was collected, evaporated to dryness and redissolved in 0.5 mL of 0.1% HOAc and the evaporation process was repeated. Sodium nitrate (2 mg, 24 μmol) in 1 mL of TFA was added to the dry residue and reacted at 4°C for 5 min. The products were confirmed to be [^{18}F]3-fluoro-L-tyrosine and [^{18}F]FNT by use of HPLC and ^{19}F NMR spectroscopy. The present separation method offers the advantage, over our previously described method (*vide supra*)¹⁰¹ of avoiding the use of a buffered mobile phase and a second HPLC purification step. The TFA was evaporated and the sample was redissolved in 0.1% HOAc and used for characterization. Preparative HPLC

conditions used for the products of fluorination of 3-nitro-L-tyrosine and for the study of the relative reactivity of [^{18}F]F₂ towards L-tyrosine and 3-nitro-L-tyrosine were identical to those described above except that the mobile phase was an aqueous solution comprised of 20% CH₃CN and 0.1% TFA. Under these conditions, L-tyrosine eluted at 8.5 min and [^{18}F]FNT eluted at 9.5 min.

Aliquots of the reaction mixture and of purified [^{18}F]FNT were analyzed on a reverse phase HPLC column (Phenomenex, ODS-2, 0.9 x 25 cm) and an aqueous solution of 20% CH₃CN with 0.1% TFA as the mobile phase using a flow rate of 3.0 mL min⁻¹. Under these conditions, 3-fluoro-L-tyrosine and [^{18}F]FNT eluted at 5.5 and 7.5 min, respectively (Figure 2.6). The identity of the peak eluting at 5.5 min was confirmed by spiking the reaction mixture with 3-fluoro-DL-tyrosine.

2.5 Dose Preparation and Quality Control

The radiochemical purities of [^{18}F]fluoro-L-DOPA (96 ± 2% for 2- and 6- fluoro isomers and 91 ± 4% for 5-fluoro isomer) and [^{18}F]3-F- α -MT (98 ± 2%) were determined by analytical HPLC analysis of an aliquot of the quality control sample. Pure [^{18}F]2-, [^{18}F]5- or [^{18}F]6-fluoro-L-DOPA and [^{18}F]3-F- α -MT in 0.1% acetic acid were separately collected in a pyrogen-free 10 mL vial and a 0.1 mL sample was removed for quality control. Ascorbic acid (ca. 1 mg) and 0.6 mL of 10% sodium chloride in water (sterile and pyrogen-free) were added and the solution was transferred through 0.22 μm sterile filter (Millipore) into a 10 mL sterile vial. Each batch passed quality control tests for pH

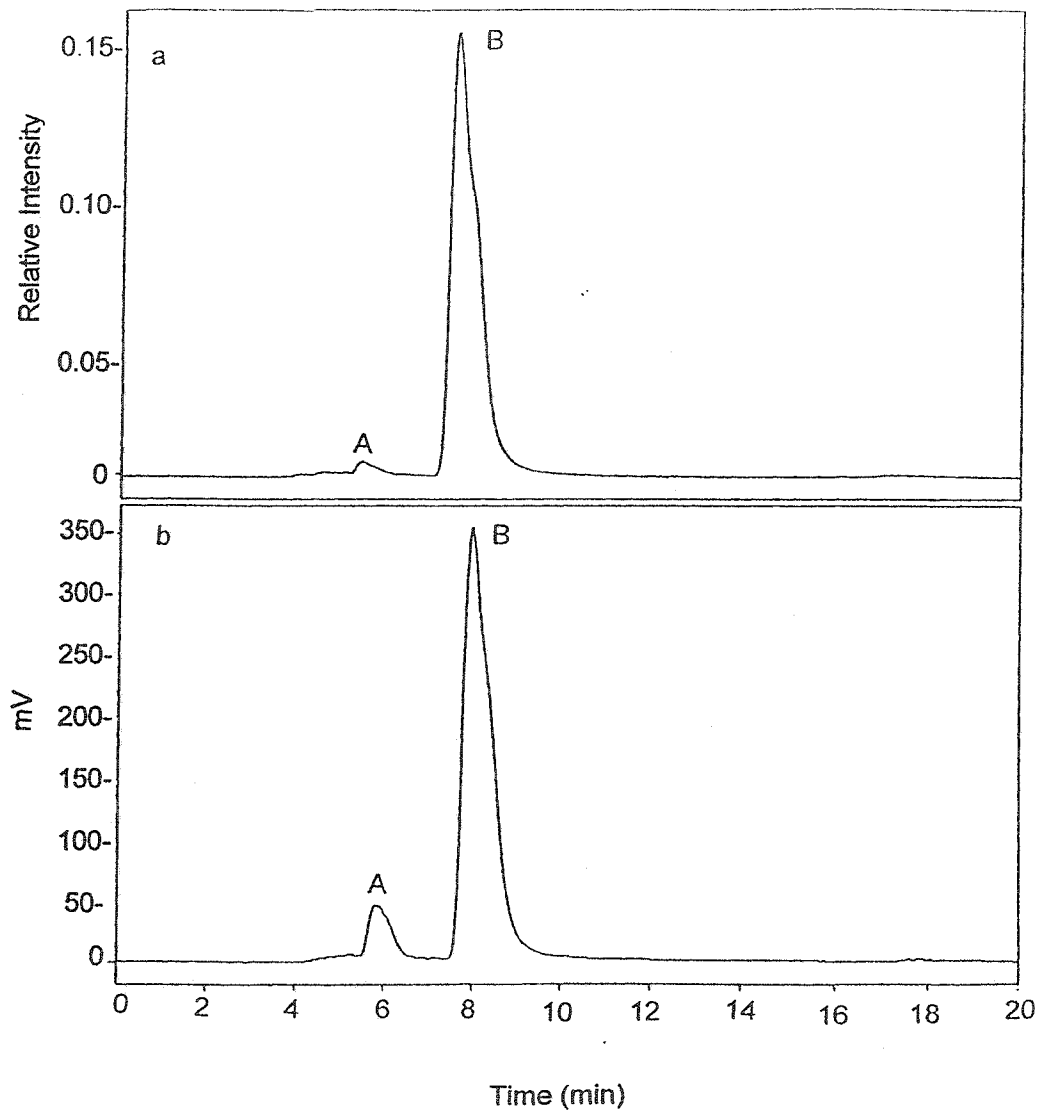


Figure 2.6. HPLC trace of the reaction mixture after the nitration of [^{18}F]3-fluoro-L-tyrosine (A) using NaNO_3 in TFA solvent at 4 °C for 5 min to produce [^{18}F]FNT (B) (eq. 2.4): (a) UV, $\lambda = 275$ nm and (b) [^{18}F]-radioactivity trace.

(5 - 6), sterility and pyrogenicity. The radiochemical yields were determined as the ratio of ^{18}F activity in the peaks of interest (decay corrected to the beginning of the experiment), to the ^{18}F activity in the reaction vessel after all of the fluorine gas had been bubbled through the amino acid solution.

2.6 Nuclear Magnetic Resonance Spectroscopy

Proton, ^{13}C and ^{19}F NMR spectra were recorded on a Bruker Avance 200 (4.6976 T), Avance 300 (7.0463 T) or Avance DRX-500 (11.7440 T) spectrometer. Typical acquisition parameters are given in Table 2.1. For low-temperature work, the NMR probe was cooled using a nitrogen flow and variable temperature controller (BV-T 2000).

The ^1H , ^{13}C , ^{19}F and ^{129}Xe NMR spectra were referenced at room temperature to external Me_4Si , Me_4Si , CFCl_3 , and XeOF_4 , respectively. The chemical shift convention used is that a positive (negative) sign indicates a chemical shift to high (low) frequency relative to that of the reference compound.

Table 2.1 Typical NMR Spectroscopic Parameters for ^1H , ^{13}C , ^{19}F and ^{129}Xe NMR

Spectroscopy.

Acquisition Parameter	^1H	^{13}C	^{19}F	^{129}Xe
$B_0 = 4.6976 \text{ T}$				
SF	200.200	50.328	188.372	
TD	16 K	16 K	32 K	
SW (kHz)	4.1	12.6	17.4	
Hz/Pt	0.25	0.77	0.53	
AQ (s)	2.02	0.652	0.939	
NS	8	25000	500	
$B_0 = 7.0463 \text{ T}$				
SF	300.135	75.469	282.404	
TD	16 K	16 K	32 K	
SW (kHz)	4.505	17.857	33.8	
Hz/pt	0.55	2.180	1.03	
AQ (s)	1.819	0.459	0.131	
NS	8	5000	1000	
$B_0 = 11.7440 \text{ T}$				
SF	500.130	125.771	470.592	139.086
TD	32 K	32 K	32 K	32 K
SW (kHz)	5.734	28.986	44.248	38.4
Hz/pt	0.18	0.89	0.675	1.17
AQ (s)	2.857	0.586	0.741	0.426
NS	32	21000	100	5000

2.6.1 2-D HSQC

The ^{13}C NMR chemical shifts of L- α -MT were assigned using a ^{13}C spin sort and were found to follow the same trend for tyrosine¹⁰² despite differences in concentration and pH. The ^{13}C NMR chemical shifts for 3-F- α -MT were assigned using an inverse-detected ^1H - ^{13}C 2-D chemical shift correlation experiment. The spectra were acquired using the pulse field gradient version of the heteronuclear single quantum coherence (HSQC) pulse sequence. The FID's in the F2 (^1H) dimension were recorded over a 3.655 kHz spectral width in 1K memories. The 128 FID's collected in the F1 (^{13}C) dimension were obtained over a 21.368 kHz spectral width. Each FID was acquired in 2 scans. The fixed delays during the pulse sequence were a 1.0 s relaxation delay and a delay for polarization transfer.

2.6.2 2-D ROESY

The 2-D ROESY spectra were acquired in 16 scans for each of the 256 FIDs that contained 2K data points in the F2 dimension over a 3.931 kHz spectral width. A 1.0 s relaxation delay was used between acquisitions. A mixing time of 800.0 ms was used. Zero-filling in the F1 dimension produced a 1K x 1K data matrix with a digital resolution of 3.839 Hz/point in both dimensions.

2.6.3 2-D EXSY

Two-dimensional ^{19}F - ^{19}F EXSY spectra were acquired at 470.55 MHz using the pulse sequence 90° - t_1 - 90° - t_m - 90° -ACQ. A temperature of 15 °C was used in order to slow

down the formation of HF_2^- , while maintaining a soluble solution. In the F1 dimension, 256 FIDs were recorded, with each FID acquired in 48 scans over a 60 kHz spectral width. Mixing times of 400 ms and 800 ms were employed.

2.6.4 Single Selective Inversion

Single selective inversion experiments were conducted as previously described¹⁵ and the full observed relaxation, under the combined influence of spin-lattice relaxation and chemical exchange was analyzed using the CIFIT program (available from Alex D. Bain).²³ The equimolar samples of XeF_2 and $[\text{N}(\text{CH}_3)_4][\text{F}]$ were prepared in CH_3CN solvent with concentrations of 0.18 M and 0.36 M, as described previously.¹⁴

2.7 Raman Spectroscopy

Low-temperature (-155 to $-165\text{ }^\circ\text{C}$) Raman spectra were recorded on a Bruker RFS 100 FT Raman spectrometer using a 1064-nm excitation laser as previously described.¹⁰³ Spectra were recorded in glass or $\frac{1}{4}$ -in. FEP sample tubes using laser powers of 200 mW and a total of 300 scans.

2.8 Computational Methods

The theoretical calculations discussed in Chapter 8 (DFT, MP2 and ELF) were conducted by Dr. Reijo J. Suontamo, Department of Chemistry, University of Jyväskylä, Finland. The details of these computations will be described in a subsequent publication.¹⁰⁴

2.9 PET Scanning Protocol

Two healthy, 55 year old (control) subjects participated in this study. The study was designed in accordance with the Institutional Review Board, McMaster University. The subjects fasted for four hours prior to the examination. They were not pretreated with carbidopa, as it has been shown that this increases the radioactivity in the brain, but not the specific accumulation in the striatum.¹⁰⁵ Subjects were examined in an ECAT ART,¹⁰⁶ after intravenous injection of between 3 and 5 mCi of [¹⁸F]5-, and [¹⁸F]6-fluoro-L-DOPA. Subject 1 was also injected with 4 mCi of [¹⁸F]2-fluoro-L-DOPA. Studies were conducted within a three-month interval.

The subject's head was immobilized in a head holder. Subjects were scanned for a total of 120 min. Images were reconstructed (by Prof. Claude Nahmias and co-workers, Departments of Nuclear Medicine and Physics and Astronomy, Hamilton Health Sciences and McMaster University, respectively) as previously described. Regions of interest (ROIs) were drawn with reference to a standard neuroanatomical atlas¹⁰⁷ around the right and left caudate nuclei, the right and left putamina, and the cerebellum for the 6-fluoro-L-DOPA study. These regions were then transferred to the 2- and 5-fluoro-L-DOPA studies. The decay-corrected time activity curves in these ROIs were then obtained for the duration of the study. An influx constant (K_i)¹⁰⁸ was calculated for each of the regions using the cerebellum as the tissue reference.¹⁰⁹

CHAPTER 3

RADIOCHEMICAL AND NMR SPECTROSCOPIC INVESTIGATION OF THE SOLVENT EFFECT ON THE ELECTROPHILIC ELEMENTAL FLUORINATION OF L-DOPA: SYNTHESIS OF [¹⁸F]5-FLUORO-L-DOPA

3.1 Introduction

In the present study, ¹⁸F-labelling and NMR spectroscopy were used to investigate the effect of the solvent acidity on the reactivity and selectivity of F₂ towards L-DOPA. The application of ¹⁸F-labelled fluoro-L-DOPA is of interest for the investigation of movement disorders in man. It is known, for example, that the clinical features of Parkinson's disease, muscular rigidity, immobility, flexed posture and tremor are associated with marked deficiencies of striatal dopamine.¹⁰ Garnett, *et al.*¹¹⁰ first demonstrated the use of [¹⁸F]5-fluoro-DL-DOPA to study intracerebral L-DOPA transport and metabolism in live monkeys. They later pioneered the use of [¹⁸F]6-fluoro-L-DOPA, in conjunction with PET, to visualize the regional distribution of intracerebral dopamine

in the living human brain.¹¹ Subsequently, [^{18}F]6-fluoro-DOPA was also used to show that the accumulation of ^{18}F was reduced in the contra lateral putamen of patients suffering from hemiparkinsonism.¹² Whereas [^{18}F]6-fluoro-DOPA shows a very specific accumulation in the brain, [^{18}F]2-fluoro-DOPA appears not to enter the brain at all.¹¹ The fate of [^{18}F]5-fluoro-DOPA in the human brain is not known because of the lack of an efficient method to produce clinically useful quantities of [^{18}F]5-fluoro-L-DOPA. Ever since these findings, there have been numerous efforts to develop an efficient method to introduce ^{18}F into the aromatic ring of L-DOPA.

The direct fluorination of L-DOPA, using either fluorine gas or acetyl hypofluorite produced mainly 2- and 6-fluoro-L-DOPA.^{58,100,112} To date, the only method reported for the synthesis of [^{18}F]5-fluoro-DOPA is by the Balz-Schiemann reaction (see section 1.4) in which the fluorine in diazonium fluoroborate was labelled with ^{18}F by exchange with [^{18}F]HF.¹¹³ The theoretical maximum radiochemical yield is only 20% because ^{18}F is introduced into the aromatic ring by thermal decomposition of the labelled fluoroborate anion. In practice, the radiochemical yield ranged from 0.1 - 2%. Moreover, the Balz-Schiemann reaction produced a mixture of D- and L-[^{18}F]5-fluoro-DOPA, and because the enzyme L-aromatic amino acid decarboxylase is stereospecific, use of the racemic mixture would be equivalent to injection of two radiotracers, thereby doubling the radiation dose to the patient. More recently, a method has been developed to separate [^{18}F]5-fluoro-L-DOPA from the reaction mixture following the Balz-Schiemann reaction,¹¹⁴ however, these methods are not suitable for human studies. In this study, a reliable method for production of mCi quantities of [^{18}F]5-fluoro-L-DOPA by the direct

fluorination of L-DOPA with [^{18}F]F₂ is described.

3.2 Results and Discussion

3.2.1 Identification of 5-Fluoro-L-DOPA

The negative ion electrospray mass spectrum of the compound eluting at 12 min after the second HPLC separation (see section 2.4.1) gave a peak at $m/z = 214$ [M-H]⁻. The ¹H NMR spectrum of 5-fluoro-DOPA in D₂O revealed multiplets at 6.35 - 6.38 (2H, aromatic), 4.01 (1H, X part of the ABX spin system on the side-chain) and 2.91 and 2.80 ppm (AB part of the ABX spin system). The ¹⁹F NMR spectrum showed a doublet at -134.7 ppm (³J_{H6-F} = 9.0 ± 0.3 Hz).

Earlier work in our laboratory⁵⁸ showed that direct fluorination of L-DOPA in anhydrous BF₃/HF produces monofluorinated L-DOPA in 40% radiochemical yield (theoretical maximum is 50%) with respect to [^{18}F]F₂. The high electrophilic fluorination yield in anhydrous HF was explained by the fact that HF is not only resistant to oxidative attack by fluorine, but also promotes electrophilic substitution by an S_N2-type reaction mechanism.⁵⁵ The orientation for fluorination, however, results mainly in 2- and 6-fluoro-DOPA (eq. 2.1) and was surprising because the electron donating substituents at C3 and C4 are expected to direct the electrophile to C2, C5 and C6. In the present work, we have shown that changing the acidity of the reaction medium can significantly influence the orientation of fluorination in L-DOPA.

The direct fluorination of L-DOPA in TFA, formic acid or 10% TFA in glacial acetic acid changed the orientation of fluorination significantly producing mainly 2- and

5-fluoro-DOPA (Table 3.1). Radiochemical and ^1H and ^{13}C NMR spectroscopic methods were used to investigate the effect of solvents on the orientation of aromatic fluorine substitution in DOPA.

3.2.2 ^1H and ^{13}C NMR Spectroscopic Studies of Solvent Effects on the Fluorination of L-DOPA

The ^1H NMR chemical shifts of L-DOPA in various protic solvents are listed in Table 3.2. The results of the radiofluorination of L-DOPA in formic acid and 10% TFA in glacial acetic acid are very similar (Table 3.1) and therefore only 10% TFA-D in DOAc was used for NMR characterization. The basic feature of ^1H NMR spectrum of L-DOPA consisted of multiplets at 2.89 - 3.62 ppm (2H, AB part of ABX spin system on the side-chain), 4.15 - 4.70 ppm (1H, X part of ABX spin system) and at 6.54 - 7.05 ppm (3H, aromatic). The $-70\text{ }^\circ\text{C}$ ^1H NMR spectrum of L-DOPA in HF contained an additional intense signal at 8.40 ppm (HF solvent) and a quadrupole-broadened signal at 6.06 ppm (3H) corresponding to the protonated amine of the side-chain. The ^1H NMR spectrum of L-DOPA in BF_3/HF showed high-frequency shifts for all resonances relative to the resonances of L-DOPA in HF. In addition, the resonance corresponding to the carboxylic acid proton was observed at 10.07 ppm. The ^{13}C NMR chemical shifts for L-DOPA were similar in all solvents except for a significant high-frequency shift for the ^{13}C resonance of the carboxylic carbon when BF_3/HF was used as the solvent (Table 3.3).

Table 3.1 Radiochemical Yield and Orientation of Electrophilic Elemental Fluorination of L-DOPA in Acidic Solvents.

Solvent	Radiochemical Yield (%) ^a	Orientation of Fluorination		
		2-FDOPA (%)	5-FDOPA (%)	6-FDOPA (%)
BF ₃ /HF	40	35	5	60
HF	30	35	5	60
TFA	9	90	10	0
50%TFA in HOAc	5.3	56	44	0
30% TFA in HOAc	6.4	55	45	0
HCOOH	6.5	48	52	0
10% TFA in HOAc	5.5	46	54	0
10% TFA, 2% Ac ₂ O in HOAc	7.6	57	43	0
10% TFA, 20% Ac ₂ O in HOAc	5.2	50	50	0
30% TFA in Ac ₂ O	1.4	28	72	0
2.5% TFA in HOAc	1.3	51	49	0
HOAc	0	0	0	0

^aRadiochemical yield = (¹⁸F activity in FDOPA) ÷ (¹⁸F activity in the reaction vessel).

Table 3.2. ^1H NMR Chemical Shifts (ppm) of L-DOPA in Acidic Solvents.

Solvent (T, °C)	C2-H	C5-H	C6-H	-CH ₂	-CH	NH ₂	COOH
BF ₃ /HF (-70) ^a	6.82	6.86	6.74	3.12 2.89	4.46	6.43	10.07
HF (-70)	6.65	6.73	6.60	3.07 2.81	4.15	6.06	-
TFA-D (30)	7.05	7.09	6.94	3.62 3.37	4.7	-	-
10% TFA-D/DOAc (30)	6.69	6.67	6.54	3.17 3.02	4.33	-	-

^a Coupling constants (± 0.3 Hz) $^2J_{\text{AB}} = -15.1$, $^3J_{\text{AX}} = 4.8$, $^3J_{\text{BX}} = 10.6$, $^3J_{\text{H5H6}} = 8.0$.

Table 3.3. ^{13}C NMR Chemical Shifts (ppm) of L-DOPA in Acidic Solvents.

Solvent(T, °C)	$\delta^{13}\text{C}$ (ppm)								
	C-1	C-2	C-3	C-4	C-5	C-6	<u>CH</u> ₂	<u>CH</u>	<u>COOH</u>
BF ₃ /HF (-70)	128.2	119.3	139.6	140.4	118.9	126.2	34.2	55.4	183.1
HF (-70)	127.6	118.1	141.0	140.8	118.6	124.8	33.8	55.1	172.8
TFA-D (30)	127.7	119.1	145.7	145.4	119.5	125.1	36.7	57.4	174.5
10% TFA-D /DOAc (30)	127.0	118.1	146.4	145.8	117.6	123.1	36.5	56.2	173.1

When aromatic compounds containing a ring activating substituent, OR, are dissolved in a strong acid, protonation occurs at the ring carbon *para* to the OR group and not at the oxygen atom.¹¹⁵ It has been argued that ring protonation on the carbon *para* to the OR group allows delocalization of the positive charge resulting in a quinonoid structure. Olah and Mo¹¹⁶ used superacid media of varying acidities to show that the ratio of ring protonation to oxygen protonation decreased when the acidity of the medium was decreased. Protonation of both the oxygen and the ring carbon has also been observed at low temperatures when anisole is dissolved in HF saturated with BF₃.¹¹⁷ In the present study, the -70 °C ¹H and ¹³C NMR spectra of L-DOPA in BF₃/HF showed no evidence for protonation of the ring carbon or the phenolic oxygen. However, unambiguous evidence for the protonation of the carboxylic group on the side-chain was obtained from the presence of the acidic proton at 10.07 ppm in the ¹H NMR spectrum and a 10 ppm chemical shift of the carboxylic carbon to higher frequency in the ¹³C NMR spectrum. These findings confirm the absence of ring protonation and also concur with the higher radiochemical yield of fluoro-DOPA resulting from elemental fluorination of L-DOPA in BF₃/HF (Table 3.1). Aromatic ring protonation in L-DOPA would be expected to render the ring more resistant to electrophilic fluorination, and dramatically reduce the yield of fluoro-DOPA.

3.2.3 Radiochemical Yield of [¹⁸F]Fluoro-L-DOPA

Radio-HPLC traces of the reaction mixtures after the electrophilic fluorination of L-DOPA in TFA, 10% TFA in glacial acetic acid and formic acid are shown in Figure

3.1. The peaks eluting at 11 and 12 min were assigned to 2- and 5-fluoro-DOPA, respectively, by comparing the relative ^{18}F activities present in these peaks to the relative intensities of the ^{19}F NMR signals at -139.6 and -134.7 ppm. The radiochemical yields of [^{18}F]2- and 5-fluoro-DOPA were determined as the ratio of ^{18}F activity in the peaks eluting at 11 and 12 min, respectively, to the total ^{18}F activity in the reaction vessel. The determination of radiochemical yield and the characterization of [^{18}F]6-fluoro-DOPA has been described elsewhere.⁵⁸

Because only one fluorine atom in [^{18}F]F₂ is labelled with ^{18}F , the theoretical maximum radiochemical yield for electrophilic fluorination using [^{18}F]F₂ is 50%. Our results on the direct fluorination of L-DOPA (Table 3.1) clearly show that the radiochemical yield of monofluorinated product increases with increasing acidity of the reaction medium. The relatively high yield of fluoro-DOPA obtained in the low temperature (-70 °C) reactions in HF (30%) and in BF₃/HF (40%) is due to the protonation of side-chain functional groups (amine and carboxylic acid), which protects the substrate from oxidation by fluorine. The low radiochemical yield of fluoro-DOPA for reactions carried out in TFA (9%), formic acid (6.5%) and in 10% TFA in HOAc (5.5%) is also predictable because the relatively high temperatures (0 to 10 °C) used during the fluorination may promote competitive reactions either by the oxidation of unprotected hetero-atoms or by free radical initiated reactions. It should be noted that removal of any traces of water that may be present in the TFA system, by the addition of 2 - 20% acetic anhydride to the solvent, did not improve radiochemical yields significantly.

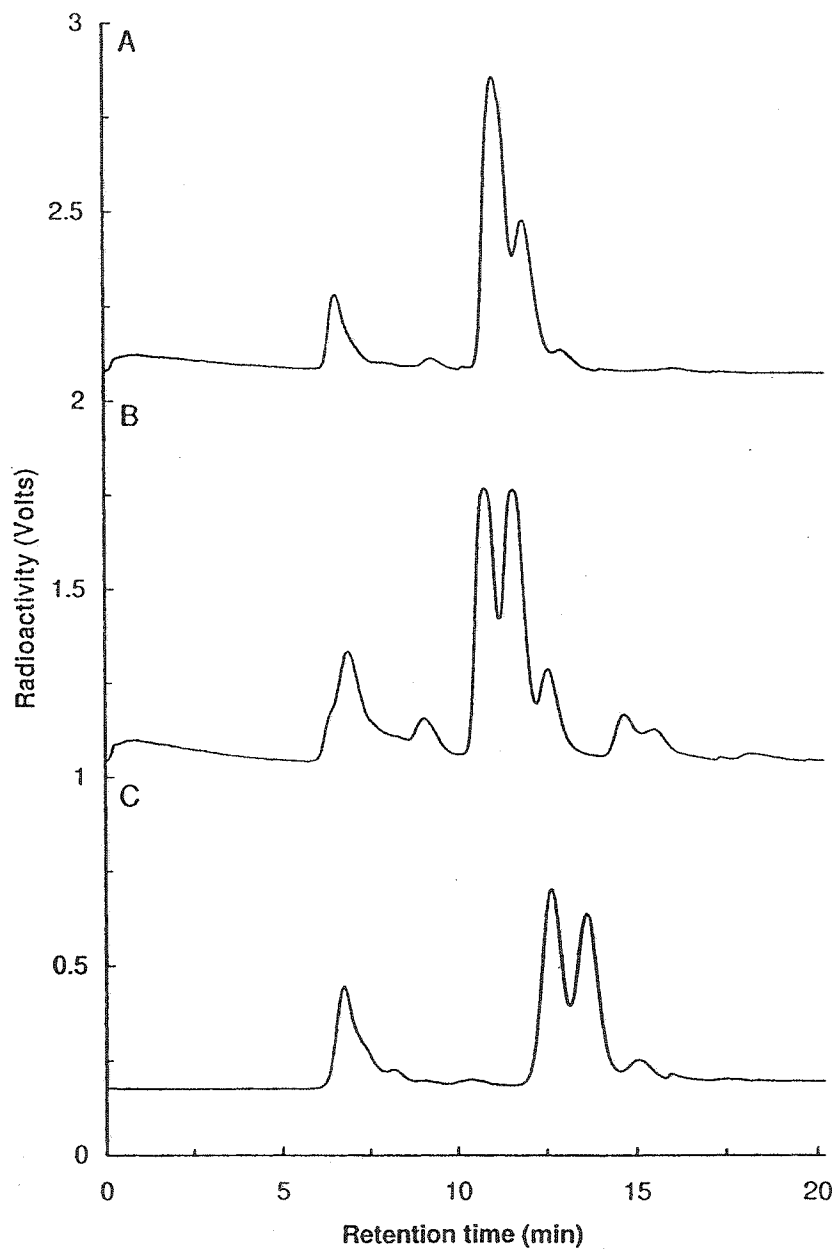


Figure 3.1. Radiochromatogram of the Reaction Mixture After the Radiofluorination of L-DOPA in (A) TFA (B) 10% TFA in CH_3COOH and (C) HCOOH .

3.2.4 Solvent Effect on the Orientation of Aromatic Fluorine Substitution in DOPA

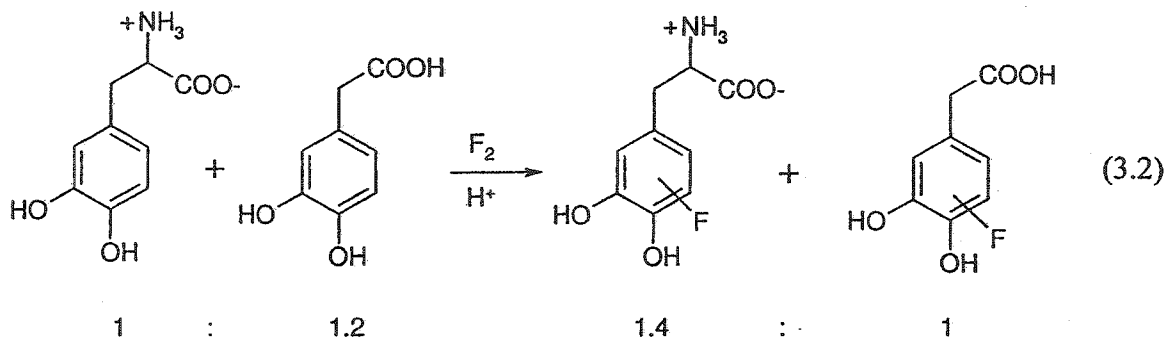
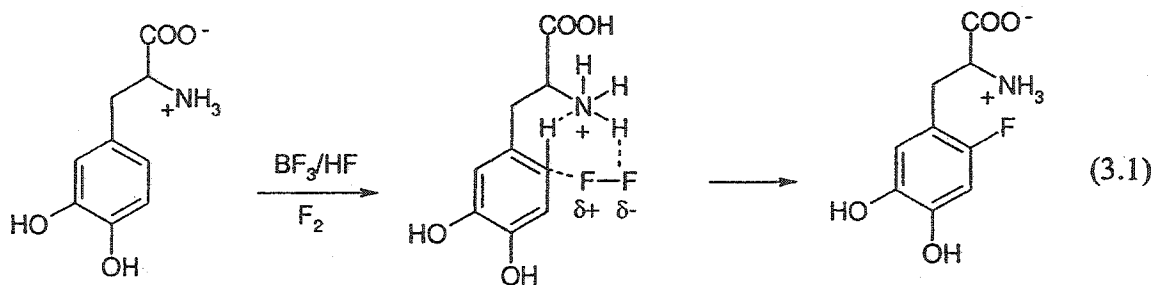
The relative amounts of 2-, 5- and 6-fluoro-DOPA formed varied considerably depending upon the solvent used (Table 3.1). When HF or BF₃/HF was used as the solvent medium, substitution was favoured at C2 (35%) and C6 (60%). When the solvent acidity was reduced and TFA was the solvent, the substitution occurred almost exclusively at C2 (90%) and further lowering of the acidity to formic acid or to 10% TFA in HOAc resulted in almost equal fluorine attack at C2 (45%) and C5 (55%).

Cacace and Wolf¹¹⁸ used dilute [¹⁸F]F₂ in neon to study the substrate selectivity and orientation of aromatic substitution by molecular fluorine. They established that fluorination of substituted benzenes and toluenes proceeded with similar selectivity and orientation as had been observed for other halogens. Since the OH group is known to be an *ortho*- and *para*- directing substituent, the ring carbons C2, C5 and C6 in L-DOPA would be the positions favoured for attack by an incoming electrophile. However, based on the observed selectivity of fluorine substitution (Table 3.1), a significant change in electron density is expected at the ring carbons when the solvent is changed from HF or BF₃/HF to TFA or 10% TFA in HOAc. Since ¹³C NMR chemical shifts are sensitive to changes in electron density at the aromatic ring carbons, significant changes in ¹³C NMR spectra of L-DOPA in different solvents may also be expected. Ding, *et al.*¹¹⁹ used a similar argument to rationalize changes in the radiochemical yields of nucleophilic aromatic substitution by ¹⁸F-fluoride with changes in electron density at the reaction center (¹³C NMR chemical shifts) for a series of structurally related electron-rich aromatic compounds. These authors reported that low-frequency shifts in ¹³C resonance at the

reaction center resulted in higher radiochemical yields for nucleophilic substitution of fluoride. In the present study, the ^{13}C NMR spectra of L-DOPA in different solvents (Table 3.3) show that C6 is the least shielded (highest frequency) ring carbon relative to C2 and C5; the latter having almost the same chemical shift. The formation of 2- and 5-fluoro-DOPA, in nearly equal amounts after the fluorination of L-DOPA in 10% TFA in HOAc, is in agreement with the ^{13}C NMR chemical shifts of C2 and C5. The complete absence of 6-fluoro-DOPA suggests preferential substitution of fluorine *ortho* to hydroxyl groups at C3 and C4. A similar preference for *ortho* substitution was reported during the fluorination of phenylalanine where the ratio of 2-fluorophenylalanine to 4-fluorophenylalanine (*ortho* to *para*) was found to be 6.5 : 1.¹¹² The near-regiospecific fluorination of DOPA in TFA produces 90% 2-fluoro-DOPA and is surprising because the OH group at C3 and C4 is expected to direct the incoming electrophile to their respective *ortho* positions, C2 and C5. Moreover, the near-identical ^{13}C NMR chemical shifts of C2 and C5 (119.1 and 119.5 ppm) suggest similar electron densities at C2 and C5, and little preference for electrophilic attack of fluorine at C2 or C5. The relatively high radiochemical yield of 6-fluoro-DOPA in HF (and similarly in BF_3/HF) is even more surprising because the ^{13}C NMR chemical shifts indicate that the lowest electron density occurs at C6 (124.8 ppm), compared to those of C2 and C5 (118.1 and 118.6 ppm). Similar to our evaluation of the use of NMR chemical shifts for the prediction of orientation of electrophilic fluorination, Kilbourn and co-workers¹²⁰ have affirmed that the correlation between ^{13}C NMR chemical shifts of an aromatic ring carbon bearing a leaving group and the yield of nucleophilic displacement with n.c.a. $^{18}\text{F}^-$ is applicable to a

number of structurally related compounds this concept cannot be generalized to aromatic rings with different leaving groups or ring substituents.

Preferential substitution of fluorine at C2 and C6 can be explained by a neighbouring group effect from the protonated amine of the side-chain which could facilitate substitution on the ring by removing the developing fluoride ion during or after the formation of the aromatic carbon-fluorine bond (equation 3.1). Further evidence for the role of protonated amine during electrophilic fluorination was obtained from the radiofluorination of an equimolar quantity of DOPA and 3,4-dihydroxy-phenylacetic acid using $[^{18}\text{F}]\text{F}_2$ (equation 3.2). In both compounds the aromatic ring is activated mainly by the OH groups and have equal numbers of favored sites for electrophilic attack. Therefore, both compounds are expected to show similar reactivities towards $[^{18}\text{F}]\text{F}_2$. Involvement of the protonated amine function during the formation of the aromatic carbon-fluorine bond is consistent with the formation of higher ratios of fluoro-DOPA to fluoro-3,4-dihydroxy-phenylacetic acid (1.4 : 1). Taylor, *et al.*¹²¹ first demonstrated the effect of the neighboring carboxylic group on electrophilic thallation and subsequently Coenen, *et al.*¹¹² have explained the results of direct fluorination of phenylalanine by a similar neighboring group effect from the side-chain.



3.2.5 Direct Fluorination Using Acetyl Hypofluorite

The synthesis of acetyl hypofluorite and its versatility as a mild fluorinating agent was first demonstrated by Rozen, *et al.*¹²² The use of [¹⁸F]CH₃COOF for the radiofluorination of various derivatives of L-DOPA to produce 2- and 6-fluoro-DOPA has been reported.^{100,112,123,124} In an effort to obtain a higher radiochemical yield of 5-fluoro-DOPA, the fluorination of L-DOPA with CH₃COOF was investigated because CH₃COOF is a milder fluorinating agent than F₂ and should result in fewer oxidative products when the reaction is carried out in aqueous acid. Results from the electrophilic fluorination of L-DOPA using acetyl hypofluorite are shown in (Table 3.4). No attempt was made to carry out the reaction in HF solvent because acetyl hypofluorite and HF

undergo fluorine exchange. Since $[^{18}\text{F}]\text{CH}_3\text{COOF}$ itself is produced from $[^{18}\text{F}]\text{F}_2$ gas, the maximum radiochemical yield of $[^{18}\text{F}]\text{CH}_3\text{COOF}$ is only 50%. Therefore, the radiochemical yield of $[^{18}\text{F}]\text{fluoro-DOPA}$ produced using $[^{18}\text{F}]\text{CH}_3\text{COOF}$ (Table 3.4) is only 50% of the radiochemical yield using $[^{18}\text{F}]\text{F}_2$ (Table 3.1). The fluorination of L-DOPA using $[^{18}\text{F}]\text{CH}_3\text{COOF}$ was not pursued in detail because of the low radiochemical yield and poor fluorination selectivity.

Table 3.4. Radiochemical Yield and Isomeric Distribution of Fluoro-DOPA After the Fluorination of L-DOPA Using Acetyl Hypofluorite.

Solvent	Radiochemical Yield (%) ^a	Orientation of Fluorination		
		[¹⁸ F]FDOPA	2-FDOPA	5-FDOPA
TFA	7.0	75	25	0
10% TFA in HOAc	4.5	80	20	0
HOAc	0	0	0	0

^aRadiochemical yield = (amount of ¹⁸F in FDOPA) ÷ (amount of ¹⁸F in the reaction vessel).

3.3 Conclusion

The aim of the present work has been to develop a fast and efficient method to produce clinically useful quantities of [^{18}F]5-fluoro-L-DOPA. To that end we have shown that direct fluorination of L-DOPA in glacial acetic acid containing 10% TFA or formic acid are suitable methods. Starting with 350 mCi of [^{18}F]F₂, 5 ± 0.5 mCi of [^{18}F]5-fluoro-L-DOPA has been produced after 65 min of synthesis time. Based on the simplicity and reproducibility of the method, this is the most efficient method available at this time to produce clinically useful quantities of [^{18}F]5-fluoro-L-DOPA. We have also shown that the ^{13}C NMR chemical shifts of the aromatic ring carbons are not necessarily a reliable probe for predicting the orientation of electrophilic substitution when CH₃COOF and F₂ are used as fluorinating agents.

CHAPTER 4

THE EFFECT OF AROMATIC FLUORINE SUBSTITUTION IN L-DOPA ON THE *IN VIVO* BEHAVIOUR OF [¹⁸F]2-, [¹⁸F]5- AND [¹⁸F]6-FLUORO-L-DOPA IN THE HUMAN BRAIN

4.1 Introduction

It is known that the clinical features of Parkinson's disease, muscular rigidity, bradykinesia and rest tremor, are associated with marked deficiencies of striatal dopamine.¹⁰ These observations, corroborated many times by means of autopsy examinations,¹²⁵ have led to the use of L-DOPA, the metabolic precursor of dopamine, to alleviate the symptoms of Parkinson's disease.¹²⁶ A proposal that ¹⁸F-labelled DOPA might be a specific tracer for intracerebral dopamine inspired the synthesis of [¹⁸F]5-fluoro-DL-DOPA.¹¹³ Following an intravenous injection of [¹⁸F]5-fluoro-DL-DOPA in a monkey, Garnett and co-workers¹¹⁰ used simple γ -ray detectors to monitor ¹⁸F-activity. These authors used a three-compartment explanatory model to derive fractional rate constants for the forward and backward transport of L-DOPA across the blood-brain barrier, and for the formation and degradation of neuronal dopamine. It was concluded

that this technique could be extended to man and used to investigate the role of DOPA and dopamine in the control of mood and locomotion.¹¹⁰ The lack of an efficient synthesis of [¹⁸F]5-fluoro-L-DOPA had prevented it from being studied in the human brain.

Subsequently, Garnett and co-workers¹¹ pioneered the use of [¹⁸F]6-fluoro-L-DOPA, in conjunction with PET, to visualize the regional distribution of intracerebral dopamine in the living human brain. Fluorine-18 labelled 6-fluoro-L-DOPA was further used to show that the accumulation of ¹⁸F was reduced in the contralateral putamen of patients suffering from hemiparkinsonism.¹² These findings were the first demonstration of a disturbance of intrastriatal dopamine metabolism in patients suffering from Parkinson's disease. Although the *in vivo* metabolism of [¹⁸F]6-fluoro-L-DOPA in the human brain is known,^{127,128} the metabolic fate of 2- and 5-fluoro-DOPA in the human brain has not been reported.

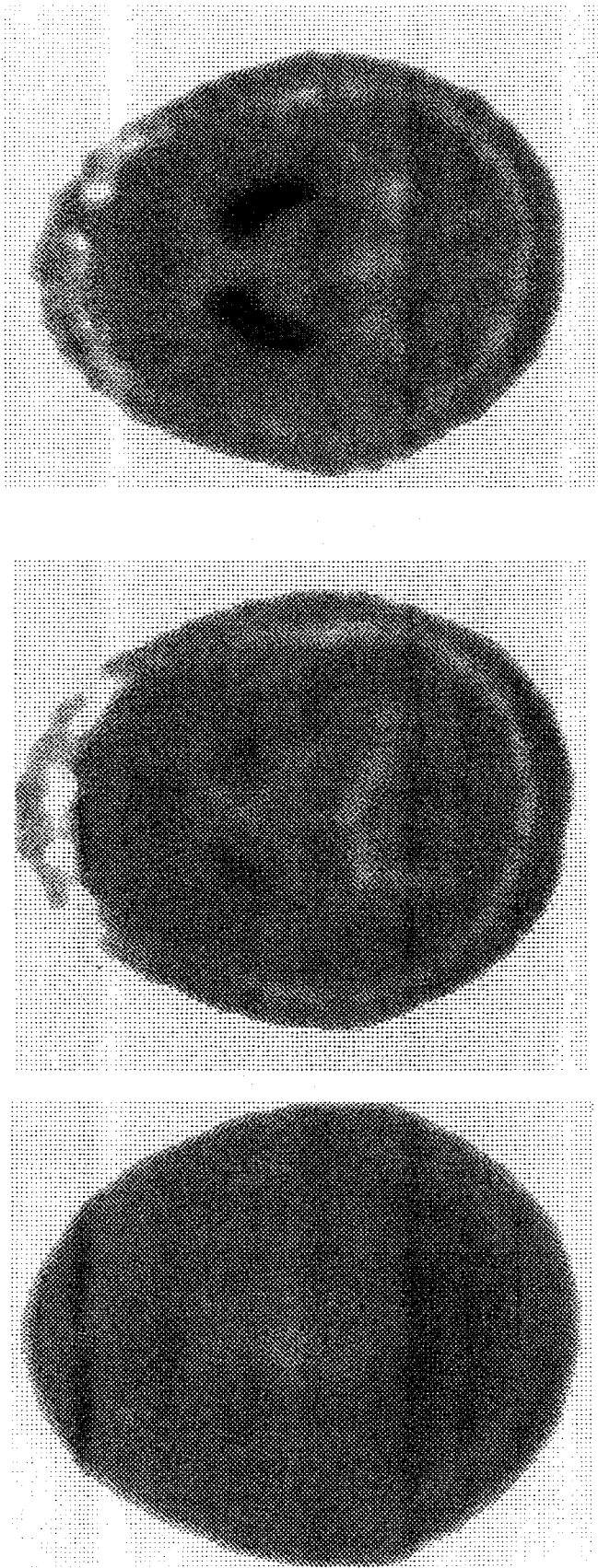
The fate of [¹⁸F]5-fluoro-DOPA in the human brain is not known because low yielding Balz-Schiemann reactions were the only methods described for its synthesis.^{114,113} The present chapter reports a comparative study of the time course and distribution of radioactivity in the human brain after [¹⁸F]2-, [¹⁸F]5- and [¹⁸F]6-fluoro-L-DOPA have been injected.

4.2 Results and Discussion

The distributions of [¹⁸F]2-, [¹⁸F]5- and [¹⁸F]6-fluoro-L-DOPA in a transaxial plane at the level of the striata in Subject 1 from 60 to 120 minutes after injection are

shown in Figure 4.1. There is large accumulation of [^{18}F]6-fluoro-dopamine in the striata, whereas, there is a very small accumulation of radioactivity in the grey matter and basal ganglia following injection of [^{18}F]2- and [^{18}F]5-fluoro-L-DOPA. The time courses of [^{18}F]2-, [^{18}F]5- and [^{18}F]6-fluoro-L-DOPA for Subject 1 are shown in Figure 4.2. The striatal influx constant (K_i), using a cerebellar input function, was determined to be $0.0027 \pm 0.0026 \text{ min}^{-1}$ for [^{18}F]2-fluoro-L-DOPA, $0.0035 \pm 0.0019 \text{ min}^{-1}$ for [^{18}F]5-fluoro-L-DOPA and $0.0106 \pm 0.0019 \text{ min}^{-1}$ for [^{18}F]6-fluoro-L-DOPA (note the large uncertainty on the K_i value for [^{18}F]2-fluoro-L-DOPA). The very low uptake, if any, of [^{18}F]2-fluoro-dopamine in the brain confirms a previous report that cerebral dopaminergic structures do not accumulate ^{18}F following injection of [^{18}F]2-fluoro-L-DOPA.¹²⁹ The distribution and K_i values obtained with [^{18}F]5-fluoro-L-DOPA ($0.0030 \pm 0.0007 \text{ min}^{-1}$) and [^{18}F]6-fluoro-L-DOPA ($0.0090 \pm 0.0005 \text{ min}^{-1}$) for Subject 2 were similar to those for Subject 1.

There are marked differences in the distribution and kinetics of the three ring fluorinated isomers of L-DOPA. For example, [^{18}F]2-fluoro-L-DOPA does not appear to cross the blood brain barrier. In contrast, [^{18}F]5-fluoro-L-DOPA appears to be taken up and cleared from both the cerebellum and striatum as indicated by the shape of the time-activity curves. Fluorine-18 labelled 6-fluoro-L-DOPA clearly enters the brain and shows that ^{18}F preferentially accumulated in the striata. The *fluorine effect* (see section 1.1) seen in our study is similar to that seen in a previous study,¹³⁰ which showed that the substitution of fluorine for hydrogen at positions 2, 5 or 6 on the aromatic ring of



[¹⁸F]2-fluoro-L-DOPA

[¹⁸F]5-fluoro-L-DOPA

[¹⁸F]6-fluoro-L-DOPA

Figure 4.1. Distribution of [¹⁸F]2- (left), [¹⁸F]5- (middle) and [¹⁸F]6- (right) fluoro-L-DOPA in Subject 1, 60 to 120 minutes after intravenous injection of the tracer. The transaxial section, at the level of the basal ganglia, is at the same level in all three studies. The images have been normalized to each other. Note the intense retention of radioactivity in the striata (darkest regions) following administration of [¹⁸F]6-fluoro-L-DOPA

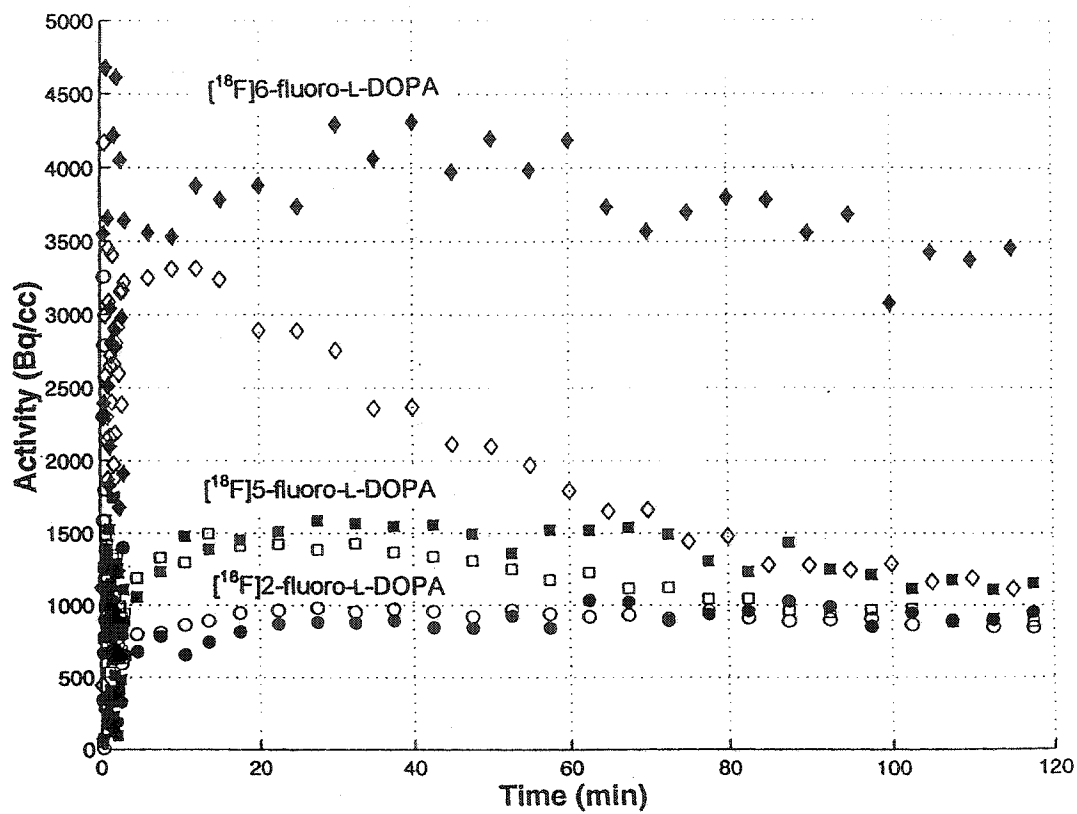


Figure 4.2. Time course of radioactivity in the striata (solid symbols) and the cerebellum (open symbols) after an intravenous injection of [^{18}F]2- (circles), [^{18}F]5- (squares), and [^{18}F]6- (diamonds) fluoro-L-DOPA.

norepinephrine (NE) dramatically alters the specificity of these analogues to their respective receptors. The 2-fluoro-isomer of NE is a β -adrenergic agonist with little α -activity, 6-fluoro-NE is an α -agonist with little β -agonist activity, whereas, 5-fluoro-NE displays both α - and β -adrenergic activity comparable to endogenous NE.

The distribution of [^{18}F]2- and [^{18}F]6-fluoro-L-DOPA has been studied in the carbidopa-pretreated male hooded rat.¹³¹ These authors showed that [^{18}F]2-fluoro-L-DOPA is not decarboxylated by the enzyme aromatic amino acid decarboxylase (AADC) in the rat striatum and is rapidly *O*-methylated by the enzyme catechol-*O*-methyltransferase (COMT). Although this study compared the metabolism of [^{18}F]2- and [^{18}F]6-fluoro-L-DOPA, these authors did not evaluate the metabolic fate of the 5-fluoro isomer of L-DOPA. Several studies involving 5-fluoro-DOPA have been conducted using racemic mixtures of DL-DOPA, both *in vitro*^{132,133,134} and *in vivo*.^{135,136,110} Oldendorf¹³⁷ has shown that D-DOPA does not cross the blood brain barrier and in our laboratory, we did not observe uptake of ^{18}F in the striatum when a normal subject was injected with [^{18}F]6-fluoro-D-DOPA.¹³⁸ Therefore, evaluations of previous studies using 2-fluoro-DL-DOPA and 5-fluoro-DL-DOPA are further complicated by the presence of D-enantiomers. Only three studies, all of which have been *in vitro* metabolic studies,^{139,140,141} have been reported evaluating [^{18}F]5-fluoro-L-DOPA. Wiese and co-workers^{134,140} have shown that 5- and 6-fluoro-DOPA enantiomers reproducibly undergo *O*-methylation and that COMT inhibitors may prove to be effective for PET application with 5- and 6-fluoro-L-DOPA.¹⁴¹ Although these authors compared the metabolism of 5- and 6-fluoro-L-

DOPA, the metabolism of the 2-fluoro isomer of L-DOPA was not considered in their studies.

Cross-species determinations of enzymatic activities in [^{18}F]6-fluoro-L-DOPA-PET studies are often equivocal because *in vitro* determinations obtained from animal models and humans are substantially different.^{128,142} Furthermore, a study comparing the 5- and 6-fluoro isomers of DOPA also stated that cerebral metabolism cannot be exclusively elucidated by *in vitro* enzyme assays.¹⁴⁰ Several factors are involved in human *in vivo* studies that play a major role in understanding the biological imaging of the dopaminergic pathway using [^{18}F]fluoro-L-DOPA.^{128,143} In addition to transport across the blood-brain barrier, the central availability of fluoro-L-DOPA is affected by peripheral metabolism. The enzymatic reaction rates are dependent upon the availability of the substrate and their affinities for AADC and COMT. The accumulation of fluorodopamine in the striata is further dependent upon its ability to be stored in vesicles within the nigrostriatal neurons, and its later release along with endogenous dopamine.¹⁴⁴

Compared with L-DOPA, 2-fluoro-DOPA has a higher affinity for COMT¹³³ and a substantially lower affinity for AADC.¹³¹ This suggests that 2-fluoro-L-DOPA is rapidly *O*-methylated (at position 3) in the periphery, thereby depleting the supply of 2-fluoro-L-DOPA to the brain. If present in the brain, [^{18}F]2-fluoro-L-DOPA would be further *O*-methylated, leaving even smaller amounts available for enzymatic decarboxylation to [^{18}F]2-fluoro-dopamine. To our knowledge, no investigation has been carried out to determine if 2-fluoro-dopamine can be stored within the vesicles of the dopaminergic neurons. Alternatively, the very low uptake of [^{18}F]2-fluoro-L-DOPA in the brain could

also be attributed to its relatively poor transport across the blood-brain barrier.¹³¹

In contrast with 2-fluoro-DOPA, it has been shown that 5-fluoro-DOPA is comparable with L-DOPA as a substrate for AADC,¹³² and 5-fluoro-L-DOPA crosses the blood-brain barrier to an extent that is similar to that of L-DOPA.¹¹⁰ Interestingly, no evidence for substantial retention of 5-fluoro-dopamine in the striatum was obtained in our study. The affinity of 5-fluoro-DOPA for COMT was determined to be higher than L-DOPA and comparable with that of 2-fluoro-DOPA.¹³³ The increased phenolic ionization produced by fluorine at the 5-position on the aromatic ring of DOPA which, similar to 2-fluoro-DOPA, is situated *ortho* to an activating hydroxyl group, likely promotes the formation of 4-*O*-methylated derivative.¹³⁹ The influence of fluorine substitution on the site of enzymatic *O*-methylation when fluorine is situated *ortho* to one of the phenolic groups has also been noted for norepinephrine.¹⁴⁵ The relatively high affinity of COMT towards [¹⁸F]2- and [¹⁸F]5-fluoro-L-DOPA compared with L-DOPA and [¹⁸F]6-fluoro-L-DOPA¹⁴⁶ compromises their utility as PET tracers. The use of a COMT inhibitor may reveal specific uptake of [¹⁸F]5-fluoro-dopamine in the striata, because 5-fluoro-DOPA was shown to have an affinity towards AADC comparable with that of L-DOPA.¹³²

The role of COMT cannot be solely responsible for the *fluorine effect* when tracing *in vivo* dopaminergic function with ring fluorinated isomers of L-DOPA. For example, DeJesus and Mukherjee¹⁴⁷ have proposed ¹⁸F-labelled derivatives of L-*meta*-tyrosine (*FmT*) as useful tracers for the study of intracerebral dopamine metabolism. Because the peripheral metabolism of *FmT* is simpler than that of [¹⁸F]6-fluoro-L-DOPA,

[¹⁸F]6-*FmT* has been proposed as a superior agent with which to study intracerebral metabolism in health and disease in humans.¹⁴⁸ Unlike [¹⁸F]6-fluoro-DOPA, *FmT* are not substrates for COMT since they lack the necessary enediol moiety,¹⁴⁹ but are substrates for AADC.¹⁵⁰ It has since been shown that the site of ring fluorination on *L-meta*-tyrosine alters its biological properties, i.e., [¹⁸F]6-*FmT* is superior for the assessment of dopamine metabolism in the brain using PET, when compared with [¹⁸F]2-*FmT*¹⁵¹ and [¹⁸F]4-*FmT*.¹⁵²

4.3 Concluding Remarks

In the present study, the time course and distribution of [¹⁸F]2-, [¹⁸F]5- and [¹⁸F]6-fluoro-L-DOPA in the human brain are presented. Only [¹⁸F]6-fluoro-dopamine shows specific accumulation in the striata, making [¹⁸F]6-fluoro-L-DOPA the only useful ring-fluorinated isomer of L-DOPA for the study of the dopaminergic pathway. This study illustrates the importance of isomeric and radiochemical purities in radiopharmaceutical design.

CHAPTER 5

SELECTIVITY OF ELEMENTAL FLUORINE TOWARDS L-TYROSINE AND L- α -METHYLTYROSINE IN ACIDIC MEDIA AND THE SYNTHESSES OF THEIR [^{18}F]3-FLUORO AND [^{18}F]3,5-DIFLUORO DERIVATIVES

5.1 Introduction

Fluorine-18 labelled 2-fluoro-2-deoxy-D-glucose (FDG) has become the standard imaging agent against which other imaging agents for tumour detection by means of PET are compared. Inoue and co-workers¹⁵³ have shown that [^{18}F]3-fluoro-L- α -methyltyrosine (3-F- α -MT) has higher tumour-to-normal cortex counts and higher tumour-to-white matter cortex counts than FDG in patients with brain tumours. The same group has further revealed that the uptake of FDG was significantly lower than that of 3-F- α -MT in experimental breast tumour models.^{154,155} The syntheses of [^{18}F]2- and 3-F- α -MT have been reported by fluorination of L- α -methyltyrosine (L- α -MT) in TFA using [^{18}F]AcOF.¹⁵⁶ The radiochemical yield for [^{18}F]2- and 3-F- α -MT (1 : 5.7), with respect to [^{18}F]AcOF, was $20.3 \pm 5.1\%$.¹⁵⁶ Since [^{18}F]AcOF is produced from [^{18}F]F₂, the

radiochemical yield of the fluoro isomers can only be $10.2 \pm 2.6\%$ with respect to $[^{18}\text{F}]\text{F}_2$. Several reports^{153,154,157,158} have affirmed the need for a more efficient synthetic protocol in order for 3-F- α -MT to be shared by other medical institutions. In this paper, we describe an efficient synthesis of 3-F- α -MT by direct fluorination of L- α -MT with $[^{18}\text{F}]\text{F}_2$ in anhydrous HF (eq. 2.2).

A second issue addressed in the present chapter involves the syntheses and characterization of $[^{18}\text{F}]$ 3,5-difluoro derivatives of tyrosine and L- α -MT. Kirk¹⁵⁹ has synthesized “cold” 3-fluoro-L-tyrosine and 3,5-difluoro-L-tyrosine, however, these multi-step syntheses are too time consuming to be of use for ^{18}F -labelling studies. In the present study the syntheses of $[^{18}\text{F}]$ 3,5-difluoro derivatives L-tyrosine and L- α -MT by direct fluorination are also reported for the first time (eq. 2.3).

5.2 Results and Discussion

5.2.1 Identification of 3-F- α -MT

Preparative HPLC analysis of the reaction mixture obtained after the direct fluorination of L- α -MT with $[^{18}\text{F}]\text{F}_2$ in HF (eq. 2.2) revealed a strong UV peak at 17 min and a weak peak at 20 min. A comparison of the retention time, as well as spiking the reaction mixture with authentic L- α -MT, enabled us to assign the earlier peak to L- α -MT. The fraction eluting at 20 min contained 81% of the total radioactivity found in the reaction mixture. The positive electrospray mass spectrum of the compound eluting at 20 min from the reaction mixture (eq. 2.2) showed a protonated molecular ion at $m/z = 214$ $[\text{M} + \text{H}]^+$. The ^1H NMR spectrum of the sample revealed one less proton in the aromatic

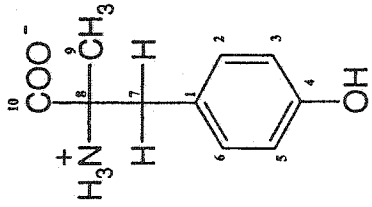
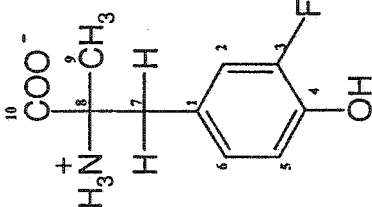
region when compared with the ^1H spectrum of L- α -MT (Table 5.1). The ^{19}F NMR spectrum consisted of a doublet of doublets at -136.8 ppm, consistent with the ^{19}F NMR spectrum of 3-F- α -MT reported in the literature.¹⁵⁶ A multiplet similar to that in the ^{19}F NMR spectrum of 2-fluoro-L-tyrosine⁵⁶ was observed at -114.8 ppm (<4% by integration) when HF or BF_3/HF was the solvent. The ^{13}C NMR chemical shifts of 3-F- α -MT (Table 5.1) agreed with the values predicted using empirically derived substituent parameters for fluorine.¹⁰²

Analytical HPLC analysis of the reaction mixture (eq. 2.2) is shown in Figure 2.4 where it can be seen that L- α -MT eluted at 9 min (UV) and 3-F- α -MT eluted at 12 (UV) and 12.5 min (radioactivity). The reaction mixture from equation (2.3) showed these peaks as well as two additional radioactive peaks eluting at 3.5 and 13.5 min when formic acid, TFA or BF_3/HF were the solvents.

5.2.2 Identification of 3,5-Difluoro Isomers

Figure 2.5 shows the analytical HPLC chromatograms of the reaction mixture (eq. 2.3), where 0.13 M BF_3/HF was the solvent. The peak eluting at 13.5 min during the analytical HPLC analysis (25 min during the preparative HPLC separation) was identified as [^{18}F]3,5-difluoro-L- α -methyltyrosine. The positive ion electrospray mass spectrum of this peak gave a protonated molecular ion at $m/z = 232$ $[\text{M}+\text{H}]^+$. The ^{19}F NMR spectrum could be analyzed as an AA'XX' spin system centered at -132.2 ppm. The coupling

Table 5.1. ^1H and ^{13}C NMR Parameters for L- α -MT and 3-F- α -MT.

Compound	^1H chemical shift, ppm	Coupling Constant, Hz	^{13}C Chemical shift ^b , ppm
 L- α -MT	H9		C-1
	1.06		124.6
	H7 _A		C-2
	2.46		132.2
	H7 _B		C-3
	2.69	$^2J(\text{H7}_A-\text{H7}_B), -14.6$	C-4
	H3 and H5		C-5
	6.30	$^3J(\text{H2}-\text{H3}), 8.3$	C-6
	H2 and H6		C-7
	6.55	$^3J(\text{H5}-\text{H6}), 8.3$	C-8
		C-9	
		C-10	
		173.2	
 3-F- α -MT ^a	H9		C-1
	1.43		126.1
	H7 _A		C-2
	2.84		117.8
	H7 _B		C-3
	3.11	$^2J(\text{H7}_A-\text{H7}_B), -14.6$	C-4
	H6		C-5
	6.76	$^4J(\text{H2}-\text{H6}), 2.0; ^5J(\text{H6}-\text{F}), 0.8$	C-6
	H5		C-7
	6.83	$^3J(\text{H5}-\text{H6}), 8.7; ^4J(\text{H5}-\text{F}), 8.7$	C-8
H2		C-9	
6.87	$^3J(\text{H2}-\text{F}), 12.0$	C-10	
		174.3	
		126.2	
		119.2	
		150.5	
		142.1	
		117.3	
		127.8	

^aThe ^{19}F chemical shift is -136.8 ppm (with respect to external CFCl_3 at 30°C).

^bCalculated values using fluorine substituent parameters are shown in parentheses.

constants obtained from spectral fitting¹⁶⁰ were ${}^3J_{\text{HF}} = 1.2$ Hz; ${}^5J_{\text{HF}} = -2.9$ Hz; ${}^4J_{\text{HH}} = 11.4$ Hz; ${}^4J_{\text{FF}} = 11.5$ Hz. These couplings were confirmed by use of ${}^{19}\text{F}$ NMR spectral simulation (Figure 5.1).¹⁶¹ The ${}^1\text{H}$ NMR spectrum revealed the methyl proton at 1.54 ppm, an AB spin pattern centered at 3.08 ppm (2H on side-chain, ${}^2J_{\text{HH}} = -14.6$ Hz), and an AA'XX' spin pattern centered at 6.81 ppm (2H, aromatic) which corresponded to that observed in the ${}^{19}\text{F}$ NMR spectrum.

The coupling between the two fluorines and the two protons on the aromatic ring of L- α -MT was confirmed by acquiring the ${}^{19}\text{F}$ $\{{}^1\text{H}; 6.81$ ppm $\}$ NMR spectrum and ${}^1\text{H}$ $\{{}^{19}\text{F}; -132.2$ ppm $\}$ NMR spectrum. The AA'XX' spin systems were decoupled to a singlet in both the ${}^1\text{H}$ and ${}^{19}\text{F}$ spectra (Figure 5.2). In order to verify that the AA'XX' spin system arises from the 3,5-difluoro isomer and not from the 2,6-difluoro isomer, the ${}^1\text{H}$ NMR spectrum of difluorinated L- α -MT was studied by 2-dimensional rotating frame Overhauser enhancement spectroscopy (ROESY). The ROESY spectrum showed cross-peaks between the methylene protons on the side-chain and the protons at the 2- and 6-positions of the aromatic ring (Fig. 5.3). The concentration of the sample was too low for characterization by ${}^{13}\text{C}$ NMR spectroscopy.

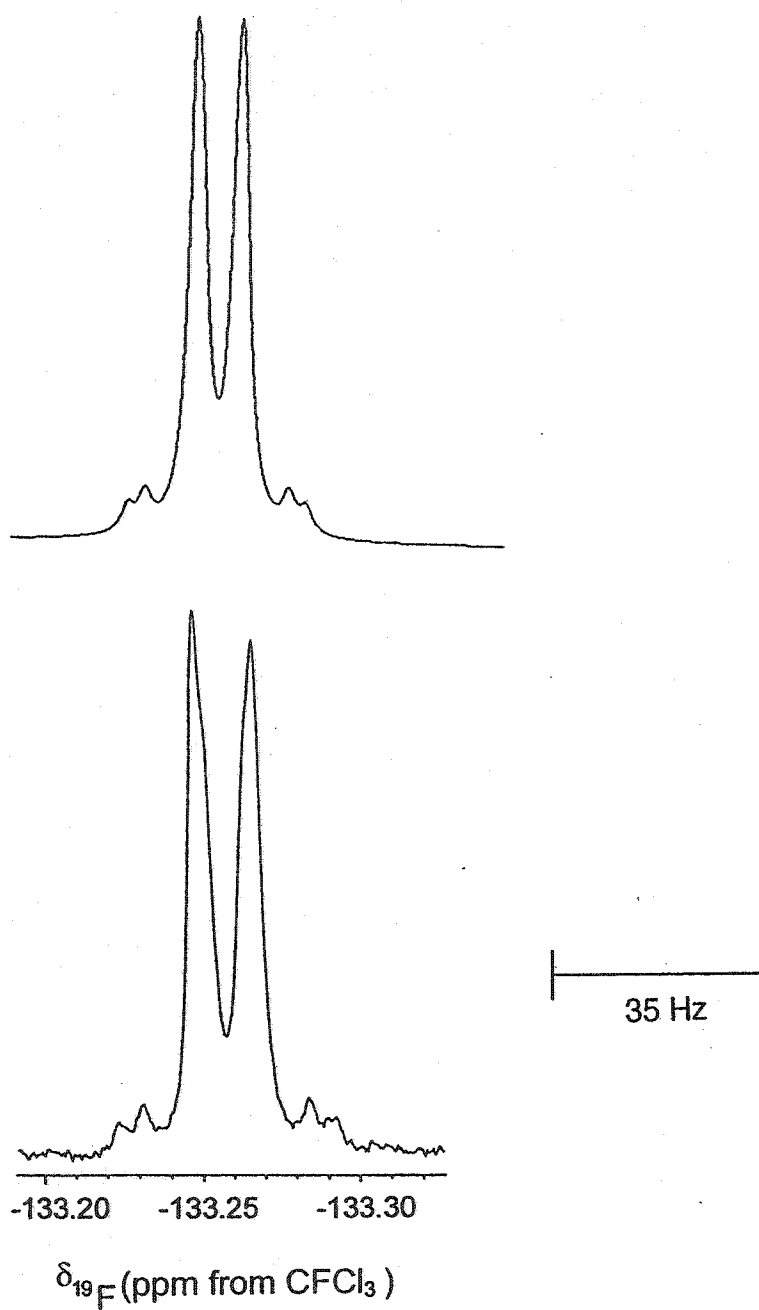


Figure 5.1 Experimental (bottom) and simulated (top) ^{19}F NMR spectrum of 3,5-difluoro-L- α -MT.

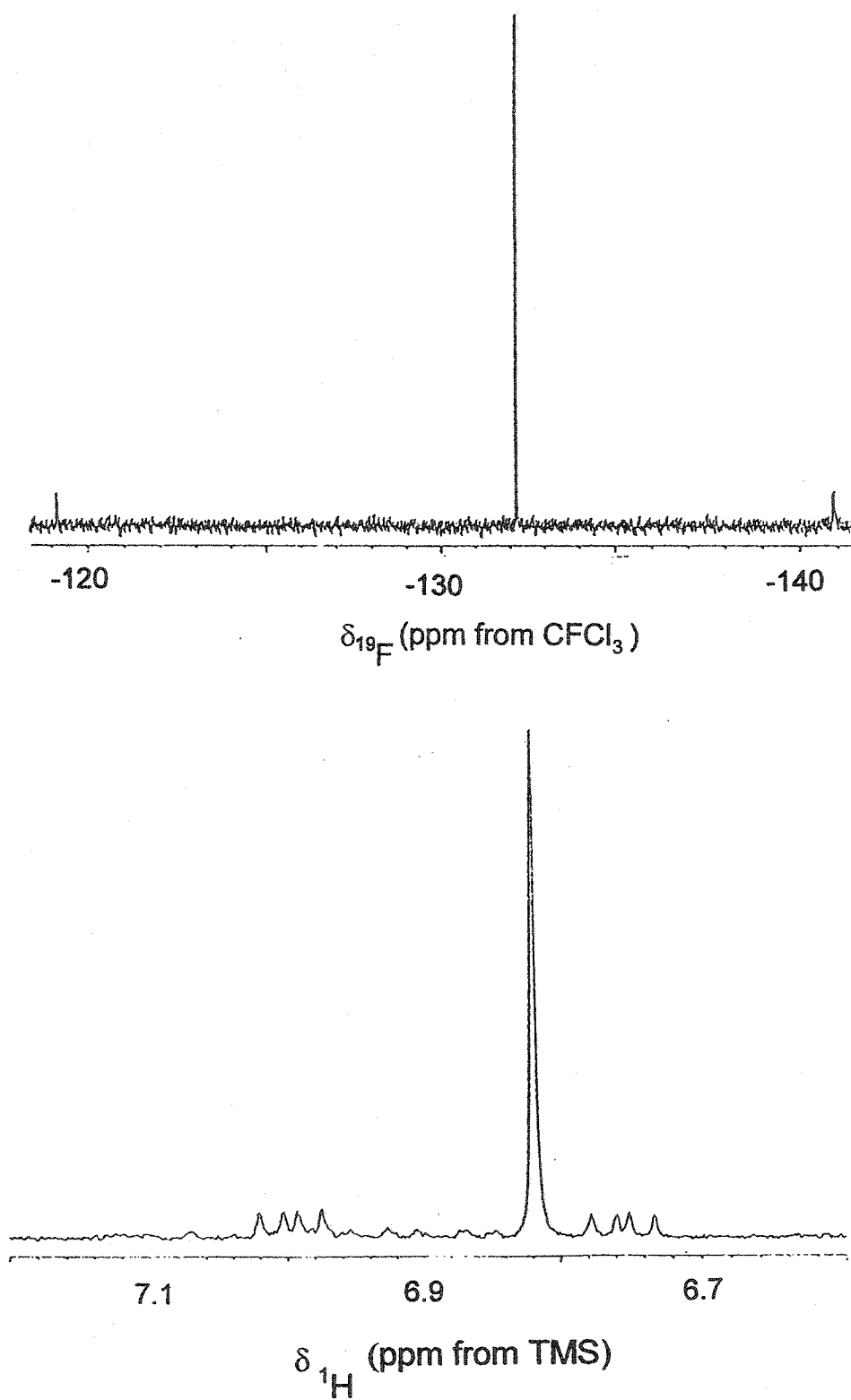


Figure 5.2. ^{19}F $\{^1\text{H}; 6.81 \text{ ppm}\}$ NMR spectrum (top) and ^1H $\{^{19}\text{F}; -132.2 \text{ ppm}\}$ NMR spectrum (bottom) of $[^{18}\text{F}]3,5\text{-difluoro-L-}\alpha\text{-methyltyrosine}$.

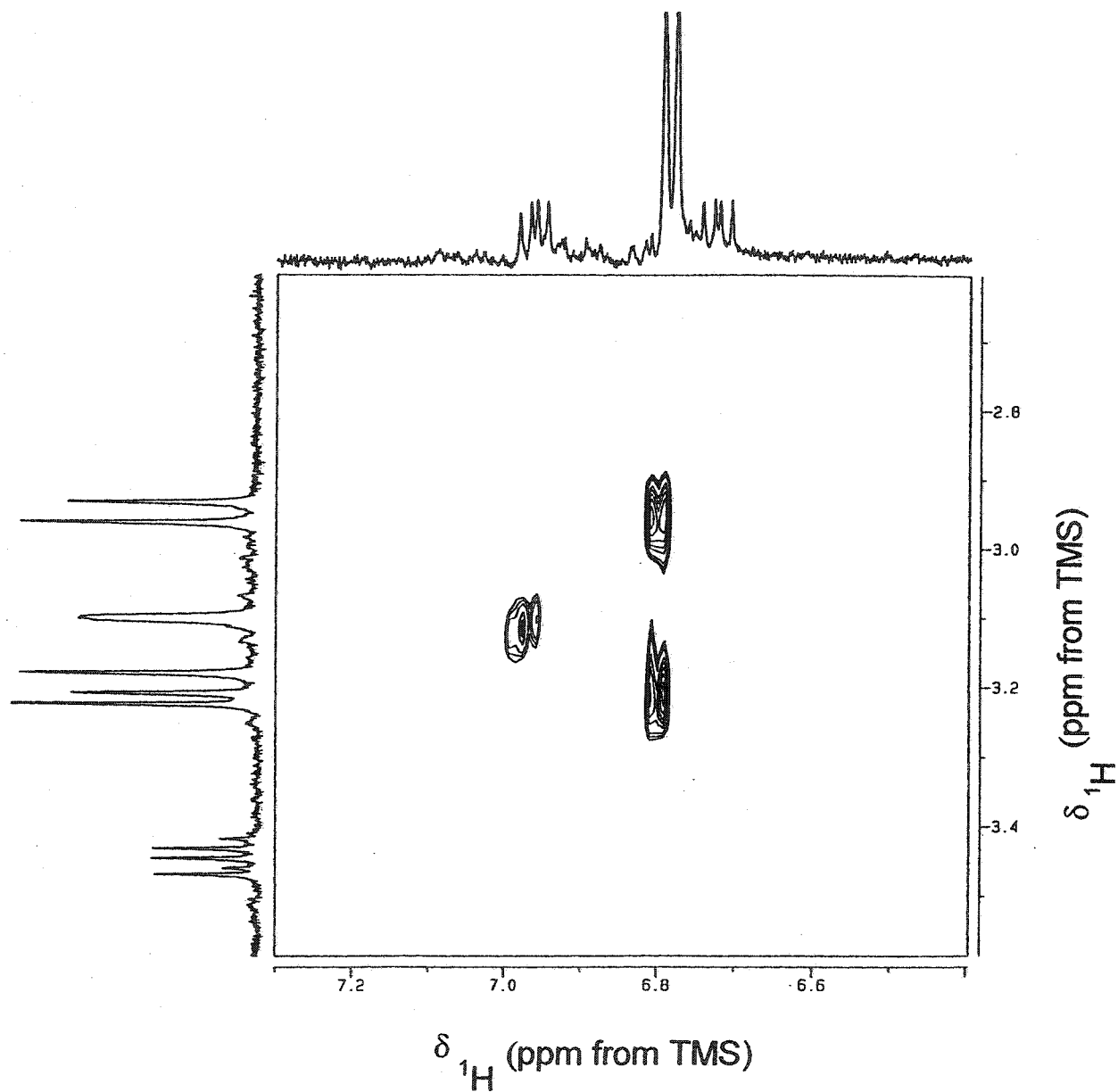
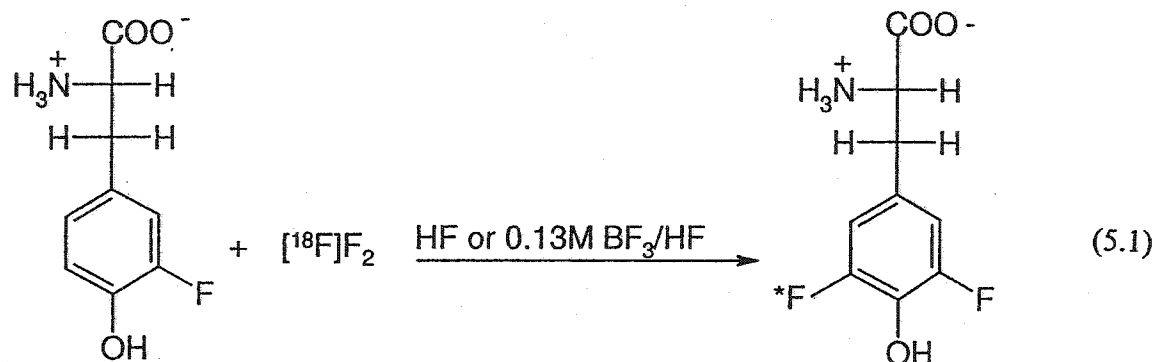


Figure 5.3. A 2-D ROESY NMR spectrum showing through space correlations between the aromatic and side-chain protons of 3,5-difluoro-L- α -MT, in an unpurified mixture.

Fluorine-18 labelled 3,5-difluoro-tyrosine was synthesized by direct fluorination of L-tyrosine in acidic media and by direct fluorination of 3-fluoro-DL-tyrosine in HF or 0.13 M BF_3/HF (eq. 5.1). The 3,5-difluoro-tyrosine had a ^{19}F NMR chemical shift of -132.2 ppm ($^3J_{\text{HF}} = 1.9$ Hz; $^5J_{\text{HF}} = -2.4$ Hz; $^4J_{\text{HH}} = 11.3$ Hz; $^4J_{\text{FF}} = 11.4$ Hz) and showed a protonated molecular ion at $m/z = 218$ $[\text{M}+\text{H}]^+$ in the positive ion electrospray mass spectrum.



5.2.3 Proton and ^{13}C NMR Spectra of L- α -MT in Various Solvents

Table 5.2 describes the ^1H and ^{13}C NMR spectra of L- α -MT in various solvents. The ^1H NMR spectrum of L- α -MT in HF at -70 °C consisted of an AA'BB' spin pattern at 6.79 ppm (2H, aromatic) and 6.62 ppm (2H, aromatic), a broad singlet ($\Delta\nu_{1/2}$, 30 Hz) at 6.04 ppm (NH_3^+), an AB spin pattern at 3.06 and 2.77 ppm (2H, CH_2), and a singlet at 1.40 ppm (3H, CH_3). Two additional signals were observed in the ^1H NMR spectrum of L- α -MT in BF_3/HF that were not observed when HF solvent was used: a sharp singlet at

10.09 ppm (carboxylic acid proton) and a broad singlet ($\Delta\nu_{1/2}$, 78 Hz) at 12.93 ppm (protonated hydroxyl group). All other signals followed a similar trend, except that they were shifted to higher frequencies relative to those in HF solvent. It is also noteworthy that the proton chemical shifts of L- α -MT in strong acids (HF and BF₃/HF) differ from those acquired in D₂O/DCl, where lower frequency shifts were observed for the aromatic protons, and there was no evidence for the protonated hydroxyl group, the carboxylic acid proton or the protonated amine group. The ¹³C NMR spectrum of L- α -MT in BF₃/HF was similar to that of L- α -MT in HF and in D₂O/DCl except that the carboxylic acid carbon in BF₃/HF was shifted to higher frequency and the aromatic carbon at C4 was shifted to lower frequency.

5.2.4 Influence of Solvent Acidity on Radiochemical Yield of Fluoro-tyrosine

Derivatives

During the direct fluorination of L-tyrosine or L- α -MT, the radiochemical yield (with respect to [¹⁸F]F₂) increased with increasing solvent acidity (Table 5.3), i.e., the yield of 3-F- α -MT ranged from 15% (HCOOH) to 28% (TFA) to 30% (HF). In an attempt to further improve the radiochemical yields of the 3-fluoro isomers, the acidity of the solvent was increased using BF₃/HF mixtures. However, in all experiments employing BF₃/HF, the radiochemical yields of 3-F- α -MT decreased (15 – 26%) and significant quantities of the 3,5-difluoro isomers were produced.

Table 5.2. ^{13}C and ^1H (in parentheses) NMR Chemical Shifts for L- α -Methyltyrosine in Various Solvents.

Solvent (T, °C)	COOH	C α	CH ₃	CH ₂	C-1	C-2/C-6	C-3/C-5	C-4
		(NH ₃ ⁺)						(OH ₂ ⁺)
BF ₃ /HF (-70)	187.1 (10.09)	62.0 (6.53)	19.0 (1.48)	39.7 (3.15)	129.6	132.9 (7.11)	117.3 (7.03)	146.7 (12.93)
HF (-70)	175.2	62.6 (6.04)	19.9 (1.40)	40.4 (2.92)	125.0	130.7 (6.79)	115.6 (6.62)	151.9
D ₂ O/DCI (+30)	173.2	60.7	21.3 (1.06)	41.3 (2.48)	124.6	132.2 (6.55)	115.7 (6.30)	155.1

Table 5.3. Radiochemical Yields for Fluorinated Tyrosine Derivatives Resulting from the Direct Fluorination of Substrate in Acidic Media with [^{18}F]F $_2$.

Substrate	Solvent	Radiochemical Yield (%) ^a	
		3-Fluoro	3,5-Difluoro
L- α -methyltyrosine	Formic acid	13	2
	TFA	27	1
	HF	30	0
	BF $_3$ /HF (0.056 M)	25	1
	BF $_3$ /HF (0.13 M)	11	5
	BF $_3$ /HF (0.29 M)	12	3
L-tyrosine	Formic acid	12	4
	TFA	30	4
	HF	30	0
	BF $_3$ /HF (0.13 M)	12	6

^aRadiochemical Yield = (amount of ^{18}F in fluorinated tyrosine analog) \div (amount of ^{18}F in reaction vessel).

5.2.5 Radiochemical Yields of [^{18}F]3-Fluoro-L-tyrosine and 3-F- α -MT

The highest radiochemical yields of the 3-fluoro isomers of the tyrosine derivatives with respect to [^{18}F]F₂ in the present study were obtained by direct fluorination in HF or TFA (Table 5.3). Similar results have been found by direct fluorination of tyrosine in HF,⁵⁶ and TFA¹¹² with [^{18}F]F₂. The high electrophilic fluorination yields in HF are attributed to the inertness of HF to oxidative attack by fluorine and the ability of HF to promote electrophilic substitution by an S_N2 type process.⁵⁵ Recent studies reveal that protic solvents promote electrophilic fluorination of aromatic compounds, and the electrophilic reactivity and selectivity of fluorine varies significantly with the acidity of the reaction medium.^{162,54}

A previous study conducted in our laboratory has shown that BF₃/HF mixtures are efficient solvent media for the production of [^{18}F]fluoro-L-DOPA by elemental fluorination of L-DOPA.⁵⁸ Radiochemical yields of [^{18}F]fluoro-L-DOPA were highest when L-DOPA was directly fluorinated in BF₃/HF solvent (40%),⁵⁸ when compared with yields in HF (35%)⁹⁹ and TFA (9%)^{112,162} solvents. The high yield for [^{18}F]fluoro-L-DOPA is expected because the two hydroxyl groups activate the ring towards electrophilic attack by fluorine. Unlike the radiochemical yield of fluoro-L-DOPA, which increased upon going from HF to BF₃/HF solvent, the radiochemical yield of fluoro-L- α -MT decreased in BF₃/HF. One explanation may be that the reactivity of L-DOPA in BF₃/HF towards electrophilic fluorination was not reduced to the same extent as for L- α -MT presumably because of an additional activating hydroxyl group on the aromatic ring.

A similar decrease in radiochemical yield was also observed during the direct fluorination of L-*meta*-tyrosine when going from HF to BF₃/HF.⁵⁷

5.2.6. Orientation of Fluorination and the Formation of [¹⁸F]3,5-Difluoro

Derivatives of L-Tyrosine and L- α -MT

The direct fluorination of L-tyrosine or L- α -MT with [¹⁸F]F₂ produces the 3-fluoro isomer as the major ¹⁸F-containing product in all solvents used in the present study (Table 5.3). Cacace and Wolf¹¹⁸ have studied the orientation of direct liquid phase fluorination of substituted aromatics and have suggested that the fluorinations proceed through a mechanism that is similar to that for ionic halogenation reactions of aromatic compounds. The formation of 3-fluoro isomers by the direct fluorination of the precursor is consistent with this latter mechanism because the electron donating properties of the hydroxyl group render the position *ortho* to the hydroxyl group more susceptible to electrophilic attack. Misaki¹⁶³ has reported similar results when phenol and *para*-cresol were used as the substrates for direct fluorinations.

Preparative HPLC analysis of the reaction mixture after fluorination of L-tyrosine or L- α -MT in formic acid, TFA or BF₃/HF mixtures showed an additional peak eluting at 25 min, which gave a signal in the ¹⁹F NMR spectrum at -132.2 ppm. Similar results were obtained when AcOF was the fluorinating agent. Tomiyoshi and co-workers¹⁵⁶ have observed a compound, co-produced with 3-F- α -MT during the fluorination of L- α -MT in TFA using [¹⁸F]AcOF, having a similar ¹⁹F NMR chemical shift (-134.1 ppm; originally

referenced to TFA, but converted here to an external CFCl_3 reference) which they have assigned to 2-fluoro-L- α -methyltyrosine. The ^{19}F NMR chemical shift, however, differs significantly from the ^{19}F chemical shift of 2-fluoro-tyrosine (-115.8 ppm).⁵⁶ Our detailed characterization has confirmed that the compound co-produced with 3-F- α -MT having a ^{19}F NMR chemical shift of -132.2 ppm is 3,5-difluoro-L- α -methyltyrosine. This is in agreement with a study by Kirk¹⁶⁴ that reports the ^{19}F NMR chemical shift of 3,5-difluorotyramine hydrochloride at -131.4 ppm (originally referenced to hexafluorobenzene, but converted here to an external CFCl_3 reference).

The formation of 3,5-difluorinated derivatives are surprising since a 3:1 excess of precursor to fluorinating agent should favor monosubstitution on the aromatic ring. Hatano and co-workers¹⁶⁵ have observed a difluorinated analog of L-DOPA co-produced during electrophilic synthesis of [^{18}F]6-fluoro-L-DOPA when a 3:1 molar ratio of precursor to fluorinating agent was used. Assuming that the 3,5-difluoro derivatives are produced in a step-wise manner, we conducted the direct fluorination of 3-fluoro-DL-tyrosine in HF and 0.13 M BF_3/HF with [^{18}F]F₂ (eq. 5.1) which gave [^{18}F]3,5-difluoro-DL-tyrosine in 12% and 13% radiochemical yields, respectively. This result is even more surprising because the direct fluorination of L-tyrosine and L- α -MT in HF is regiospecific towards the formation of the 3-fluoro isomer, and 3,5-difluoro compounds are not produced. A recent study by Chambers and co-workers¹⁶⁶ has systematically investigated the fluorination of 1,4-disubstituted aromatic compounds and found that complex mixtures of products are often obtained. These authors concluded “although fluorine acts

in many situations as a simple electrophile, there is clearly much yet to learn about the range of mechanistic preferences”.

5.2.7 Proton and ^{13}C NMR Spectroscopic Studies of the Solvent Effect on the Radiochemical Yield of 3-F- α -MT

In the present study we have demonstrated that the radiochemical yield of 3-F- α -MT is influenced by the acidity of the reaction medium. Proton and ^{13}C NMR spectroscopy were used to investigate the effect of solvent on the radiochemical yield of 3-F- α -MT and to show deactivation of the aromatic ring of L- α -MT when BF_3/HF is the solvent.

Results from the low-temperature ^1H and ^{13}C NMR study (Table 5.2) show that the oxygen on the hydroxyl group of L- α -MT is protonated in BF_3/HF solution, which is observed as a broad singlet in the ^1H NMR spectrum at 12.93 ppm, and from the shielding of the *ipso*-carbon in the ^{13}C NMR spectrum. Further evidence for the protonation of the oxygen on the hydroxyl group is evident from the chemical shifts of the aromatic protons, which are shifted to higher frequency in BF_3/HF when compared with the chemical shifts of L- α -MT in HF. These chemical shift differences indicate that all aromatic proton environments are deshielded upon dissolution of L- α -MT in BF_3/HF as a result of deactivation of the aromatic ring by the protonated hydroxyl group.

The ^1H NMR spectrum of L- α -MT at $-70\text{ }^\circ\text{C}$ (Table 5.2) in BF_3/HF showed no evidence for ring protonation of L- α -MT. In contrast, Brouwer *et al.*¹¹⁷ obtained evidence

for the protonation of both the oxygen and the ring carbon of anisole in HF saturated with BF_3 at low temperatures. This could arise for two reasons: (1) the concentrations of BF_3 in HF used in the present study were approximately 0.13 M, compared with the saturated solution of BF_3 in HF used by Brouwer *et al.*¹¹⁷ which would favor ring protonation, (2) protonation of L- α -MT (a zwitterion) in strong acids at the carboxylate group is preferred over any other site. The observation of the acidic proton (Table 5.2) at 10.09 ppm in the $-70\text{ }^\circ\text{C}$ ^1H NMR spectrum of L- α -MT in BF_3/HF and a corresponding high-frequency shift for the carbonyl carbon in the $-70\text{ }^\circ\text{C}$ ^{13}C NMR spectrum of this sample support carboxylate protonation.

Deactivation of an aromatic ring is known to retard electrophilic aromatic substitution and is manifested in the present study when BF_3/HF mixtures are used as the solvent media, resulting in lower radiochemical yields (Table 5.3). Chambers and co-workers¹⁶⁶ have noted that the degree of protonation of the hydroxyl group of 1,4-disubstituted aromatic compounds varies with acidity of the solvent and reduces the susceptibility of the molecule towards electrophilic fluorination. It can be expected that sufficient deactivation of the aromatic ring by the protonated oxygen on the hydroxyl group of tyrosine analogs can lead to increased formation of the 2-fluoro and 2,6-difluoro compounds. The differences in isomeric distributions in BF_3/HF mixtures can also be explained by changes in electron density on the aromatic ring, which vary depending on the degree of hydroxyl group protonation.

5.3 Conclusion

The goal of the present work was to develop an efficient method to improve the radiochemical yield of [^{18}F]3-fluoro-L- α -methyltyrosine. It was shown that the direct fluorination of L- α -MT in TFA or HF with [^{18}F]F₂ produces 3-F- α -MT in 28% and 30% radiochemical yields (relative to [^{18}F]F₂), respectively; the highest reported radiochemical yields of 3-F- α -MT achieved to date. For routine production of 3-F- α -MT in a hospital environment, TFA is the preferred solvent. Furthermore, 3,5-difluoro isomers of L-tyrosine and L- α -MT were synthesized by direct fluorination for the first time.

CHAPTER 6

SYNTHESES OF [¹⁸F]5-FLUORO-3-NITRO-L-TYROSINE

6.1 Introduction

Aromatic nitration is one of the most extensively studied reactions in synthetic and theoretical chemistry.^{167,168} Aromatic nitration also occurs *in vivo* by the action of “reactive nitrogen species”, which are being increasingly proposed as contributors to tissue injury in several human diseases. The detailed mechanisms by which these species cause modifications in biomolecules is not completely understood.¹⁶⁹ The *in vivo* detection of 3-nitro-L-tyrosine is considered to be a biomarker for “reactive nitrogen species” in a biological matrix, however, the *in vivo* formation and fate of 3-nitro-L-tyrosine is a controversial subject.^{169,170,171}

A number of analytical procedures for the separation, detection and quantification of 3-nitro-L-tyrosine have been developed including UV, HPLC, GC, MS and biochemical techniques.¹⁷² Labelled compounds have also been considered for the detection and quantification of 3-nitro-L-tyrosine. For example, ¹⁵N-labelled tetranitromethane has been used to synthesize [¹⁵N]3-nitro-L-tyrosine¹⁷³ and [¹⁵N]-

labelled tyrosines in proteins¹⁷⁴ as new NMR probes for nitrotyrosines. Thus, a radiolabelled derivative of 3-nitro-L-tyrosine could be useful for the detection and quantification of 3-nitro-L-tyrosine.

The goals of the present work were to develop rapid methods for the synthesis of fluorine-18 labelled 3-nitro-L-tyrosine, which could be used as a probe in studies of the biological function of 3-nitro-L-tyrosine by means of PET. The present study reports three synthetic routes to [¹⁸F]5-fluoro-3-nitro-L-tyrosine ([¹⁸F]FNT).

6.2 Results and Discussion

Mixtures of nitric acid and sulfuric acid continue to be the most widely used nitrating agents, however, the strongly oxidizing natures of these systems and environmental considerations have led to the development of more selective reagents and methods.¹⁶⁷ Acid-catalyzed electrophilic aromatic nitration¹⁷⁵ often has the advantage that the solvents are recyclable and nitrations can be achieved under anhydrous conditions. Nitroaromatics that contain fluorine are an interesting class of compounds and have applications in the agrochemical and pharmaceutical industries.¹⁷⁶ Chambers and Skinner¹⁷⁶ have patented a synthetic route to mono- and polyfluoronitrated aromatic compounds by reacting aromatic compounds with a nitrating agent (e.g., aqueous HNO₃) in the presence of elemental fluorine. In the present work, three synthetic approaches to [¹⁸F]FNT were explored: (1) nitration of [¹⁸F]3-fluoro-L-tyrosine (2) direct fluorination of 3-nitro-L-tyrosine, and (3) a one-pot nitration followed by fluorination of L-tyrosine. Anhydrous HF and TFA were chosen as the solvents for these reactions because they

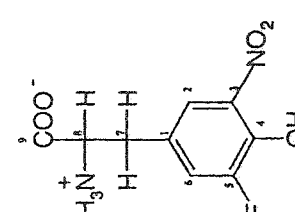
have proven to be useful for acid-catalyzed electrophilic nitration¹⁷⁷ and are ideal for the direct fluorination of aromatic amino acids.^{99,56,112,58,162,101}

6.2.1 Nitration of 3-Fluoro-DL-tyrosine and [¹⁸F]3-Fluoro-L-tyrosine

In previous work,¹³⁹ 5-fluoro-3-nitro-DL-tyrosine was synthesized by reaction of an ice-cold suspension of 3-fluoro-DL-tyrosine in water with concentrated HNO₃ and allowing the reaction to proceed below 25 °C overnight. In the present work, nitration of 3-fluoro-DL-tyrosine was carried out using an equimolar quantity of NaNO₃, in TFA (4 °C) or HF (-65 °C) solvent. Analysis of the reaction mixture using HPLC (UV, λ = 275 nm) showed that the conversion of 3-fluoro-DL-tyrosine to 5-fluoro-3-nitro-DL-tyrosine was >98% after 5 min. Characterization of 5-fluoro-3-nitro-tyrosine was conducted by use of ¹H, ¹³C and ¹⁹F NMR spectroscopy (Table 6.1).

We have previously reported the synthesis of [¹⁸F]3-fluoro-L-tyrosine by direct fluorination of L-tyrosine with a 29 ± 1% radiochemical yield.¹⁰¹ The nitration of 3-fluoro-DL-tyrosine, described above, was applied to the nitration of [¹⁸F]3-fluoro-L-tyrosine (eq. 2.4) and produced [¹⁸F]FNT with a radiochemical yield of 96 ± 2% with respect to [¹⁸F]3-fluoro-L-tyrosine. Analytical HPLC analysis of the reaction mixture after nitration of [¹⁸F]3-fluoro-L-tyrosine with NaNO₃ in TFA (eq. 2.4) is shown in Figure 2.6. The peaks eluting at 5.5 and 7.5 min correspond to unconverted 3-fluoro-L-tyrosine and [¹⁸F]FNT, respectively, as confirmed by ¹⁹F NMR spectroscopy. Furthermore, the peak assigned to 3-fluoro-L-tyrosine in the reaction mixture showed an increase in peak

Table 6.1. Proton, ^{13}C and ^{19}F NMR Parameters for FNT

	^1H chemical shift, ppm	Coupling Constant, Hz	^{13}C Chemical shift ^b , ppm	Coupling Constant, Hz
	H7 _A	$^2J(\text{H7}_A\text{-H7}_B)$, -14.6	C-1	$^3J(\text{C1-F})$, 6.9
	H7 _B	$^3J(\text{H7}_A\text{-H8}_x)$, 5.72	C-2	$^4J(\text{C2-F})$, 2.3
	H8 _x	$^3J(\text{H7}_B\text{-H8}_x)$, 7.31	C-3	$^3J(\text{C3-F})$, 3.1
	H6	$^3J(\text{H6-F})$, 10.7	C-4	$^2J(\text{C4-F})$, 16.1
	H2	$^5J(\text{H2-F})$, 2.0	C-5	$^1J(\text{C5-F})$, 246.9
		$^4J(\text{H2-H6})$, 2.0	C-6	$^2J(\text{C6-F})$, 19.2
			C-7	41.1
			C-8	60.2
			C-9	177.5

5-fluoro-3-nitro-tyrosine^a^aThe ^{19}F chemical shift is -130.7 ppm with respect to external CFCl_3 at 30 °C.^bCalculated values using fluorine substituent parameters are shown in parentheses.

area when spiked with 3-fluoro-DL-tyrosine.

6.2.2 Fluorination of 3-Nitro-L-tyrosine

The direct fluorination of 3-nitro-L-tyrosine using [^{18}F]F₂ (eq 2.5) resulted in radiochemical yields of 13 and 15% in TFA and HF, respectively, for [^{18}F]FNT. Structural characterization of FNT was accomplished by use of ^1H , ^{13}C and ^{19}F NMR spectroscopies and positive ion electrospray mass spectrometry, which showed a protonated molecular ion at $m/z = 245$ $[\text{M}+\text{H}]^+$. The syntheses and preparative HPLC purifications of [^{18}F]FNT were completed within 1 h. It should be noted that 3-nitro-L-tyrosine was not separated from [^{18}F]FNT under the HPLC conditions used in this study. In view of the significantly lower radiochemical yield in equation 2.5, compared with that resulting from direct nitration of [^{18}F]3-fluoro-L-tyrosine in equation 2.4, the development of HPLC methods to optimize this separation were not pursued further.

6.2.3 One-Pot Nitration and Fluorination of L-Tyrosine

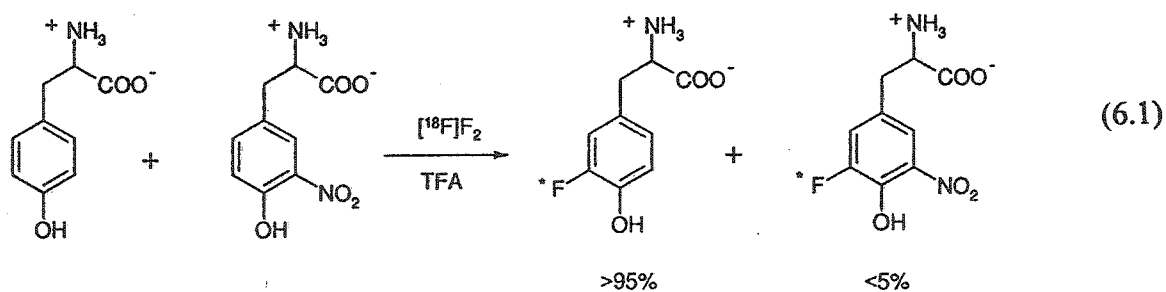
One-pot nitrations of L-tyrosine in TFA and HF solvents, followed by fluorination using [^{18}F]F₂, were also carried out in the present study (eq. 2.6). The conversion of L-tyrosine to 3-nitro-L-tyrosine was >98% (determined by HPLC; UV, $\lambda = 275$ nm). The products of these reactions were characterized by ^1H , ^{13}C and ^{19}F NMR spectroscopies and by positive ion electrospray mass spectrometry, which showed protonated molecular ions at $m/z = 227$ and 245 $[\text{M}+\text{H}]^+$ corresponding to 3-nitro-L-tyrosine and [^{18}F]FNT, respectively.

Substitutions at positions 3- and 5- on the aromatic ring of L-tyrosine were expected in view of the higher electron densities at these positions that arise from the electron donating properties of the hydroxyl group. In Chapter 5 it was shown that the same sites are susceptible to electrophilic aromatic substitution in L-tyrosine and L- α -methyltyrosine.¹⁰¹ The radiochemical yield of [^{18}F]FNT, after a one-pot nitration of L-tyrosine using NaNO_3 followed by fluorination with [^{18}F]F $_2$ (eq. 2.6), was 14 and 12% in TFA and HF, respectively.

6.2.4 Relative Reactivity of [^{18}F]F $_2$ Towards L-Tyrosine and 3-Nitro-L-tyrosine

The radiochemical yields of [^{18}F]FNT resulting from the direct fluorination of 3-nitro-L-tyrosine (eqs. 2.5 and 2.6; $13.5 \pm 1.5\%$) are lower than those resulting from the direct fluorination of L-tyrosine in TFA (28%) and HF (30%). The lower radiochemical yields in the present work are not surprising because the electron withdrawing nitro group renders the aromatic ring less susceptible to electrophilic aromatic substitution. Cacace and Wolf¹¹⁸ have reported that the relative reactivity of aromatic substrates with F $_2$ increases with increasing activation of the aromatic ring in the order: nitrobenzene \ll benzene $<$ toluene \ll anisole. Because the radiochemical yield of an ^{18}F -labelled fluoroaromatic compound is indicative of the efficiency of fluorine substitution on the aromatic ring, it was of interest to determine the relative reactivity of [^{18}F]F $_2$ towards three-fold molar excesses of both L-tyrosine and 3-nitro-L-tyrosine in TFA at 4 °C (eq. 6.1). The results of this competition experiment revealed that the reactivity of fluorine towards L-tyrosine was considerably higher than towards 3-nitro-L-tyrosine, which was

determined from the distribution of radioactivity and peak integration after preparative HPLC and from integration of the ^{19}F NMR spectrum of the reaction mixture. The combined radiochemical yield of $[\text{}^{18}\text{F}]\text{3-fluoro-L-tyrosine}$ and $[\text{}^{18}\text{F}]\text{FNT}$ was 26% (relative to $[\text{}^{18}\text{F}]\text{F}_2$), with >95% of the activity arising from $[\text{}^{18}\text{F}]\text{3-fluoro-L-tyrosine}$. Figure 6.1 shows HPLC traces of the reaction mixture resulting from this competition experiment. The peaks eluting at 4, 5.5 and 7.5 min correspond to (an) unknown fluorine-containing species, $[\text{}^{18}\text{F}]\text{3-fluoro-L-tyrosine}$ and $[\text{}^{18}\text{F}]\text{FNT}$, respectively. These results clearly show that the aromatic ring of L-tyrosine is more susceptible to substitution by fluorine, under the present experimental conditions, than the relatively deactivated aromatic ring of 3-nitro-L-tyrosine, accounting for the lower radiochemical yield after fluorination of 3-nitro-L-tyrosine when compared with that of L-tyrosine in TFA.¹⁰¹



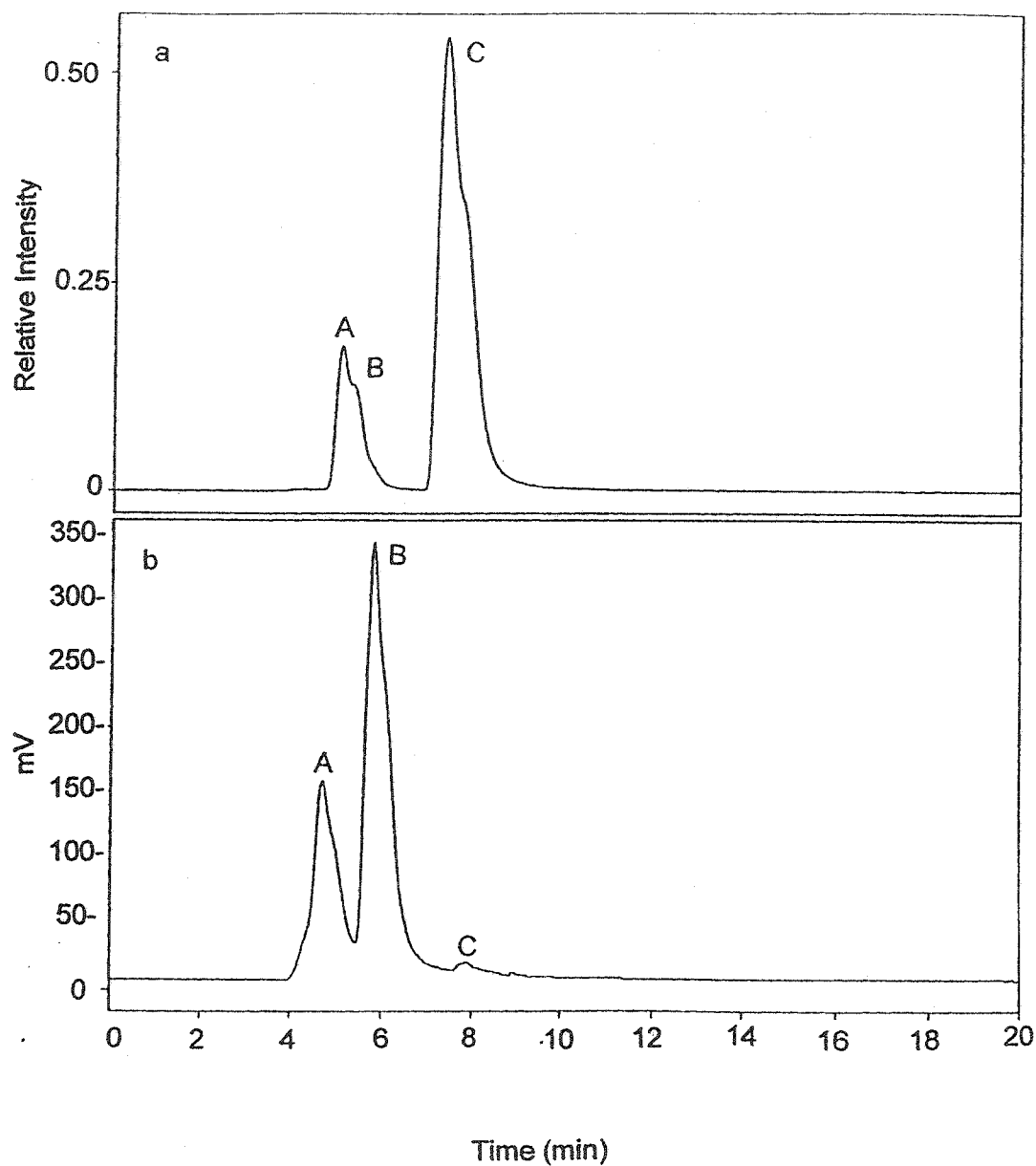


Figure 6.1 HPLC trace showing the relative reactivity of $[^{18}\text{F}]\text{F}_2$ towards three-fold molar excesses of both L-tyrosine and 3-nitro-L-tyrosine in TFA solvent at $4\text{ }^\circ\text{C}$ (eq. 6.4). The labels A, B, and C correspond to unidentified fluorine-containing species, $[^{18}\text{F}]\text{3-fluoro-L-tyrosine}$ and $[^{18}\text{F}]\text{FNT}$, respectively: (a) UV, $\lambda = 275\text{ nm}$ and (b) $[^{18}\text{F}]$ -radioactivity trace.

6.2.5 Comparison of the Synthetic Routes to [^{18}F]FNT

Of the three new synthetic methods for [^{18}F]FNT that are described in the present study (eq. 2.4, 2.5 and 2.6), the direct nitration of [^{18}F]3-fluoro-L-tyrosine (eq. 2.4) is the preferred route because the nitration of [^{18}F]3-fluoro-L-tyrosine is fast (5 min) and efficient ($96 \pm 2\%$ conversion to [^{18}F]FNT). This method also produces [^{18}F]FNT of high radiochemical purity because all of the L-tyrosine precursor is easily removed immediately following fluorination with [^{18}F]F $_2$. The present study also showed that fluorination of L-tyrosine is more efficient than fluorination of the relatively deactivated aromatic ring of 3-nitro-L-tyrosine. However, the one-pot method of nitration followed by fluorination of L-tyrosine (eq. 2.4) offers an alternative general route to the syntheses of nitrofluoroaromatic compounds. For ^{18}F -labelled nitrofluoroaromatic compounds requiring high specific activity for PET applications, nucleophilic methods using no-carrier-added $^{18}\text{F}^-$ can be used for the syntheses of ^{18}F -aromatics,⁴¹ and the resulting compounds should prove to be easily nitrated, as established by the present study.

6.3. Conclusions

Efficient synthetic methods leading to the syntheses of [^{18}F]FNT have been developed in the present study. The direct nitration of [^{18}F]3-fluoro-L-tyrosine using NaNO_3 in TFA at 4 °C produced [^{18}F]FNT with a radiochemical yield of $96 \pm 2\%$ with respect to [^{18}F]3-fluoro-L-tyrosine within 5 min. This method offers the highest radiochemical purity and yields of [^{18}F]FNT at this time and is well suited for the routine

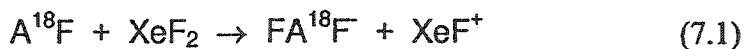
production of [^{18}F]FNT in a hospital environment. The present work also establishes that [^{18}F]FNT can be synthesized by direct fluorination of 3-nitro-L-tyrosine in TFA or HF solvent using [^{18}F]F₂ in a radiochemical yield of 13.5 ± 1.5 % relative to [^{18}F]F₂.

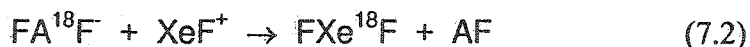
CHAPTER 7

ON THE PREPARATION OF FLUORINE-18 LABELLED XeF₂ AND CHEMICAL EXCHANGE BETWEEN FLUORIDE ION AND XeF₂

7.1 Introduction

Xenon difluoride has been extensively used as a fluorinating agent for a wide variety of inorganic and organic compounds.⁶¹ Fluorine-18 labelled XeF₂ has been synthesized^{62,63} and used to prepare positron emitting medical imaging agents such as [¹⁸F]2-fluoro-2-deoxy-D-glucose⁶⁴ and [¹⁸F]6-fluoro-L-DOPA.⁶⁵ Fluorine-18 labelled XeF₂ was first prepared in our laboratories⁶² by treating SO₂ClF solutions of XeF₂ with [¹⁸F]HF, [¹⁸F]SiF₄ or [¹⁸F]AsF₅. The exchanges are attributed to the Lewis acid properties of the labelled fluorides (eq 7.1 and 7.2). Our laboratories have since shown that [¹⁸F]XeF₂ can also be synthesized by the thermochemical reaction of carrier-added [¹⁸F]F₂ and Xe.⁶³ Appelman¹⁷⁸ has also shown that very slow fluorine exchange occurs between XeF₂ and aqueous H¹⁸F (ca. 0.8% after 2 h at 0 °C).

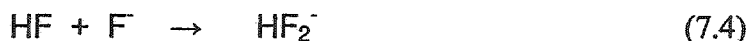
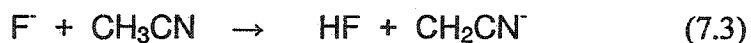




A recent study by Pike *et al.*⁶⁶ reports that no-carrier-added (n.c.a.) ¹⁸F-labelled KF and CsF, sequestered by 2,2,2-crypt (1,10-diaza-4,7,13,16,21,24-hexaoxabicyclo[8.8.8]hexacosane), undergo fluorine exchange with XeF₂ at room temperature in CH₂Cl₂ and CHCl₃ solvents. The study also reports that the exchange was inhibited in CH₃CN solvent. It was claimed that the 2,2,2-crypt-M⁺ cation (M = K or Cs) catalyzes ionization of XeF₂ in chlorinated solvents. Exchange experiments conducted in CH₂Cl₂ solutions required a large molar excess of XeF₂ relative to the cryptand (molar ratio of XeF₂ : 2,2,2-crypt : Cs₂CO₃ used in a typical exchange experiment was 56 : 1 : 0.29) for "efficient" exchange of n.c.a. ¹⁸F⁻ ion. When 2,2,2-crypt-K⁺ and CHCl₃ solvents were used, ≤ 90% of the radioactivity was incorporated into XeF₂, however, yields were reported to be highly variable. This work is at apparent odds with earlier ¹⁸F-labelling experiments which have shown that fluoride, in the form of [N(*n*-Bu)₄][¹⁸F], does not exchange with XeF₂ in CH₂Cl₂ solvent after 30 min at room temperature.¹⁷⁹

Fluoride ion and XeF₂ are known to react with a number of organic solvents. Christie and Wilson¹⁸⁰ have demonstrated, by ¹H and ¹⁹F NMR spectroscopy, that anhydrous [N(CH₃)₄][F], so-called "naked fluoride", reacts with CH₃CN, CH₂Cl₂, and CHCl₃ solvents at room temperature. These authors have shown that fluoride ion reacts relatively slowly with CH₃CN to form HF₂⁻ and CH₂CN⁻ anions, according to equations

7.3 and 7.4. Fluoride ion was also reported to react slowly with CH_2Cl_2 , forming CH_2ClF as the only reported fluorination product, but rapidly with CHCl_3 , resulting in all three possible halogen exchange products, CHCl_2F , CHClF_2 , and CHF_3 in a 2 : 3 : 1 molar ratio. Holloway *et al.*¹⁸¹ showed, using ^1H and ^{19}F NMR spectroscopy, that XeF_2 reacts with CH_2Cl_2 and CHCl_3 , over a period of two days at room temperature. The reaction of XeF_2 with CH_2Cl_2 yielded predominantly CH_2ClF , CHCl_2F , and HF , with CH_2F_2 , CHClF_2 , CCl_2F_2 , and CFCl_3 as minor (< 0.5%) products, and that with CHCl_3 yielded CHCl_2F , CHClF_2 , CHCl_3 and HF . Based on these findings, the authors suggested CH_3CN or chlorofluorocarbons might be more appropriate solvents for XeF_2 when the kinetics of the desired fluorination reactions are slow.



The aforementioned work and failed attempts in the present study to repeat the work of Pike *et al.*⁶⁶ have led to the critical reassessment of the interaction of [2,2,2-crypt-K][F], and other fluoride ion sources, with XeF_2 in CH_2Cl_2 and CH_3CN solvents under rigorously anhydrous conditions by use of one- and two-dimensional NMR techniques. Previous work⁶⁶ has shown that radiochemical yields in CHCl_3 were highly variable. This is not surprising because fluoride ion has been shown to rapidly react with CHCl_3 to form all three possible solvent exchange products, CHCl_2F , CHClF_2 , and

CHF_3 ,¹⁸⁰ and because XeF_2 has been shown to react with CHCl_3 to form CHFCl_2 , CHF_2Cl , CFCl_3 , and HF .¹⁸¹ Consequently, the role of CHCl_3 as a fluoride ion exchange medium was not reinvestigated in the present study.

7.2 Results and Discussion

7.2.1 Reaction of XeF_2 with 2,2,2-crypt and KF in CH_2Cl_2 Solvent

In the present work, equimolar mixtures of XeF_2 , KF, and 2,2,2-crypt in CH_2Cl_2 solvent detonated, under rigorously anhydrous conditions, when rapidly warmed from -196°C to room temperature. The heat of reaction was, however, effectively dissipated in experiments where $[\text{2,2,2-crypt-K}][\text{F}]$ was initially dissolved in CH_2Cl_2 , followed by XeF_2 addition at ca. -140°C to the frozen mixture and slow warming to room temperature over a period of ca. 1 h. The reaction mixture slowly changed from a colorless to a brown solution. The ^{19}F NMR spectrum of this sample was complex and several fluorination products were observed. The absence of characteristic ^{19}F signals for XeF_2 ,¹⁸² HF ¹⁸³ or HF_2^- ¹⁸⁴ in the ^{19}F NMR spectrum indicated that chemical exchange may occur between two or more of these species, and/or all of the XeF_2 had reacted with the 2,2,2-crypt- K^+ to form HF and HF_2^- , which underwent rapid fluorine exchange. The dominant ^{19}F resonance was a broad singlet at -162.8 ppm ($\Delta\nu_{1/2}$, 46 Hz). Christie and Wilson¹⁸⁴ have observed broad, exchange-averaged resonances for $\text{F}^-/\text{HF}_2^-/\text{HF}$ mixtures in mixed water (10%)/ CH_3CN solutions ranging from -118 to -170 ppm ($\Delta\nu_{1/2}$, 80 Hz), which have chemical shifts that are dependent upon the mole ratios of the components. Very weak triplets arising from CH_2F_2 at -142.1 ppm ($^2J_{\text{HF}}$, 49 Hz), and CH_2ClF at -168.9 ppm ($^2J_{\text{HF}}$,

48 Hz) were also observed. In addition, a series of weak, equally intense pairs of ^{19}F NMR resonances appears at -79.9, -80.2; -85.5, -86.2 ppm, which have chemical shifts that are similar to those of the CF_2 resonances in perfluoro-2,2,2-crypt ($\text{OCF}_2\text{CF}_2\text{O}$, -81.4 ppm, s; OCF_2 , -87.0 ppm, t, $^3J_{\text{FF}} \sim 1$ Hz; NCF_2 , -88.5 ppm, t, $^3J_{\text{FF}} \sim 1$ Hz).¹⁸⁵ It is therefore likely that partially fluorinated 2,2,2-cryptands result from oxidative fluorination of 2,2,2-crypt by XeF_2 . A second series of weak and equally intense ^{19}F resonances also appeared at -126.9, -127.2; -131.7, -131.9 ppm. Although the detailed characterization of all fluorination products was beyond the scope of the present work, these findings clearly demonstrate that alkali metal (K^+ and Cs^+) 2,2,2-cryptands are not inert in these reactions and therefore do not function as “catalysts”, as previously claimed.⁶⁶

7.2.2 Stability of XeF_2 and 2,2,2-crypt in CH_2Cl_2 Solvent

The reactivity of XeF_2 with 2,2,2-crypt in the absence of KF was also investigated in CH_2Cl_2 solvent. Samples of XeF_2 and 2,2,2-crypt were prepared in an equimolar ratio in CH_2Cl_2 solvent and warmed from -196°C to room temperature over a period of ca. 1 h. A brown-colored solution resulted, similar to that arising from the reaction of [2,2,2-crypt-K][F] and XeF_2 in CH_2Cl_2 (*vide supra*). The ^{19}F NMR spectrum revealed several fluorination products, among which was an intense, broad singlet at -162.6 ppm ($\Delta\nu_{1/2}$, 35 Hz) that is attributable to HF_2^-/HF exchange. The corresponding ^1H resonance was observed as a broad singlet at 12.65 ppm ($\Delta\nu_{1/2}$, 40 Hz) and is intermediate with respect to those of HF (7.00 ppm)¹⁸³ and HF_2^- (16.20 ppm) in CH_2Cl_2 (this work; see section 7.2.4).

Two series of weak and equally intense pairs of ^{19}F NMR resonances (-78.7, -79.2; -86.3, -87.0; -87.4, -87.9; -93.7, -94.4 ppm and -127.3, -127.5; -127.8, -128.1; -132.6, -132.8; and -142.3, -142.6 ppm) that are similar to those observed for the $\text{XeF}_2/2,2,2\text{-crypt/KF}$ system described above were observed, which are indicative of cryptand fluorination by XeF_2 . The ^1H NMR spectrum of this sample revealed, in addition to CH_2Cl_2 (5.34 ppm) solvent, unreacted 2,2,2-crypt ($\text{OCH}_2\text{CH}_2\text{O}$, 3.58 ppm, s; OCH_2 , 3.66 ppm, t, $^3J_{\text{HH}} = 5$ Hz; NCH_2 , 3.00 ppm, t, $^3J_{\text{HH}} = 5$ Hz) and a broad line (12.72 ppm, $\Delta\nu_{1/2}$, 56 Hz) that is assigned to HF and HF_2^- undergoing rapid proton exchange. It is reasonable to assume that protonated nitrogen centers of the fluorination products and unreacted 2,2,2-crypt may serve as the counterions, however, the NH protons can be expected to undergo chemical exchange with HF/HF_2^- and therefore may also be represented by the resonance at 12.72 ppm. Several very weak, broad features were also observed in the ^1H NMR spectrum between 6 and 10 ppm.

A sample containing a 33 : 1 molar ratio of XeF_2 to 2,2,2-crypt was warmed from -196 °C to room temperature over a period of 1 h and produced a two-phase mixture with a clear lower density layer and a minor yellow, higher density layer. Unlike the equimolar sample of XeF_2 and 2,2,2-crypt, the ^{19}F NMR spectrum of the 33 : 1 molar ratio of XeF_2 to 2,2,2-crypt revealed the presence of XeF_2 (-175.1 ppm; $^1J(^{129}\text{Xe}-^{19}\text{F})$, 5605 Hz), and a second weaker XeF_2 resonance in the second phase (-178.4 ppm; $^1J(^{129}\text{Xe}-^{19}\text{F})$, 5630 Hz), as well as a doublet arising from CHCl_2F (-81.0 ppm; $^2J_{\text{HF}}$, 53 Hz), and triplets arising from CH_2F_2 (-142.9 ppm; $^2J_{\text{HF}}$, 49 Hz) and CH_2ClF (-170.4; $^2J_{\text{HF}}$, 48 Hz). The ^{19}F NMR spectrum also showed intense resonances at -176.4 and -181.2

ppm with linewidths of 220 and 200 Hz, respectively that are assigned to HF and HF₂⁻ undergoing rapid fluorine exchange in their respective phases. The corresponding ¹H resonances were observed at 11.64 and 11.27 ppm and had linewidths of 64 and 22 Hz, respectively. Although, the ¹H NMR spectrum of this sample was complicated by the presence of a second phase, it is noteworthy that 2,2,2-crypt was not observed, as in the equimolar sample, confirming that 2,2,2-crypt had fully reacted when a 33 : 1 molar excess of XeF₂ in CH₂Cl₂ solvent had been allowed to react at room temperature for 1 h. These findings clearly contradict the previous study,⁶⁶ which claims that a 56 : 1 molar ratio of XeF₂ to 2,2,2-crypt is required to achieve “efficient” exchange with ¹⁸F⁻ ion in CH₂Cl₂, and further confirms that 2,2,2-crypt is not inert under these reaction conditions. The NMR spectra show that large amounts of HF and HF₂⁻ corresponding to the fluorination of the CH₂ groups of 2,2,2-crypt and the solvent by XeF₂. The fluorination products that result from the reaction of XeF₂ with 2,2,2-crypt are likely contained in the second, higher density phase. Scale-up of the reaction for the purpose of characterizing the 2,2,2-crypt fluorination products was not attempted because of the exothermicity of the reaction in CH₂Cl₂. In view of the 56 : 1 molar ratio of XeF₂ : 2,2,2-crypt in the previous report,⁶⁶ and the 33 : 1 molar ratio of XeF₂ : 2,2,2-crypt in the present study, it is clear that a significant amount of XeF₂ survives in the presence of HF generated in these reactions. Hydrogen fluoride has already been shown in our earlier ¹⁸F studies to promote fluorine exchange by acting as a weak fluoride ion acceptor towards XeF₂ (eq 1 and 2).⁶² Therefore, the exchange reported in the previous work⁶⁶ cannot possibly arise from exchange of free F⁻ ion with XeF₂, but must arise from HF/HF₂⁻ exchange with XeF₂,

where HF is in very large excess relative to HF_2^- in these n.c.a. ^{18}F exchange studies.

7.2.3 Reaction of $[\text{N}(\text{CH}_3)_4][\text{F}]$ and XeF_2 in CH_2Cl_2 Solvent

Christe and co-workers⁹³ reported the synthesis of the “naked fluoride ion” source, anhydrous $[\text{N}(\text{CH}_3)_4][\text{F}]$. They demonstrated that $[\text{N}(\text{CH}_3)_4][\text{F}]$ reacts with CH_3CN and chlorinated solvents.¹⁸⁰ In the present study, an equimolar sample of $[\text{N}(\text{CH}_3)_4][\text{F}]$ and XeF_2 in CH_2Cl_2 solvent was prepared to investigate the role of fluoride ion in chemical exchange with XeF_2 in the absence of 2,2,2-crypt. Reaction took place over a period of one day at room temperature without color change. The ^{19}F NMR spectrum revealed the presence of CH_2F_2 , CHCl_2F and CH_2ClF , in addition to XeF_2 and fluoride ion, and further confirmed that the fluorination of 2,2,2-crypt- M^+ by XeF_2 was responsible for the vigorous reactions that occurred in equimolar mixtures of XeF_2 and $[\text{2,2,2-crypt-K}][\text{F}]$ in CH_2Cl_2 solvent at room temperature (see section 7.2.1). In order to verify that $[\text{2,2,2-crypt-K}][\text{F}]$ demonstrates a reactivity similar to that of $[\text{N}(\text{CH}_3)_4][\text{F}]$ in CH_3CN and CH_2Cl_2 solvents, $[\text{2,2,2-crypt-K}][\text{F}]$ was studied in these solvents by ^1H and ^{19}F NMR spectroscopy.

7.2.4 Reactions of $[\text{2,2,2-crypt-K}][\text{F}]$ with CH_3CN and CH_2Cl_2 Solvents

The ^{19}F NMR spectrum of $[\text{2,2,2-crypt-K}][\text{F}]$ in CH_3CN , after 1 h at room temperature, showed two signals, a weak singlet (-75 ppm; $\Delta\nu_{\text{F}}$, 167 Hz) corresponding to F^- , and an intense doublet (-147.1 ppm; $^1J_{\text{HF}}$, 121 Hz) assigned to HF_2^- .¹⁸⁰ The ^1H NMR spectrum showed, in addition to the solvent line (CH_3CN , 1.96 ppm) and 2,2,2-

crypt (OCH₂CH₂O, 3.57 ppm, s; OCH₂, 3.52 ppm, t, ³J_{HH} = 5.5 Hz; NCH₂, 2.55 ppm, t, ³J_{HH} = 5.5 Hz), a triplet at 16.33 ppm (¹J_{HF}, 121 Hz) characteristic of HF₂⁻.¹⁸⁰ Using saturated solutions of anhydrous [N(CH₃)₄][F] as the fluoride ion source, CH₂CN⁻ has been previously detected as a broad singlet (linewidth not reported) at 9.1 ppm in the ¹H NMR spectrum, which was found to increase in intensity with time (up to several days).¹⁸⁰ In the present study, CH₂CN⁻ was not observed when [2,2,2-crypt-K][F] was allowed to react in CH₃CN at room temperature over a 1 h period, likely because of the lower concentration of fluoride ion and shorter reaction time used when compared with the previous study,¹⁸⁰ and the expected breadth of the resonance. This study confirms previous work which showed that the major product resulting from the reaction of fluoride ion with CH₃CN is HF₂⁻ when either [N(CH₃)₄][F]¹⁸⁰ or [2,2,2-crypt-K][F]¹⁸⁶ is used as the fluoride ion source.

The ¹⁹F NMR spectrum of [2,2,2-crypt-K][F] in CH₂Cl₂, after 1 h at room temperature, showed a weak singlet (-115 ppm; Δν_{1/2}, 242 Hz) for F⁻ and a triplet (-169.7 ppm; ¹J_{HF}, 48.0 Hz), characteristic of CH₂ClF. The ¹H NMR spectrum of the same sample showed CH₂ClF (5.92 ppm, d, ²J_{HF}, 48.0 Hz), in addition to the solvent line (CH₂Cl₂, 5.34 ppm), and 2,2,2-crypt (OCH₂CH₂O, 3.57 ppm, s; OCH₂, 3.49 ppm, t, ³J_{HH} = 5.5 Hz; NCH₂, 2.53 ppm, t, ³J_{HH} = 5.5 Hz). A triplet was also observed in the present work in the ¹⁹F NMR spectrum (-142.8 ppm; ²J_{HF}, 49.9 Hz) that is characteristic of CH₂F₂.¹⁸⁷ The triplet expected for CH₂F₂ in the ¹H NMR spectrum was not observed because it was masked by the CH₂Cl₂ solvent signal (the ¹H chemical shift of CH₂F₂ is reported at 5.62 ppm¹⁸⁸). The ¹⁹F NMR spectrum of the HF₂⁻ anion was observed as a

doublet (-156.3 ppm; $^1J_{\text{HF}}$, 122 Hz) and showed a triplet (16.20 ppm; $^1J_{\text{HF}}$, 122 Hz) in the ^1H NMR spectrum. Christe and Wilson¹⁸⁰ showed that CH_2Cl_2 undergoes slow halogen exchange with $[\text{N}(\text{CH}_3)_4][\text{F}]$ at room temperature, giving CH_2ClF as the main reaction product, but did not report the presence of CH_2F_2 . However, it was shown in the present study, using ^{19}F NMR spectroscopy, that a sample of $[\text{N}(\text{CH}_3)_4][\text{F}]$ in CH_2Cl_2 , after 1 h at room temperature, resulted in the formation of CH_2F_2 as the major product, with CH_2ClF as the minor product (the molar ratio of $\text{F}^- : \text{CH}_2\text{F}_2 : \text{CH}_2\text{ClF}$ was 2.2 : 6.8 : 1.0). The formation of CH_2F_2 as a major product in this reaction is not surprising and is consistent with previous halogen exchange reactions between CH_2Cl_2 and alkali metal fluorides. Fukui and Kitano¹⁸⁹ synthesized CH_2ClF and CH_2F_2 in 19 and 17% yields, respectively, by passing CH_2Cl_2 through a mixture of NaF and KF in $\text{HO}(\text{CH}_2)_2\text{OH}$ at 180 - 200 °C, and Verbeek and Sundermeyer¹⁹⁰ synthesized CH_2F_2 in 82% yield (34% conversion) by reaction of CH_2Cl_2 with a KF-HF melt at 300 °C. In agreement with the work of Christe and Wilson,¹⁸⁰ HF_2^- was not observed in the present work when $[\text{N}(\text{CH}_3)_4][\text{F}]$ was allowed to react with CH_2Cl_2 for 1 h, whereas, reaction of [2,2,2-crypt-K][F] in CH_2Cl_2 resulted in the formation of HF_2^- after 1 h at room temperature. These findings further demonstrate that the previously reported⁶⁶ exchange reaction between XeF_2 and [2,2,2-crypt-K][^{18}F] was not catalyzed by 2,2,2-crypt, but rather resulted from exchange among HF, HF_2^- and XeF_2 , as described above (see section 7.2.2) and in the previous work from our laboratories.⁶²

7.2.5 Fluoride Ion and HF Exchange with XeF₂

A 2-D ¹⁹F-¹⁹F EXSY experiment demonstrates that fluoride ion exchanges with XeF₂ in CH₃CN solvent. The off-diagonal correlations (Figure 7.1) confirm exchange between an initially equimolar mixture of [N(CH₃)₄][F], -71.5 ppm ($\Delta\nu_{1/2} = 267$ Hz) and XeF₂, -178.2 ppm; ¹J(¹²⁹Xe-¹⁹F), 5657 Hz. It was also shown that HF₂⁻ (-143.8 ppm; ¹J_{HF}, 120 Hz) does not exchange with XeF₂ or fluoride ion on the NMR timescale under the experimental conditions used in this study. The HF₂⁻ anion present in these samples was derived from fluoride attack on the solvent (eq 7.3 and 7.4), as previously reported.¹⁸⁰ The ¹⁹F exchange is postulated to proceed through the formation of trifluoroxenate(II), XeF₃⁻, anion as the exchange intermediate (eq 7.5). The existence of the XeF₃⁻ anion will be discussed in the proceeding chapter and a subsequent publication.¹⁰⁴



Fluorine exchange between XeF₂ and HF has been established on the radiochemical timescale, as well as on the NMR timescale by use linewidth measurements in variable-temperature ¹⁹F and ¹²⁹Xe NMR spectra.^{191,192} In the present work, exchange of XeF₂ with HF was studied by variable-temperature ¹⁹F and ¹²⁹Xe NMR spectroscopy using a saturated solution of XeF₂ in anhydrous HF solvent, in order to estimate the standard enthalpy of formation for this exchange reaction. The ¹⁹F NMR

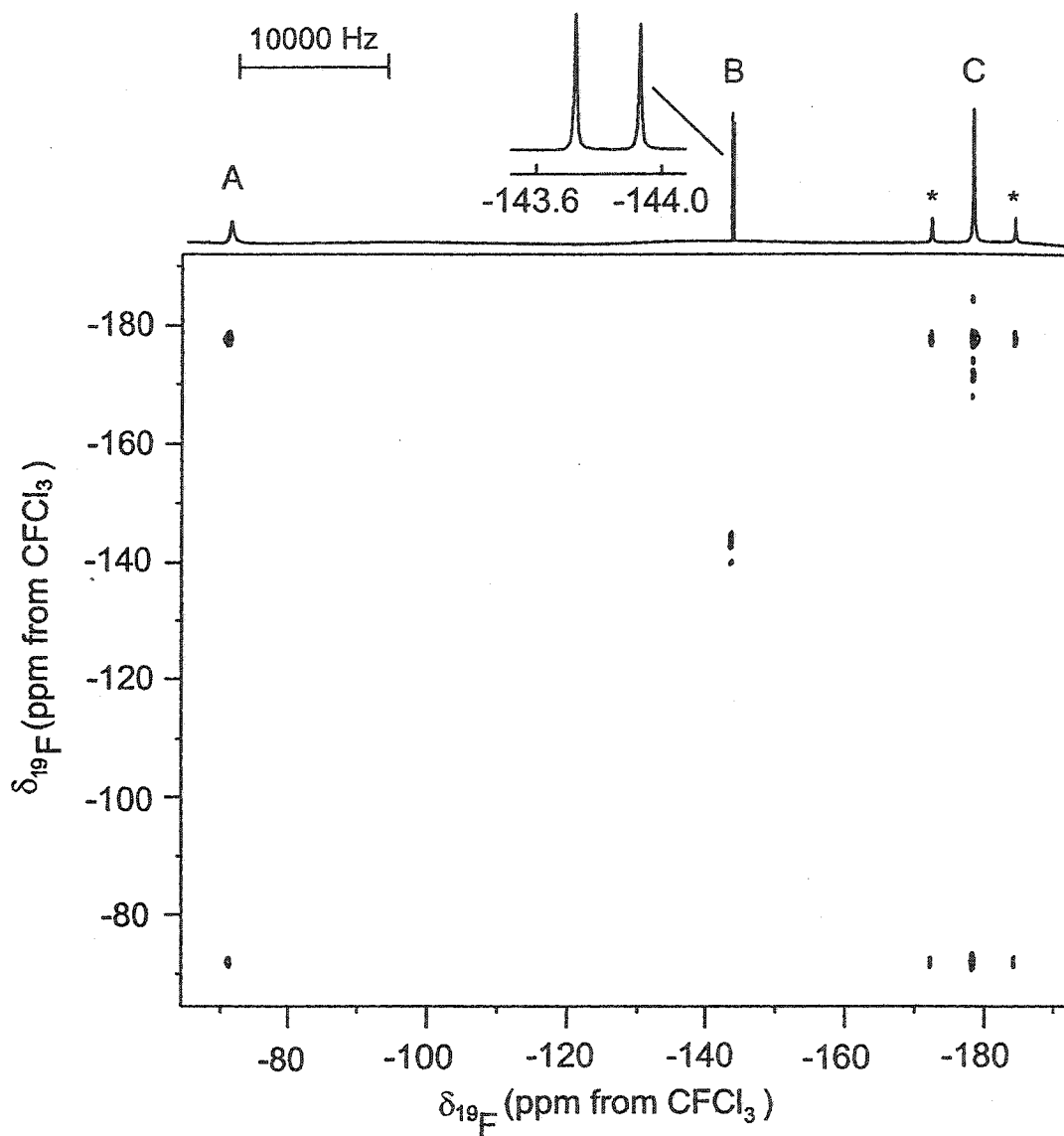


Figure 7.1. 2-D ^{19}F - ^{19}F EXSY spectrum of an equimolar sample of XeF_2 and $[\text{N}(\text{CH}_3)_4][\text{F}]$ in CH_3CN solvent, acquired at 15°C using a mixing time of 400 ms. The labels A, B, and C refer to F^- , HF_2^- ($^1J_{\text{HF}}$, 120 Hz), and XeF_2 ($^1J(^{129}\text{Xe}-^{19}\text{F})$, 5657.2 Hz), respectively.

spectra were acquired over a temperature range of -80 to 30 °C. The spectra revealed significant line broadening, however, overlap between the ^{19}F signal of XeF_2 and the ^{129}Xe - ^{19}F satellites occurred with the HF signal in the ^{19}F NMR spectra. The ^{129}Xe NMR spectra showed only a triplet for XeF_2 and significant line broadening between -27 °C and 30 °C (Figure 7.2). The standard enthalpy of activation, ΔH^\ddagger , was determined for this sample to be 9 ± 1 kcal mol $^{-1}$, by use of exchange lineshape calculations.¹⁹³

7.2.6 On the Influence of Solvent and Vessel upon the Reactions of XeF_2 with Organic Substrates

It has been assumed that F^- ion exchange with XeF_2 proceeds by a dissociative mechanism. Ramsden and Smith¹⁹⁴ claim that Pyrex glass surfaces catalyze the ionization of XeF_2 in CH_2Cl_2 , CHCl_3 , CFCl_3 and C_6F_6 solvents to presumably form the strong electrophile XeF^+ (estimated electron affinity, 10.9 eV¹⁹⁵). There are numerous examples of stable XeF^+ salts,^{196,197} and it is well recognized in the field of noble-gas chemistry that the XeF^+ cation is only stable in a very limited number of inorganic solvent media which are not susceptible to oxidative attack, such as anhydrous HF and BrF_5 , thus the formation of the strong electrophile, XeF^+ , as a reactive intermediate in organic solvents is unlikely and unfounded. A more likely scenario involves an HF assisted exchange in which HF hydrogen bonds to and polarizes XeF_2 , followed by nucleophilic attack at xenon by the fluorine of HF. Moreover, these authors¹⁹⁴ also claimed F^- ion exchange with XeF_2 does not occur under certain conditions, such as in an FEP vessel or in CH_3CN

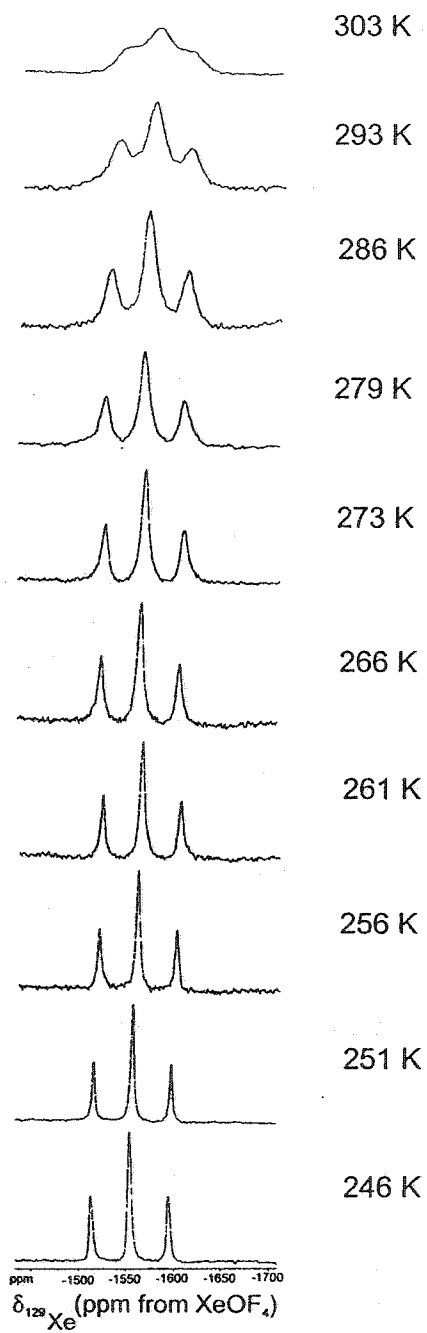
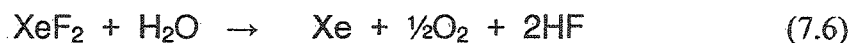


Figure 7.2. Variable-temperature ^{129}Xe NMR spectra of a sample of XeF_2 in HF .

solvent, and it was also suggested that CH₃CN inhibits the exchange of XeF₂ with [2,2,2-crypt-M][¹⁸F].⁶⁶ Contrary to these claims, a 2-D ¹⁹F-¹⁹F EXSY experiment in this study has demonstrated that fluoride ion exchanges with XeF₂ in CH₃CN solvent contained in an FEP vessel (see section 7.2.5).

Ramsden and Smith¹⁹⁴ have also claimed that the catalytic effects of glass surfaces in electrophilic fluorination reactions using XeF₂ in dry CH₂Cl₂ circumvent the need for HF in reactions described as requiring HF catalysis. The alleged surface catalysis of XeF₂/F⁻ exchange is more likely attributable to HF attack of the glass surface.

The origin of HF, as pointed out previously, may arise from occlusion of HF by XeF₂,¹⁹⁸ as well as from solvent attack by XeF₂, as described above, and from a lack of truly anhydrous conditions (eq. 7.6). Attack of glass by HF is a cyclic process, producing water which further reacts with and reduces XeF₂ to produce HF (eq. 7.6). Moreover, the H₂O/HF/glass system is repeatedly emphasized in the literature of fluorine chemistry to introduce a variety of species, including boron- and silicon-containing Lewis acids,¹⁹⁹ which may also serve as fluorine exchange catalysts.⁶²



7.2.7 The Synthesis of [¹⁸F]XeF₂ by ¹⁸F⁻ Exchange with XeF₂ in CH₂Cl₂

There are several major concerns relating to exchange of ¹⁸F-labelled fluoride ion with XeF₂ as previously reported.⁶⁶ Among these are the large molar excess of XeF₂ relative to 2,2,2-crypt (56 : 1) and the high concentration (0.285 M) of XeF₂ in CH₂Cl₂

that was required to effect exchange with n.c.a. $^{18}\text{F}^-$ ion in 1 mL of CH_2Cl_2 . Attempts to repeat the previous work⁶⁶ and to exchange 10 mCi of n.c.a. $^{18}\text{F}^-$ ion (5.8×10^{-10} mole), in the form of [2,2,2-crypt-K][^{18}F], with XeF_2 in 1 mL of CH_2Cl_2 solvent at room temperature were unsuccessful in the present study. Separate HPLC experiments (Phenomenex, Hypersil C18, $5\mu\text{m}$, 25×0.46 cm, eluted with 60% $\text{CH}_3\text{CN}/\text{H}_2\text{O}$, using a flow rate of 1.0 mL/min) were run for n.c.a. $^{18}\text{F}^-$ and XeF_2 to establish their retention times. Sharp peaks corresponding to $^{18}\text{F}^-$ (3.1 min) and XeF_2 (UV, $\lambda = 254$ nm, 3.8 min) were obtained. The chromatograms acquired for the reaction of [2,2,2-crypt-K][^{18}F] with XeF_2 in CH_2Cl_2 solvent at room temperature after 1 h were not reproducible. The UV trace showed a sharp peak with a retention time corresponding to XeF_2 (3.8 min), however, the radiochromatogram showed one broad, tailing ^{18}F -containing peak that eluted from 4 to 6 min which was not identified. The broad peak is consistent with the co-elution of several species, but no discrete $^{18}\text{F}^-$ ion peak was observed. "Cold" experiments, described in previous sections, demonstrate that the system is complex and leads to several fluorinated products. The ^{18}F exchange experiments described previously and here employed carbonate⁶⁶ or bicarbonate, respectively. Both anions are known to accelerate the decomposition of XeF_2 in aqueous media.²⁰⁰ The inability to separate $^{18}\text{F}^-$ from [^{18}F] XeF_2 in the radiochromatogram results because the ^{18}F activity is distributed among XeF_2 , F^- , HF and HF_2^- , as well as the products of solvent fluorination (*vide supra*).

Fluorine-18 exchange experiments between XeF_2 and ^{18}F -labelled fluoride ion, in the form of a tetraalkylammonium salt, were not attempted because it is difficult to obtain rigorously anhydrous ^{18}F -labelled fluoride salts. Consequently, the formation of fluoride

ion hydrates, $F^-(H_2O)_n$ ($n = 1-6$),²⁰¹ in ^{18}F -labelling experiments is expected to greatly attenuate the degree of fluoride ion "nakedness" in these studies, and the reaction of XeF_2 with coordinated water and trace amounts of other adventitious water is expected to lead to HF (eq. 7.6) and HF_2^- (eq. 7.4). Furthermore, the reaction of XeF_2 with CH_2Cl_2 is known to produce CH_2ClF , $CHCl_2F$ and HF, with CH_2F_2 , $CHClF_2$, CCl_2F_2 , and $CFCl_3$ as minor ($< 0.5\%$) products.¹⁸¹ These factors could also account for the failure of $[N(n-Bu_4)_4][^{18}F]$ to undergo exchange with XeF_2 in CH_2Cl_2 .¹⁷⁹

Because multiple fluorination side products have been shown to form in reactions of "cold" fluoride ion and XeF_2 with CH_3CN and CH_2Cl_2 solvents at room temperature after 1 h, these methods are also not practical routes for the preparation of $[^{18}F]XeF_2$ from n.c.a. $^{18}F^-$ ion. Moreover, the resulting hydrochlorofluorocarbons can be highly toxic, i.e., CH_2ClF is a known carcinogen,²⁰² and thus pose problems for medicinal use if the toxins cannot be reliably separated.

7.3 Conclusions

The present work demonstrates, by EXSY NMR studies, that XeF_2 exchanges with fluoride ion when a countercation, such as $N(CH_3)_4^+$, is employed that is oxidatively resistant to XeF_2 . The exchange is postulated to proceed through the XeF_3^- anion as the intermediate. Moreover, this study shows that a 33 : 1 molar ratio of XeF_2 to 2,2,2-crypt in CH_2Cl_2 solvent leads to fluorination of 2,2,2-crypt and CH_2Cl_2 , producing $CHCl_2F$, CH_2F_2 , CH_2ClF and large amounts of HF and HF_2^- . These findings establish that the previously claimed⁶⁶ catalytic behavior of 2,2,2,-crypt- M^+ (and its implied inertness) in

the ionization of XeF_2 and in fluoride ion exchange with XeF_2 are erroneous. Reactions of $[\text{2,2,2-crypt-K}][^{18}\text{F}]$ with XeF_2 in CH_2Cl_2 solvent in the present study were not reproducible and were complicated by fluorinated products, including large amounts of HF, that result from fluorination of 2,2,2-crypt and the solvent. The exchange observed in previous work⁷ is attributable to HF formation, in accord with earlier ^{18}F -exchange studies which have shown that HF undergoes fluorine exchange with XeF_2 by acting as a weak fluoride ion acceptor towards XeF_2 (eq. 7.1 and 7.2).⁶² It must also be concluded that exchange reactions between n.c.a. $[\text{2,2,2-crypt-M}][^{18}\text{F}]$ salts and XeF_2 in CH_2Cl_2 at room temperature are not viable routes to $[^{18}\text{F}]\text{XeF}_2$ for use in clinical work.

CHAPTER 8

AN NMR SPECTROSCOPIC STUDY OF XeF_2/F^- EXCHANGE AND THEORETICAL STUDIES OF THE XeF_3^- ANION AND ATTEMPTED SYNTHESSES OF XeF_3^- SALTS

8.1 Introduction

Xenon tetrafluoride and XeF_6 behave as fluoride ion acceptors. Xenon tetrafluoride has been shown to be a weak fluoride ion acceptor towards alkali metal fluorides and the naked fluoride ion source $[\text{N}(\text{CH}_3)_4][\text{F}]$, forming salts of the pentagonal planar XeF_5^- anion.⁹⁴ Xenon hexafluoride is a considerably stronger fluoride ion acceptor toward alkali metal fluorides,^{203,204} NOF and NO_2F ²⁰⁵ forming the XeF_7^- and XeF_8^{2-} anions. The salt, $[\text{NO}]_2[\text{XeF}_8]$, was shown, by single crystal X-ray diffraction, to contain a slightly distorted square antiprismatic XeF_8^{2-} anion.²⁰⁵ More recently, the XeF_7^- and $\text{Xe}_2\text{F}_{13}^-$ anions were characterized by X-ray crystallography as their Cs^+ and NO_2^+ salts, respectively.²⁰⁶ The XeF_7^- anion may be described as a monocapped octahedral structure and the $\text{Xe}_2\text{F}_{13}^-$ anion may be regarded as an XeF_6 molecule bridged by two long $\text{Xe}\cdots\text{F}$ bonds to an XeF_7^- anion such that the bridge fluorines avoid the axial nonbonding

electron pair of the XeF_6 molecule. Xenon hexafluoride also reacts with $[\text{NF}_4][\text{HF}_2]$ in anhydrous hydrogen fluoride to give $[\text{NF}_4][\text{XeF}_7]$ which was converted to $[\text{NF}_4]_2[\text{XeF}_8]$ by selective laser photolysis and characterized by vibrational spectroscopy.²⁰⁷

Although XeF_4 and XeF_6 behave as fluoride ion acceptors forming stable salts with a variety of cations, XeF_2 has not been shown to exhibit fluoride ion acceptor properties in solution or in the solid state. The XeF_3^- anion was first suggested by Ward²⁰⁸ to be a plausible species by consideration of diagonal relationships within the periodic table (Figure 8.1). The only prior experimental evidence for the trifluoroxenate(II) anion, XeF_3^- , is in the gas phase, which was obtained from the negative ion mass spectra of XeF_2 ²⁰⁹ and XeOF_4 .²¹⁰ Although the XeF_3^- anion has been proposed as an intermediate in the “base-catalyzed” fluorination of SO_2 by XeF_2 ,²¹¹ reasonable alternative mechanisms were subsequently proposed for this reaction which do not invoke XeF_3^- as an intermediate.²¹² It has been noted²¹² that exchange between ^{18}F -labelled fluoride ion and XeF_2 in water is not observed.¹⁷⁸ This is not surprising in view of recent findings which show that the degree of fluoride ion “nakedness” is severely compromised in aqueous solution by the formation of H-bonded fluoride ion hydrates, $(\text{H}_2\text{O})_n\text{F}^-$ ($n=1-6$).²⁰¹

The exchange between F^- and XeF_2 was observed by use of 2-D ^{19}F - ^{19}F EXSY experiments (see Chapter 7, Figure 7.1).⁶⁷ The ^{19}F exchange occurred between the “naked” fluoride ion source $[\text{N}(\text{CH}_3)_4][\text{F}]$ and XeF_2 in CH_3CN solvent at 15 °C, providing the first conclusive evidence for XeF_2 and fluoride ion exchange on the NMR

Group 15	Group 16	Group 17	Group 18
NF_4^+			
	SF_3^+		
	SF_4	BrF_2^+	
	SF_5^-	BrF_3	XeF^+
		BrF_4^-	XeF_2
			XeF_3^-

Figure 8.1. Diagonal relationships within the periodic table suggesting that XeF_3^- may be stable.

timescale.⁶⁷ The ^{19}F exchange was postulated to proceed through the formation of the trifluoroxenate(II), XeF_3^- anion (eq. 7.5).

The experimental objectives of the present study were to better define the nature of the transition state in the XeF_2/F^- exchange by NMR spectroscopy and to establish the fluoride ion acceptor properties of XeF_2 by attempting the syntheses of representative salts containing the XeF_3^- anion. Computational methods have been used to explore the nature of the intermediate in the XeF_2/F^- exchange and to arrive at the global energy minimum for the XeF_3^- anion and its corresponding geometry as well as the gas-phase fluoride ion affinity of XeF_2 relative to those of XeF_4 , XeF_6 and related fluorides. The theoretical calculations discussed in this chapter (DFT, MP2 and ELF) were provided by Dr. Reijo J. Suontamo, Department of Chemistry, University of Jyväskylä, Finland. The details of these computations will be described in a subsequent publication.¹⁰⁴

8.2 Results and Discussion

Ward²⁰⁸ suggested that the XeF_3^- anion would have an octahedral arrangement of three bond pairs and three electron lone pairs. It was subsequently noted by Liebman,²¹² who invoked the VSEPR rules,²¹³ that the *mer*-isomer (Figure 8.2 (a)) is expected to be more stable owing to the lower number (2) of lone pair – lone pair repulsions at 90° when compared with those (3) of the *fac*-isomer (Figure 8.2 (b)). Although the AX_3E_3 (E = valence electron lone pair) VSEPR arrangement of the *mer*-isomer minimizes 90° lone pair-lone pair repulsions, there are no known examples in which two or more valence

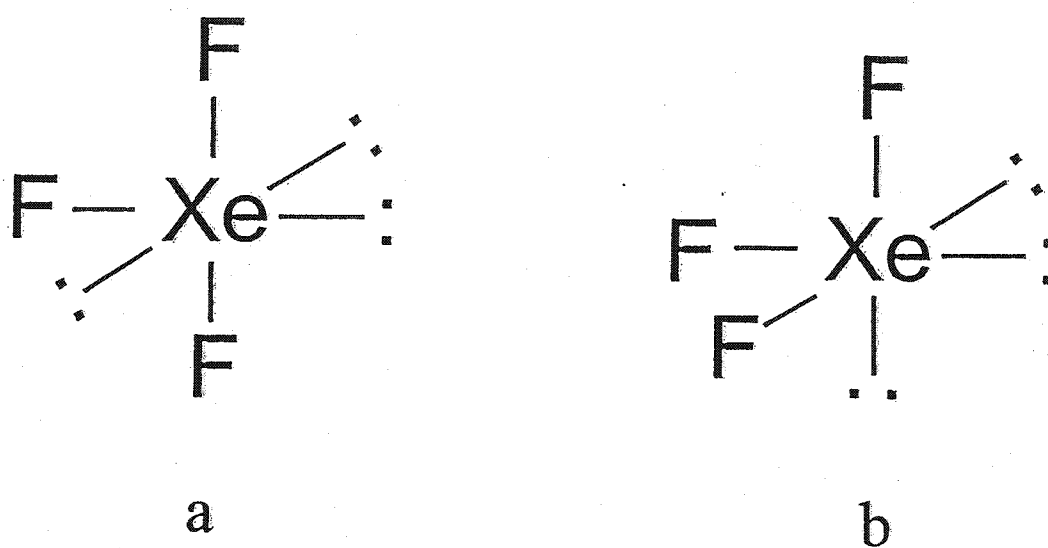


Figure 8.2. Geometries of the XeF_3^- anion depicting octahedral arrangements of bond-pairs and lone-pairs, for the meridional (a) and facial (b) arrangements, respectively.

electron lone pairs occur at approximately 90° to one another. Thus, use of VSEPR rules by Liebman in this instance may be inappropriate and renders the geometry of XeF_3^- problematic when derived from an octahedral arrangement of bond pairs and lone pairs. It was for this reason that the determination of the energy minimized geometry for the gas-phase XeF_3^- anion was undertaken using electron structure calculations.

8.2.1 Energy Minimized Geometry of the XeF_3^- Anion

The fully optimized geometry (SVWN/DZVP) for XeF_3^- is predicted to be planar and Y-shaped (C_{2v}) (Figure 8.3) and represents the first example of an AX_3E_3 arrangement. The calculated Y-shaped planar structure of the XeF_3^- anion can be rationalized in terms of the VSEPR theory with the aid of the electron localization function (ELF). The ELF calculation of XeF_2 (Figure 8.4 (a)) shows that the electron density of the three valence electron lone pairs is distributed to form a torus of electron density around the central xenon atom. The presence of a torus instead of three discrete lone pairs has been previously suggested in an X-ray crystallographic study of XeF_2 ²¹⁴ and established by ELF calculations for ClF_2^- , noting that XeF_2 is isovalent with the latter ion.²¹⁵ Starting from linear XeF_2 , the addition of a fluoride ion from above or below the plane leads to the formation of a Y-shaped XeF_3^- anion in which the torus about xenon is slightly distorted. This rationale is supported by the ELF calculations (Figure 8.4 (b))

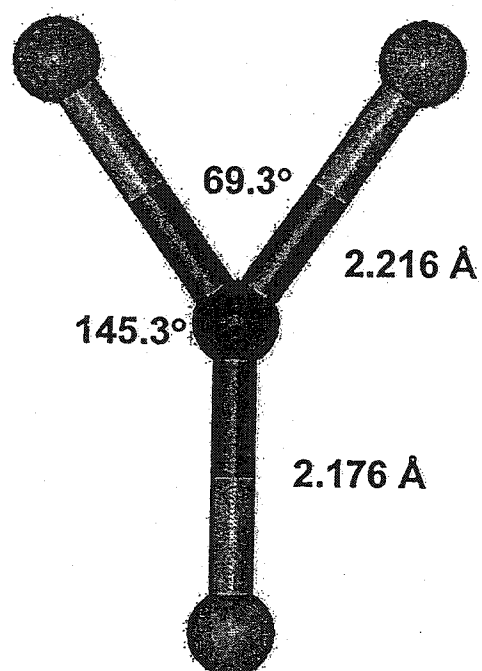


Figure 8.3. The fully optimized geometry (SVWN/DZVP) for the XeF_3^- anion.

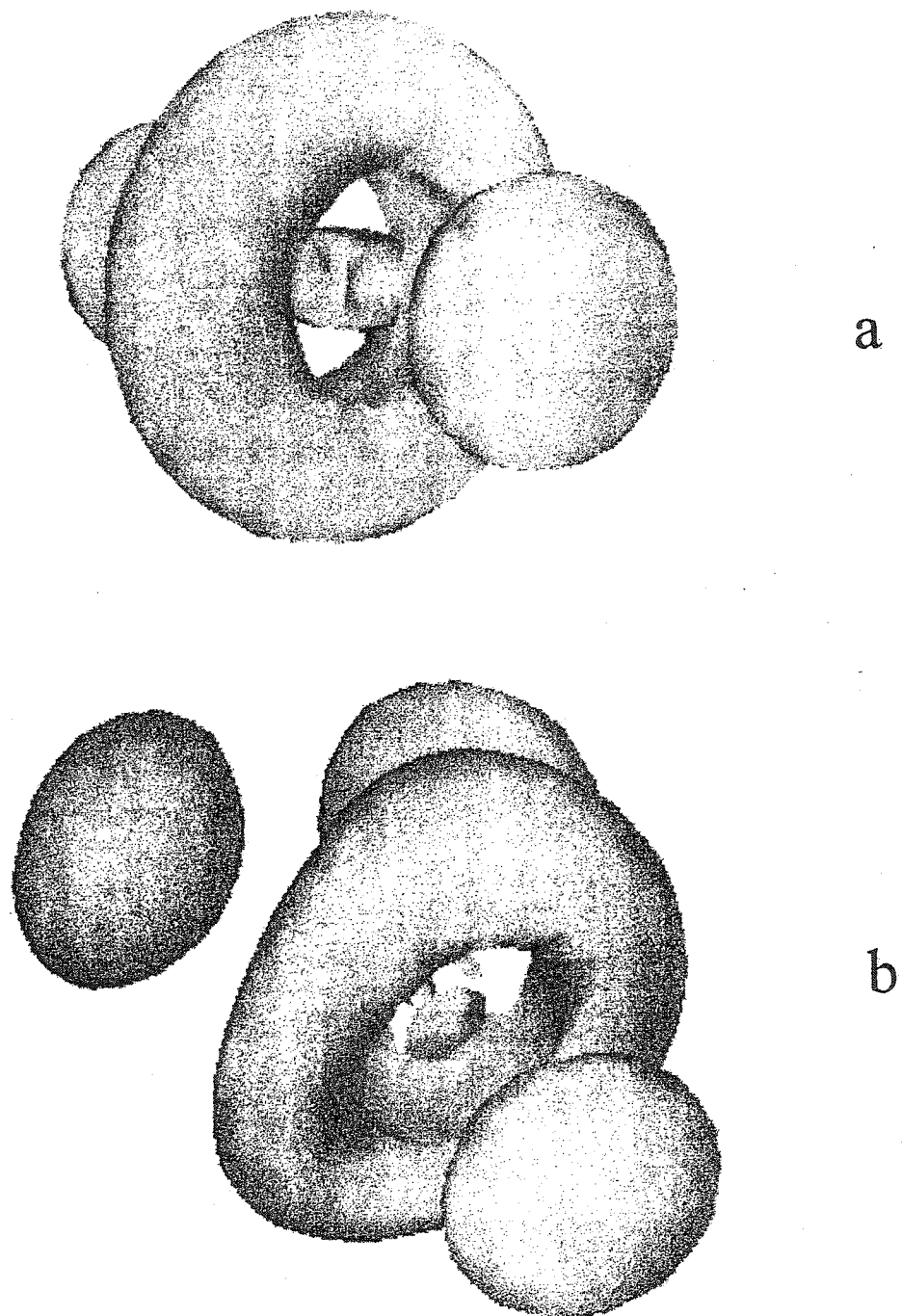


Figure 8.4. ELF calculations of (a) XeF₂ and (b) the XeF₃⁻ anion. Contours are drawn at the 0.60 localization.

It is interesting to compare the planar geometry of XeF_3^- with that of the XeF_5^- anion. The latter pentagonal planar anion has an AX_5E_2 arrangement in the xenon valence shell and is related to the AX_3E_3 arrangement of XeF_3^- (Figure 8.5) by removal of two non-adjacent fluorines from XeF_5^- and by their replacement with a torus of three electron lone pairs perpendicular to the anion plane. This results in a Y-shaped geometry for XeF_3^- which is superimposable with the XeF_5^- pentagon. Thus, the smallest F—Xe—F angle of 69.3° in XeF_3^- is nearly identical with the ideal pentagonal angle of 72° in XeF_5^- , and the larger F—Xe—F angles of 145.3° are essentially twice the ideal pentagonal angle.

8.2.2 Attempted Syntheses of Salts Containing the XeF_3^- Anion

The reaction of XeF_2 with $[\text{N}(\text{CH}_3)_4][\text{F}]$ was carried out in CH_3CN solvent at room temperature and in CHF_3 solvent at 0°C in an attempt to synthesize $[\text{N}(\text{CH}_3)_4][\text{XeF}_3]$. The Raman spectra of these samples were recorded on the samples with the solvent present and on the non-volatile residues remaining after solvent removal and only revealed bands corresponding to unreacted XeF_2 and $[\text{N}(\text{CH}_3)_4][\text{F}]^{97}$ (see sec. 2.1.3), and did not show new bands predicted for the vibrational frequencies of the XeF_3^- anion (Table 8.1).

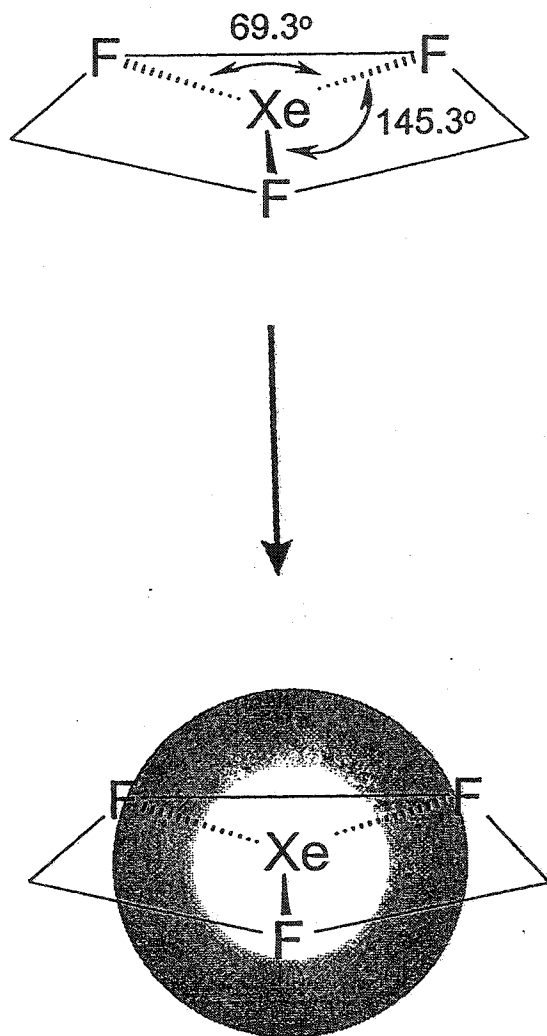


Figure 8.5. A comparison of the XeF_3^- anion geometry with that of the XeF_5^- anion.

Table 8.1. Vibrational Frequencies of the XeF_3^- Anion Calculated^a at the DFT Level of Theory^b.

Assignments (C_{2v} point symmetry)	Frequency (cm^{-1}) ^a
$\nu_1(A_1)$	437.4 (231)
$\nu_2(A_1)$	337.6 (2)
$\nu_3(A_1)$	263.2 (0)
$\nu_4(B_1)$	165.5 (27)
$\nu_5(B_2)$	319.6 (37)
$\nu_6(B_2)$	108.2 (53)

^aInfrared intensities (km mol^{-1}) are given in parentheses.

^bThe basis set used was SVWN/DZVP.

Christe²¹⁶ has shown that F₂ does not interact with [N(CH₃)₄][F] in CH₃CN or CHF₃ solvent to form [N(CH₃)₄][F₃] at low temperatures. The lack of reactivity is attributed to the high solvation energies of fluoride ion in both polar solvents. The inability to form a salt of the XeF₃⁻ anion in CH₃CN and CHF₃ solvents in the present study can be similarly explained. Christe,²¹⁶ however, did not attempt to react F₂ with [N(CH₃)₄][F] in the absence of a solvent because of the experimental difficulties anticipated in controlling the reaction.

The syntheses of the Cs⁺ and N(CH₃)₄⁺ salts containing the XeF₃⁻ anion were attempted in the absence of a solvent in the present work. Heating a four-fold molar excess of XeF₂ (m.p., 129 °C) with respect to CsF resulted in no reaction up to 170 °C. When a six-fold molar excess of XeF₂ with respect to [N(CH₃)₄][F] was heated slowly to the melting point of XeF₂, the N(CH₃)₄⁺ cation was rapidly oxidized and the sample detonated.

Christe and co-workers²¹⁷ have recently established a quantitative scale for Lewis acidities based on fluoride ion affinities and have calculated the fluoride ion affinities using *ab initio* calculations at the MP2 level of theory for more than 100 compounds, including XeF₄ (-57.1 kcal mol⁻¹). The gas-phase fluoride ion affinity of XeF₂ at 0 K was calculated at the DFT level of theory (SVWN/DZVP) in the present work, and compared with those of other known fluorides (eq. 8.1, Table 8.2).

Table 8.2. Gas-Phase Fluoride Ion Affinities^a of Selected Fluorides.

Compound	Fluoride Ion Affinity ^b (kcal mol ⁻¹)
KrF ₂	-16.4
NOF	[-17.4]
NO ₂ F	[-19.2]
XeF ₂	-21.8
HF	[-36.8]
PF ₃	[-44.9]
COF ₂	[-49.9]
XeF ₄	-60.0 [-57.1]
XeOF ₄	[-63.7]
XeF ₆	-77.7

^aCalculated at 0 K at the DFT level of theory using a SVWN/DZVP basis set.

^bThe values in brackets are from ref. (217).

The fluoride ion affinity calculated for XeF₄ in the present study is in good agreement with the previously reported value.²¹⁷ It is apparent from Table 8.1 that the fluoride ion affinity of XeF₂ (-21.8 kcal mol⁻¹) is significantly lower than those of XeF₄ (-60.0 kcal mol⁻¹) and XeF₆ (-77.7 kcal mol⁻¹). The higher fluoride ion affinities of XeF₄ and XeF₆, compared with XeF₂, are expected because both fluorides form stable fluoroanions, i.e., XeF₅⁻, XeF₇⁻, XeF₈²⁻ and Xe₂F₁₃⁻ (*vide supra*). The inability to isolate salts of the XeF₃⁻ anion in the present work is consistent with the relatively low fluoride ion affinity of XeF₂. The fluoride ion affinity of KrF₂ is only -16.4 kcal mol⁻¹ and is lower than that reported for NOF, -17.4 kcal mol⁻¹, the lowest fluoride ion affinity reported by Christe and co-workers.²¹⁷ It is noteworthy that KrF₂ has not been shown to exhibit fluoride acceptor properties,¹⁹⁷ which is also consistent with the low fluoride ion affinity of this molecule. Furthermore, variable-temperature ¹⁹F NMR spectra of KrF₂ in HF did not show significant line broadening between -80 and 15 °C, whereas XeF₂ in HF solutions clearly undergoes ¹⁹F exchange under these conditions (Chapter 7, sec. 7.2.5).

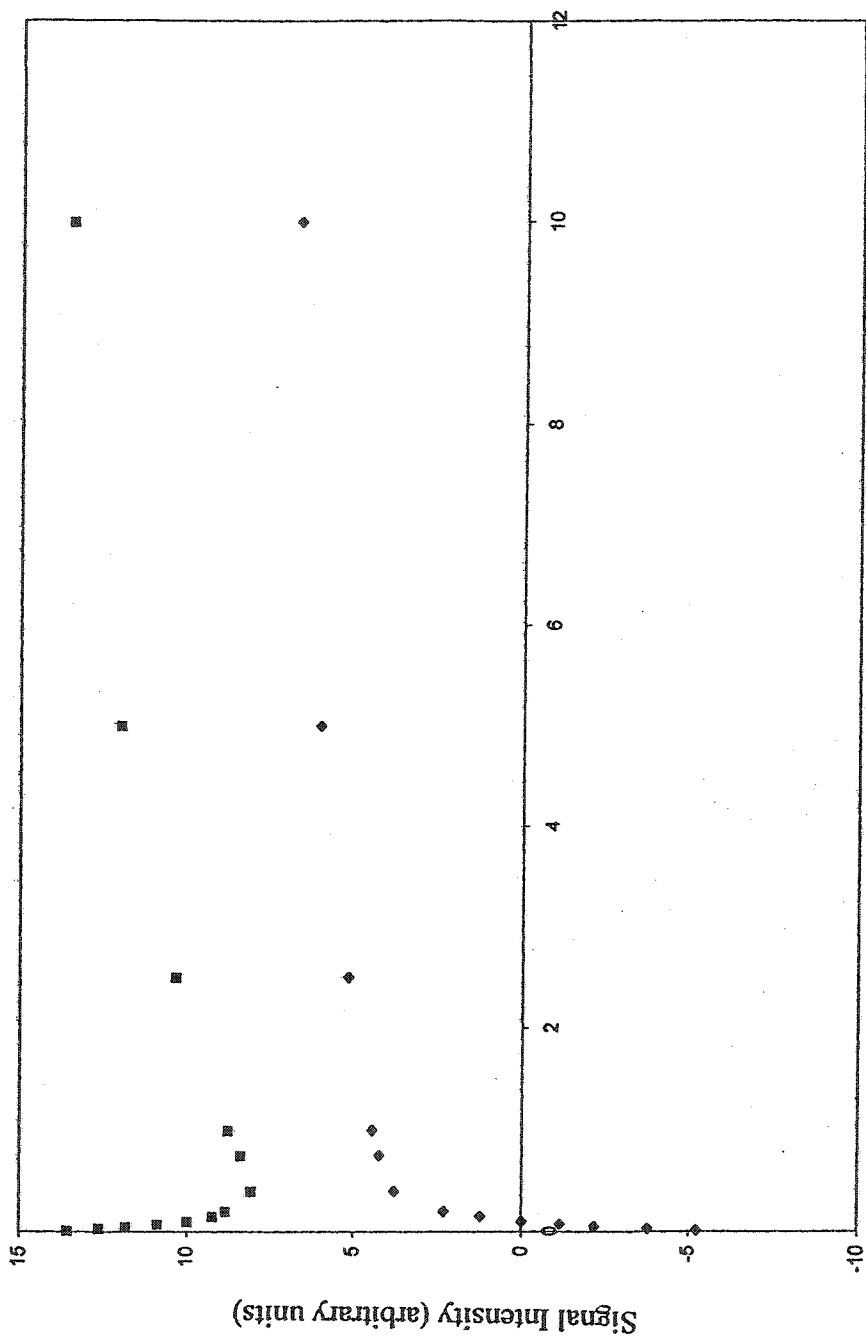


8.2.3 Intermolecular Exchange Between Fluoride Ion and XeF₂

One-dimensional NMR methods have been proclaimed to be better suited for the study of slow exchange processes than two-dimensional methods such as EXSY experiments.²¹⁸ Single selective inversion experiments are particularly useful for measuring slow exchange rates, and if such experiments can be carried out over a wide

range of temperatures, the thermodynamics of the transition state can also be investigated. The standard enthalpy of activation, ΔH^\ddagger , for intermolecular ^{19}F exchange between fluoride ion and XeF_2 was determined using equimolar samples of $[\text{N}(\text{CH}_3)_4][\text{F}]$ and XeF_2 in CH_3CN solvent in conjunction with single selective inversion NMR spectroscopic studies conducted at variable-temperatures. Figure 8.6 shows the results of a ^{19}F selective inversion experiment acquired for a sample containing 0.18 M XeF_2 and 0.18 M $[\text{N}(\text{CH}_3)_4][\text{F}]$ in CH_3CN solvent and acquired for various delay times at $-15\text{ }^\circ\text{C}$. Analysis of this intermolecular exchange process recorded over a range of temperatures from -40 to $0\text{ }^\circ\text{C}$ showed that the data were fit with a ΔH^\ddagger value of $17.7 \pm 1.2\text{ kcal mol}^{-1}$ (Figure 8.7). A more concentrated sample, 0.36 M XeF_2 and 0.36 M $[\text{N}(\text{CH}_3)_4][\text{F}]$ in CH_3CN solvent, was studied over the temperature range of -15 to $-35\text{ }^\circ\text{C}$, and the data were fit with a ΔH^\ddagger value of $13.6 \pm 1.6\text{ kcal mol}^{-1}$. The more concentrated sample exhibited a faster fluorine exchange rate than the less concentrated sample. The discrepancy between the two measured in standard activation enthalpies is not surprising considering that the single selective inversion experiments could only be conducted over relatively narrow temperature ranges owing to the onset of decomposition (fluoride ion attack on CH_3CN at higher temperatures (eq. 7.3 and 7.4).

The potential energy surface for the formation of the XeF_3^- anion from XeF_2 and F^- is under investigation by Dr. Reijo J. Suontamo, Department of Chemistry, University of Jyväskylä, Finland. This study is focused on the determination of the standard



Time (s)

Figure 8.6. Results of a selective inversion experiment conducted on a sample containing quantities of XeF₂ and [N(CH₃)₄][F] in CH₃CN solvent (0.2 M) acquired at -15 °C. The XeF₂ signal is represented by squares and the signal corresponding to fluoride ion, represented by diamonds, was selectively inverted. This figure shows the full-observed relaxation under the combined influence of spin-lattice relaxation and chemical exchange.

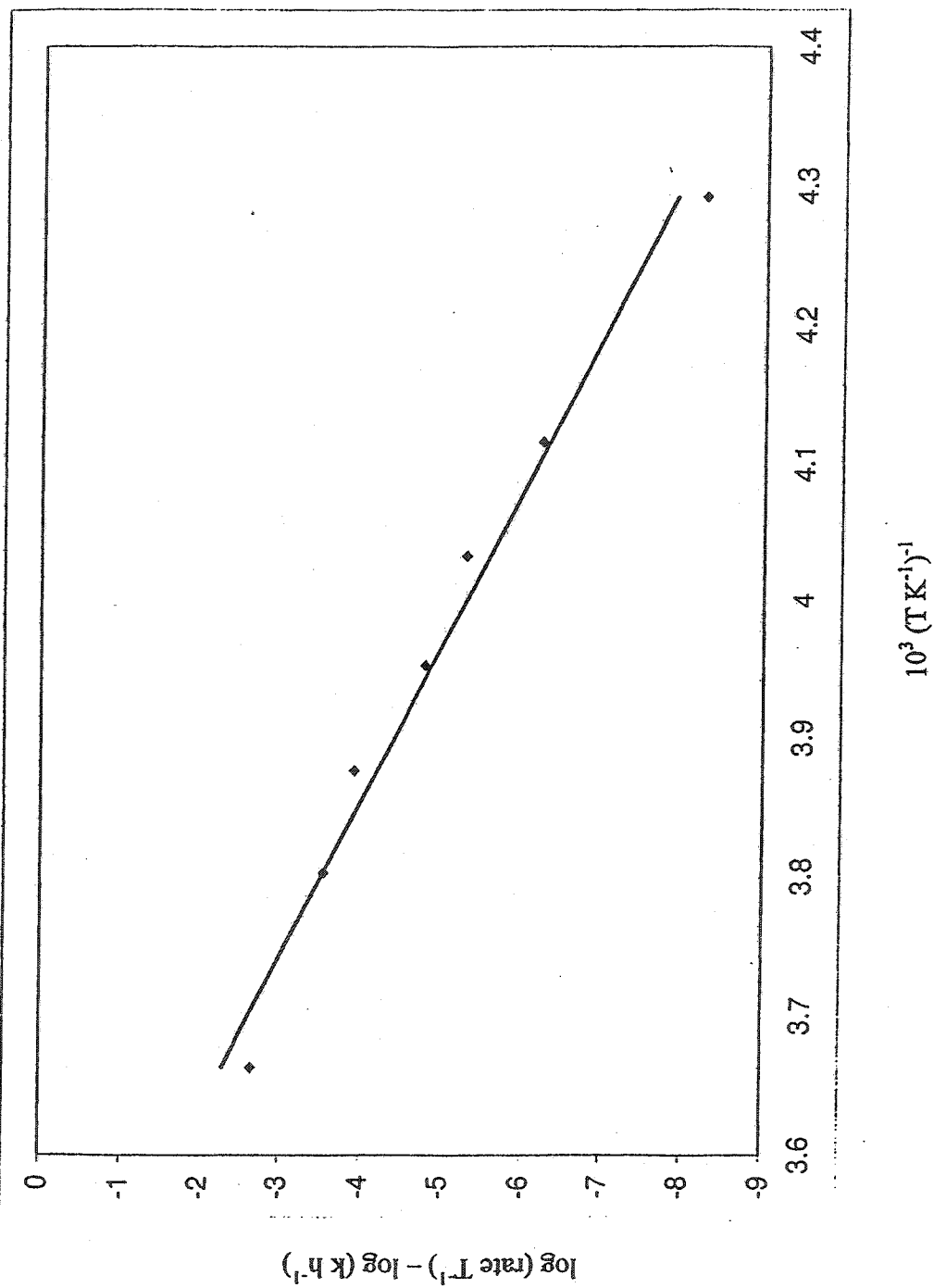


Figure 8.7. Eyring Plot of the rate data for the intermolecular ^{19}F -exchange between XeF_2 and $[\text{N}(\text{CH}_3)_4][\text{F}]$ in CH_3CN solvent (0.2 M) acquired at temperatures between -40 to 0°C .

activation parameters for this reaction with the view to compare the theoretical ΔH^\ddagger value with the experimental values determined from the NMR experiments described in this work. These studies should provide insight into the nature of the transition state and the XeF_3^- intermediate.

8.3 Conclusions

The standard enthalpy of formation for the intermolecular ^{19}F -exchange between XeF_2 and $[\text{N}(\text{CH}_3)_4][\text{F}]$ in CH_3CN solvent was measured by single selective inversion NMR spectroscopy and determined to be $17.7 \pm 1.2 \text{ kcal mol}^{-1}$ and $13.6 \pm 1.6 \text{ kcal mol}^{-1}$ for samples prepared in concentrations of 0.18 M and 0.36 M, respectively. The inability to synthesize salts containing the XeF_3^- anion in the present work is attributed to the low fluoride ion affinity of XeF_2 (-21.8 kcal/mol) relative to those of other fluoride ion acceptors. The calculated energy minimized geometry (MP2 and DFT) of the XeF_3^- anion is predicted to have an unusual Y-shaped planar structure and represents the first example of an AX_3E_3 species. The geometry of this unique species has been rationalized by use of ELF calculations, as well as in terms of the VSEPR model of molecular geometry.

CHAPTER 9

CONCLUSIONS AND DIRECTIONS FOR FUTURE WORK

9.1 Conclusions

Direct fluorination methodologies involving electrophilic fluorine sources have been significantly extended in the present work by use of ^{18}F -labelling and NMR spectroscopic studies. By judicious control of the reaction conditions and solvent acidity, a method for the site-specific electrophilic substitution of fluorine on the aromatic ring of L-DOPA was developed and used to synthesize clinically useful quantities of [^{18}F]5-fluoro-L-DOPA as a radiopharmaceutical for the first time. Prior to the present study, the fate of [^{18}F]5-fluoro-L-DOPA in the human brain was not known. Synthetic protocols developed in the present work have enabled the first human PET study involving [^{18}F]5-fluoro-L-DOPA to be conducted. In this work, the *in vivo* biodistribution of [^{18}F]5-fluoro-L-DOPA in the brain was compared with [^{18}F]2-fluoro-L-DOPA and [^{18}F]6-fluoro-L-DOPA. It was concluded that the only ring fluoro-isomer of L-DOPA that can be used for tracing intracerebral dopamine is [^{18}F]6-fluoro-L-DOPA.

The synthetic method for the development of site-specific aromatic fluorinations on L-DOPA was applied to a high yield synthesis of the tumour seeking agent [^{18}F]3-fluoro-L- α -methyltyrosine (3-F- α -MT). In this work, 3-F- α -MT was synthesized in 1 h in a formulation ready for injection, by direct fluorination of L- α -MT in anhydrous HF solvent in a 30% radiochemical yield with respect to [^{18}F]F $_2$ (theoretical maximum yield is 50%). The radiochemical yield in the present work is more than triple that of the previously reported work. The present study also served to correct the erroneously reported synthesis of 2-F- α -MT. By thorough NMR spectroscopic studies and mass spectrometry, the compound assigned as 2-F- α -MT was shown to be [^{18}F]3,5-difluoro-L- α -MT. In the course of this work, [^{18}F]3,5-difluoro-L- α -MT and [^{18}F]3,5-difluoro-L-tyrosine were synthesized for the first time.

An extension of this work with fluorinated L-tyrosine derivatives and another synthetic goal of this work was the development of a radiolabelled derivative of 3-nitro-L-tyrosine. There is significant interest in the detection of 3-nitro-L-tyrosine as a biomarker for reactive nitrogen species, which are responsible for *in vivo* nitration. This project involved the development of aromatic nitration methods, as well as direct fluorination methodologies to synthesize [^{18}F]5-fluoro-3-nitro-L-tyrosine for the first time. The synthetic protocols developed in the present studies can be applied to the syntheses of nitrofluoroaromatics.

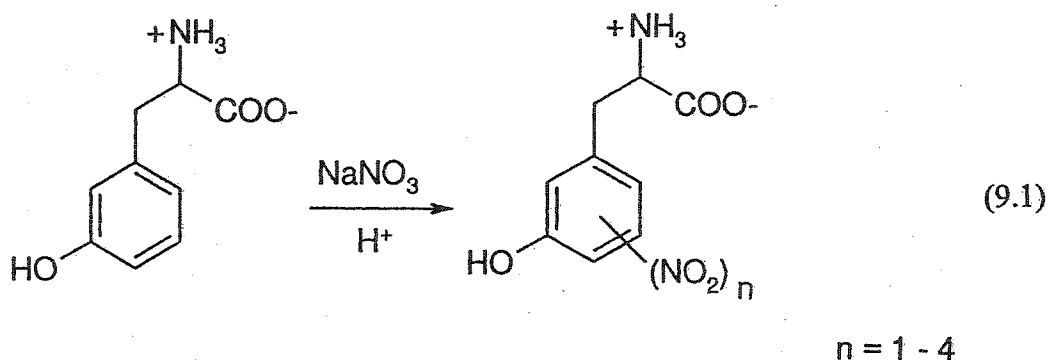
The synthesis of [^{18}F]XeF $_2$ by an exchange reaction between [2,2,2-crypt-M][^{18}F] (M = K or Cs) and XeF $_2$ in CH $_2$ Cl $_2$ solvent at room temperature was recently reported.

The inability to repeat this work in the present study led to a critical re-evaluation of the exchange between F^- and XeF_2 . By use of NMR spectroscopic studies, large amounts of HF, HF_2^- , fluorinated cryptands, chlorofluorocarbons and hydrofluorochlorocarbons were shown to result from the reaction of fluoride and XeF_2 with the solvent and reaction of XeF_2 with 2,2,2-crypt. This work has conclusively shown that the synthesis of $[^{18}F]XeF_2$ by exchange of XeF_2 with $[2,2,2\text{-crypt-M}][^{18}F]$ in CH_2Cl_2 solvent is not a viable synthetic route to PET radiopharmaceuticals.

Furthermore and contrary to the previous claims, a ^{19}F - ^{19}F EXSY and single selective inversion NMR spectroscopic studies in the present work showed that $[N(CH_3)_4][F^-]$ exchanges with XeF_2 in CH_3CN solvent under rigorously anhydrous conditions, providing the first conclusive evidence for exchange between XeF_2 and fluoride ion on the NMR timescale. The likely exchange intermediate is the trifluoroxenate(II) anion, XeF_3^- . Although XeF_3^- has been observed in the gas phase by means of gas phase mass spectrometry, attempts to isolate salts containing the XeF_3^- anion in the present work have been unsuccessful and is attributed to the low fluoride ion affinity of XeF_2 . The XeF_3^- anion would represent the first example of an AX_3E_3 (E = valence electron lone pair) species under the VSEPR formalism. The energy-minimized geometry of the XeF_3^- anion was calculated at the MP2 and DFT levels of theory and shows a planar and Y-shaped structure. The molecular geometry is rationalized by use of electron localization function calculations and VSEPR models.

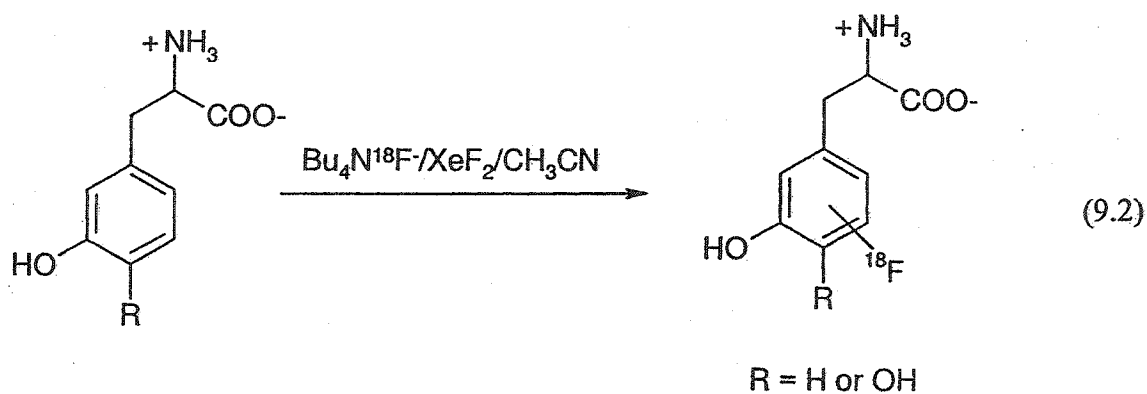
9.2 Directions for Future Work

The syntheses of biologically active nitrofluoroaromatic compounds should be extended. In particular, the direct nitration of DL-*m*-tyrosine should be investigated and the products of electrophilic aromatic nitration should be determined (eq. 9.1). Fluorine-18 labelled nitro-L-*m*-tyrosine derivatives may prove to have useful applications as radiotracers. Furthermore, high specific activity ^{18}F -labelled aromatic amino acids should prove to be easily nitrated, as established by the present studies, and a high specific activity analog of ^{18}F -5-fluoro-3-nitro-L-tyrosine could be evaluated.



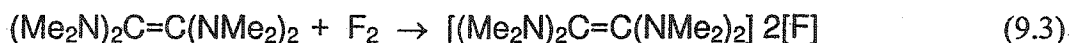
The present work has established that fluoride ion exchange with XeF_2 occurs in CH_3CN solvent. The synthesis of $[\text{}^{18}\text{F}]\text{XeF}_2$ by exchange of $^{18}\text{F}^-$ with XeF_2 would offer an alternative to using specialized $[\text{}^{18}\text{F}]\text{F}_2$ targetry presently required for generating electrophilic fluorine sources. Because nearly all medical cyclotrons routinely produce high specific activity $^{18}\text{F}^-$, $[\text{}^{18}\text{F}]\text{XeF}_2$ generated from $^{18}\text{F}^-$ could prove useful for the

syntheses of PET radiopharmaceuticals. Fluorine-18 labelled fluoride could be retained on an anion exchange column and eluted, in the absence of 2,2,2-crypt, with a solution of Bu_4NOH in CH_3CN to produce $\text{Bu}_4\text{N}^{18}\text{F}$. The $\text{Bu}_4\text{N}^{18}\text{F}$ should exchange with XeF_2 in CH_3CN to produce $[\text{}^{18}\text{F}]\text{XeF}_2$. A direct fluorination reaction of $[\text{}^{18}\text{F}]\text{XeF}_2$ with aromatic amino acids, particularly L-*m*-tyrosine and L-DOPA derivatives, should be attempted because of their utility as PET radiopharmaceuticals when labelled with ^{18}F (eq. 9.2). The reaction mixtures could be separated by HPLC and confirmed by NMR spectroscopy to verify if a product of electrophilic aromatic substitution has been synthesized.

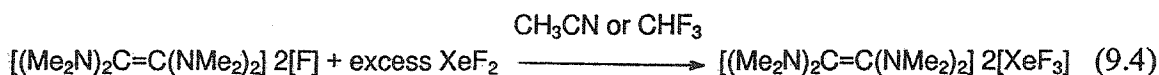


The quest for the elusive XeF_3^- and KrF_3^- anions should not be overlooked. With continued development of oxidatively resistant naked fluoride sources, direct reactions of XeF_2 with naked fluoride sources and NMR exchange experiments may lead to further experimental evidence and ultimately the syntheses of stable salts containing the XeF_3^- anion. For example, Chambers *et al.*²¹⁹ have recently reported a simple route to a salt

containing anhydrous fluoride ion by reaction of tetrakis(dimethylamino)ethene (TDAE) with elemental fluorine to produce a hexamethylguanidium fluoride analogue as shown in equation 9.3. This naked fluoride source could be used for reactions with XeF_2 in attempts to synthesize XeF_3^- and may offer advantages over $[\text{N}(\text{CH}_3)_4][\text{F}]$ because it contains a larger cation that may be able to stabilize the XeF_3^- anion.

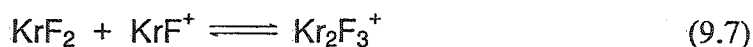
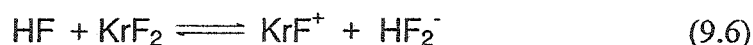


Reactions analogous to those attempted for the syntheses of salts containing the XeF_3^- anion (see Chapter 8, section 8.2.2), which made use of CH_3CN and CHF_3 as the solvent media (eq. 9.4), should be attempted using this hexamethylguanidium fluoride analogue.

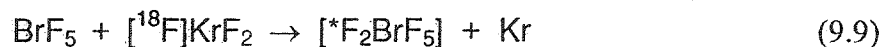
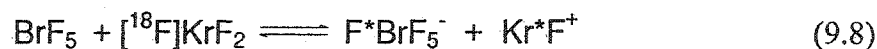


The quest for the KrF_3^- anion is particularly frustrating because KrF_2 has an even lower fluoride ion affinity ($-16.4 \text{ kcal mol}^{-1}$) than XeF_2 ($-21.8 \text{ kcal mol}^{-1}$) (see Table 8.2). The chemistry of KrF_2 has recently been reviewed.¹⁹⁷ Because KrF_2 is a much more potent oxidative fluorinating agent than any of the xenon fluorides and a better source of fluorine atoms than elemental fluorine, a synthetic route to the elusive KrF_3^- anion that makes use of an organic counteranion could not be attempted. Although fluorine exchange was not observed in a sample of KrF_2 and HF on the NMR timescale (see

Chapter 8, section 8.2.2), the exchange could be studied on the radiochemical timescale by attempting a synthesis of $[^{18}\text{F}]\text{KrF}_2$ by exchange of KrF_2 with $[^{18}\text{F}]\text{HF}$. The $[^{18}\text{F}]\text{HF}$ could be synthesized as previously described by reaction of $[^{18}\text{F}]\text{F}_2$ with H_2 in HF (eq. 9.5),³⁵ and further reacted with KrF_2 , which could promote exchange according to the equilibria shown in equations 9.6 and 9.7.



Fluorine-18 labelled KrF_2 could find applications in mechanistic and synthetic inorganic fluorine chemistry for studies ranging from main-group chemistry to lanthanide and actinide chemistry.¹⁹⁷ One such application of $[^{18}\text{F}]\text{KrF}_2$ could be to investigate the possible intermediacy of BrF_7 in the reaction of $[^{18}\text{F}]\text{KrF}_2$ with BrF_5 (eq. 9.8). If this reaction (eq. 9.9) proceeds by decomposition of BrF_7 to BrF_5 and F_2 , trapped F_2 after decomposition should contain $2/7$ of the total radioactivity.



REFERENCES

1. Silvester, M. *Spec. Chem.* 1990, 11, 392.
2. Park, B. K.; Kitteringham, N. B. *Drug Metab. Rev.* 1994, 26, 605.
3. Clark, J. H.; Wails, D.; Bastock, T. W. *Aromatic Fluorination*, CRC Press: Boca Raton; 1996, pp. 1-17.
4. Satyamurthy, N.; Namavari, M.; Barrio, J. R. *Chemtech*, 1994, 25.
5. Smart, B. E. *J. Fluorine Chem.* 2001, 109, 3.
6. Kirk, K. L. *J. Fluorine Chem.* 1995, 72, 261
7. Kirk, K. L.; Creveling, C. R. *Med. Res. Rev.* 1984, 4, 189.
8. Kirk, K. L.; Olubajo, O.; Buchhold, K.; Lewandowski, G. A.; Gusovsky, F.; McCulloh, D.; Daly, J. W.; Creveling, C. R. *J. Med. Chem.* 1986, 29, 1982.
9. Phelps, M. E. *J. Nucl. Med.*, 2000, 41, 661.
10. Iversen, L. L. *Lancet* 1982, 2, 914.
11. Garnett, E. S.; Firnau, G.; Nahmias, C. *Nature* 1983, 305, 137.
12. Garnett, E. S.; Lang, A. E.; Chirakal, R.; Firnau, G.; Nahmias, C. *Can. J. Neurol. Sci.* 1987, 14, 444.
13. "CRC Handbook of Chemistry and Physics", Lide, D. R., Ed.; 74th Ed. (Special Student Edition), CRC Press: Boca Raton, Florida, 1993. 11-37.

14. Harris, R. K. *Nuclear Magnetic Resonance Spectroscopy*. 1986, Longman Scientific & Technical, London, p. 236.
15. Winfield, J. M. *J. Fluorine Chem.* 1980, 16, 1.
16. Tewson, T. J. *Applications of Nuclear and Radiochemistry*. 1982, Pergamon Press, New York, p. 163.
17. VanBrocklin, H. F.; Pagdett, H. C.; Alvord, C. W.; Schmidt, D. G.; Bida, G. T. In *Chemists' Views of Imaging Centers*, Emran, A. M., Ed.; Plenum Press: New York, 1995; pp. 329-338.
18. Guillaume, M.; Luxen, A.; Nebeling, B.; Argentini, M.; Clark, J. C.; Pike, V. W. *Appl. Radiat. Isot.* 1991, 42, 749.
19. Worthington, J. A., Jr. In *Fluorine Chemistry*, Simons, J.H., Ed.; Academic Press: New York, 1964; Vol. 5, pp. 237-294.
20. Thomas, C. C., Jr.; Sondel, J. A.; Kerns, R. C. *Int. J. Appl. Radiat. Isot.* 1965, 16, 71.
21. Nozaki, T.; Tanaka, Y.; Shimamura, A.; Karasawa, T. *Int. J. Appl. Radiat. Isot.* 1968, 19, 27.
22. Clark, J. C.; Silvester, D. J. *Int. J. Appl. Radiat. Isot.* 1966, 17, 151.
23. Fitschem, J.; Beckmann, R.; Holm, U.; Neuert, H. *Int. J. Appl. Radiat. Isot.* 1977, 28, 781.
24. Bishop, A.; Satyamurthy, N.; Bida, G.; Phelps, M.; Barrio, J. R. *Nucl. Med. Biol.* 1996, 23, 385.

25. Ruth, T. J.; Wolf, A. P. *Radiochimica Acta*. 1979, 26, 21.
26. Nickles, R. J.; Daube, M. E.; Ruth, T. J. *Int. J. Appl. Radiat. Isot.* 1984, 35, 117.
27. Kilbourn, M. R.; Jerabek, P. A.; Welch, M. J. *Int. J. Appl. Radiat. Isot.* 1985, 36, 327.
28. Hughey, B. J.; Shefer, R. E.; Klinkowstein, R. E., Welch, M. J.; Dence, C. S.; Livni, E. *J. Nucl. Med.* 1992, 33, 932.
29. Firouzbahkt, M. L.; Schlyer, D. J., Gatley, S. J.; Wolf, A. P. *J. Nucl. Med.* 1993, 34, 69P.
30. Leonhardt, W. *Kernenergie* 1963, 6, 45.
31. Casella, V.; Ido, T.; Wolf, A. P.; Fowler, J. S.; MacGregor, R. R.; Ruth, T. J. *J. Nucl. Med.* 1980, 21, 750.
32. Blessing, G.; Coenen, H. H.; Franken, K.; Qaim, S. M. *Int. J. Appl. Radiat. Isot.* 1986, 37, 1135.
33. Ruth, T. J. *Int. J. Appl. Radiat. Isot.* 1985, 36, 107.
34. Crouzel, C.; Comar, D. *Int. J. Appl. Radiat. Isot.* 1978, 29, 407.
35. Chirakal, R.; Adams, R. M.; Firmau, G.; Schrobilgen, G. J.; Coates, G.; Garnett, E. S. *Nucl. Med. Biol.* 1995, 22, 111.
36. Straatman, M. G.; Schlyer, D. J.; Chasko, J. J. *J. Label. Compd. Radiopharm.* 1982, 19, 1373.
37. Bergman, J.; Solin, O. *Nucl. Med. Biol.* 1997, 24, 677.
38. Ruth, T. J.; Buckley, K. R.; Chun, K. S.; Hurtado, E. T.; Jivan, S.; Zeisler, S.

- Appl. Radiat. Isot.* **2001**, *55*, 457.
39. Satyamurthy, N. *J. Nucl. Med.* **2001**, *42*, 18P
 40. Kearfott, K. J.; Votaw, J. R. In *Chemists' Views of Imaging Centers*, Emran, A.M., Ed.; Plenum Press: New York, 1995; pp. 3-26.
 41. C. Lemaire, In: *Chemists' Views of Imaging Centers*, Emran, A. M., Ed.; Plenum Press: New York, 1995; pp. 367-382.
 42. Ruth, T. J.; Jivan, S.; Adam, M. J. In: *Chemists' Views of Imaging Centers*, Emran, A. M., Ed.; Plenum Press: New York, 1995; pp. 169-175.
 43. Hutchinson, J.; Sandford, G. *Top. Curr. Chem.* **1997**, *193*, 1.
 44. Schmitt, R.; von Gehren, H. *J. Prakt. Chem.* **1870**, *1*, 394.
 45. Balz, G.; Schiemann, G. *Ber. Dtsch. Chem. Ges. B.* **1927**, *60*, 1186.
 46. Haroutounian, S. A.; DiZio, J. P.; Katzenellenbogen, J. A. *J. Org. Chem.* **1991**, *56*, 4993.
 47. Adams, D. J.; Clark, J. H. *Chem. Soc. Rev.* **1999**, *28*, 225.
 48. Coenen, H. H.; Moerlain, S. M. *J. Fluorine Chem.* **1987**, *36*, 63.
 49. Luxen, A.; Barrio, J. R. *Tetrahedron Lett.* **1988**, *29*, 1501.
 50. Fukuhara, N.; Bigelow, L. A. *J. Am. Chem. Soc.* **1941**, *63*, 788.
 51. Fukuhara, N.; Bigelow, L. A. *J. Am. Chem. Soc.* **1941**, *63*, 2792.
 52. Casella, V.; Ido, T.; Wolf, A. P.; Fowler, J. S.; MacGregor, R. R.; Ruth, T. J. *J. Nucl. Med.*, **1980**, *21*, 750.
 53. Rozen, S. *Acc. Chem. Res.* **1988**, *21*, 307.

54. Chambers, R. D.; Skinner, C. J.; Hutchinson, J.; Thomson, J. J. *Chem. Soc. Perkin Trans.* 1996, 1, 605.
55. Chambers, R. D.; Hutchinson, J.; Sandford, G. *J. Fluorine Chem.* 1999, 100, 63.
56. Chirakal, R.; Brown, K. L.; Firnaeu, G.; Garnett, E. S.; Hughes, D. W.; Sayer, B. G.; Smith, R. W. *J. Fluorine Chem.* 1987, 37, 267.
57. Chirakal, R.; Schrobilgen, G. J.; Firnaeu, G.; Garnett, E. S. *Appl. Radiat. Isot.* 1991, 42, 113.
58. Chirakal, R.; Firnaeu, G.; Garnett, E. S. *J. Nucl. Med.* 1986, 26, 417.
59. Barton, D. H. R.; Godinho, L. S.; Hesse, R. H.; Pechet, M. M. *J. Chem. Soc. Chem. Commun.* 1968, 804.
60. Rozen, S. *Chem. Rev.* 1996, 96, 1717.
61. Brel, V. K.; Pirkuliev, N. Sh.; Zefirov, N. S. *Russ. Chem. Rev.* 2001, 70, 231.
62. Schrobilgen, G.; Firnaeu, G.; Chirakal, R.; Garnett, E. S. *J. Chem. Soc., Chem. Comm.* 1981, 198.
63. Chirakal, R.; Firnaeu, G.; Schrobilgen G. J.; McKay, J.; Garnett, S. *Int. J. Appl. Radiat. Isot.* 1984, 35, 401.
64. Sood, S.; Firnaeu, G.; Garnett, E. S. *Int. J. Appl. Radiat. Isot.* 1983, 34, 743.
65. Firnaeu, G.; Chirakal, R.; Sood, S.; Garnett, E. S. *J. Labelled Compd. Radiopharm.* 1981, 18, 7.
66. Constantinou, M.; Aigbirhio, F. I.; Smith, R. G.; Ramsden, C. A.; Pike, V. W. *J. Am. Chem. Soc.* 2001, 123, 1780.

67. Vasdev, N.; Pointner, B.E.; Chirakal, R.; Schrobilgen, G.J. *J. Am. Chem. Soc.* **2002**, *124*, 12863.
68. Sankar Lal, G.; Pez, G. P.; Syvret, R. G. *Chem. Rev.* **1996**, *96*, 1737.
69. Taylor, S. D.; Kotoris, C. C.; Hum, G. *Tetrahedron.* **1999**, *55*, 12431.
70. Banks, R. E.; Mohialdin-Dhaffaf, S. N.; Lal, G. S.; Sharif, I.; Syvret, R. G. *J. Chem. Soc. Chem. Commun.*, **1992**, 595.
71. Ehrenkaufner, R. H.; MacGregor, R. R. *Int. J. Appl. Radiat. Isot.* **1983**, *34*, 613.
72. Straatmann, M. G.; Welch, M. J. *J. Nucl. Med.* **1977**, *18*, 151.
73. Dogden, H. W.; Libby, W. F. *J. Chem. Phys.* **1949**, *17*, 951.
74. Azeem, M.; Gillespie, R. J. *J. Inorg. Nucl. Chem.* **1966**, *28*, 1791.
75. Christe, K. O.; Dixon, D. A.; Schrobilgen, G. J.; Wilson, W. W. *J. Am. Chem. Soc.* **1997**, *119*, 3918.
76. Appelman, E. H.; Jache, A. W. *J. Am. Chem. Soc.* **1987**, *109*, 1754.
77. Azeem, M.; Brownstein, M.; Gillespie, R. J. *Can. J. Chem.* **1969**, *47*, 4159.
78. Christe, K. O.; Wilson, W. W.; Schrobilgen, G. J.; Chirakal, R. V.; Olah, G. A. *Inorg. Chem.* **1988**, *27*, 789.
79. Christe, K. O.; Wilson, W. W.; Chirakal, R. V.; Sanders, J. C. P.; Schrobilgen, G. J. *Inorg. Chem.* **1990**, *29*, 3506.
80. Olah, G. A.; Klopman, G.; Schlosberg, R. H. *J. Am. Chem. Soc.* **1969**, *91*, 3261.
81. Olah, G. A.; Westerman, P. W.; Mo, Y. K.; Klopman, G. *J. Am. Chem. Soc.* **1972**,

- 94, 7859.
82. Chirakal, R. V. Ph.D. Thesis, McMaster University, 1991.
 83. Langen, K.-J.; Pauleit, D.; Coenen, H. H. *Nucl. Med. Biol.* **2002**, *29*, 625.
 84. Casteel, W. J., Jr.; Kolb, P.; LeBlond, N.; Mercier, H. P. A.; Schrobilgen, G. J. *Inorg. Chem.* **1996**, *35*, 929.
 85. Reinhardt, C. F.; Hume, W. G.; Linch, A. L.; Wetherhold, J. M. *J. Chem. Ed.*, **1969**, *46*, A171.
 86. Peters, D.; Miethchen, R. *J. Fluorine Chem.* **1996**, *79*, 161.
 87. Segal, E. B. *Chem. Health Saf.* **2000**, *7*, 18.
 88. Emara, A. A. A.; Schrobilgen G. J. *Inorg. Chem.* **1992**, *31*, 1323.
 89. Mercier, H. P. A.; Sanders, J. C. P.; Schrobilgen, G. J.; Tsai, S. S. *Inorg. Chem.* **1993**, *32*, 386.
 90. Lehmann, J. F.; Dixon, D. A.; Schrobilgen, G. J. *Inorg. Chem.* **2001**, *40*, 3002.
 91. Kinkead, S. A.; FitzPatrick, J. R.; Foropoulos, J., Jr.; Kissane, R. J.; Purson, J. D. In *Fluorine Chemistry Towards the 21st Century*; Thrasher, J. S.; Strauss, S. H., Eds.; ACS Symposium Series 555; American Chemical Society: Washington, D.C., 1994, Chapter 3, pp 40–55.
 92. Bezmel'nitsyn, V. N.; Legasov, V. A.; Chaivanov, B. B. *Proc. Acad. Sci. USSR, Chem. Sect.* **1977**, *235*, 365.; *Dokl. Akad. Nauk.* **1977**, *235*, 96.
 93. Christe, K. O.; Wilson, W. W.; Wilson R. D.; Bau, R.; Feng, J. *J. Am. Chem. Soc.* **1990**, *112*, 7619.

94. Christe, K. O.; Curtis, E. C.; Dixon, D. A.; Mercier, H. P.; Sanders, J. C. P.; Schrobilgen, G. J. *J. Am. Chem. Soc.* **1991**, *113*, 3351.
95. Campbell, J.; Mercier, H. P. A.; Santry, D. P.; Suontamo, R.; Borrmann, H.; Schrobilgen, G. J. *Inorg. Chem.* **2001**, *40*, 233.
96. Winfield, J. M. *J. Fluorine Chem.* **1984**, *25*, 91.
97. Berg, R. W. *Spectrochim. Acta* **1978**, *34A*, 1677.
98. Jewett, D. M.; Potocki, J. F.; Ehrenkaufner, R. E. *J. Fluorine Chem.* **1984**, *24*, 477.
99. Firnau, G.; Chirakal, R.; Garnett, E. S. *J. Nucl. Med.* **1984**, *25*, 1228.
100. Chirakal, R.; Firnau, G.; Couse, J.; Garnett, E. S. *Int. J. Appl. Radiat. Isot.* **1984**, *35*, 651.
101. Vasdev, N.; Chirakal, R.; Schrobilgen, G. J.; Nahmias, C. *J. Fluorine Chem.* **2001**, *111*, 17.
102. Kalinowski, H.; Berger, S.; Braun, S. *Carbon-13 NMR Spectroscopy*, John Wiley and Sons: New York, NY, 1988; p. 321.
103. Gerken, M.; Dixon, D. A.; Schrobilgen, G. J. *Inorg. Chem.* **2000**, *39*, 4244.
104. Vasdev, N.; Schrobilgen, G. J.; Chirakal, R.; Suontamo, R. J.; Bain, A. D., to be submitted.
105. Hoffman, J. M.; Melega, W. P.; Hawk, T. C.; Grafton, S. C.; Luxen, A.; Mahoney, D. K.; Barrio, J. R.; Huang, S. C.; Mazziotta, J. C.; Phelps, M. E. *J. Nucl. Med.* **1992**, *33*, 1472.
106. Bailey, D. L.; Young, H.; Bloomfield, P. M.; Meikle, S. R.; Glass, D.; Myers, M.

- J.; Spinks, T. J.; Watson, C. C.; Luk, P.; Peters, A. M.; Jones, T. *Eur. J. Nucl. Med.* 1997, 24, 6.
107. Tailerach, J.; Tournoux, P. *Co-Planar Stereotaxic Atlas of the Human Brain*, Thieme: New York, 1988.
108. Patlak, C. S.; Blasberg, R. B. *J. Cereb. Blood Flow Metab.* 1985, 5, 584.
109. Tedroff, J.; Acquilinius, S. M.; Laihinen, A.; Rinne, U.; Hartvig, P.; Anderson, J.; Lundqvist, H.; Haaparanta, M.; Solin, O.; Antoni, G.; Gee, A. D.; Ulin, J.; Långström, B. *Acta. Neurol. Scand.* 1990, 81, 24.
110. Garnett, E. S.; Firnau, G.; Nahmias, C.; Sood, S.; Belbeck, L. *Am. J. Physiol.* 1980, 238, R318.
111. Solin, O.; Firnau, G.; Haaparanta, M.; Chirakal, R.; Sipila, H.; Garnett, E. S. *J. Label. Comp. Radiopharm.* 1986, 23, 1106.
112. Coenen, H. H.; Franken, K.; Kling, P.; Stöcklin, G. *Appl. Radiat. Isot.* 1988, 39, 1243.
113. Firnau, G.; Nahmias, C.; Garnett, E. S. *Int. J. Appl. Radiat. Isot.* 1973, 24, 182.
114. Argentini, M.; Wiese, C.; Weinreich, R. *J. Fluorine Chem.* 1994, 68, 141.
115. Birchall, T.; Bourns, A. N.; Gillespie, R. J.; Smith, P. J. *Can. J. Chem.* 1964, 42, 1433.
116. Olah, G. A.; Mo, Y. K. *J. Org. Chem.* 1973, 38, 353.
117. Brouwer, D. M.; Mackor, E. L.; MacLean, C. *Rec. Trav. Chim.* 1966, 85, 109.
118. Cacace, F.; Wolf, A. P. *J. Am. Chem. Soc.* 1978, 100, 3639.

119. Ding, Y. S.; Shiue, C. Y.; Fowler, J. S.; Wolf, A. P.; Plenevaux, A. *J. Fluorine Chem.* **1990**, *48*, 189.
120. Rengan, R.; Chakraborty, P. K.; Kilbourn, M. R. *J. Labelled. Compd. Radiopharm.* **1993**, *33*, 563.
121. Taylor, E. C.; Kienzle, F.; Robey, R. L.; McKillop, A.; Hunt, J. D. *J. Am. Chem. Soc.* **1971**, *9*, 4845.
122. Rozen, S.; Lerman, O.; Kol, M. *J. Chem. Soc., Chem. Commun.* **1981**, 443.
123. Adam, M. J.; Ruth, T. J.; Grierson, J. R.; Abeysekera, B.; Pate, B.D. *J. Nucl. Med.* **1986**, *27*, 1462.
124. Luxen, A.; Barrio, J. R.; Bida, G. T.; Satyamurthy, N. *J. Labelled. Compd. Radiopharm.* **1986**, *23*, 1066.
125. Hornykiewicz, O. *Pharmacol. Rev.* **1966**, *18*, 925.
126. Birkmayer, W.; Hornykiewicz, O. *Wien. Klin. Wschr.* **1961**, *73*, 787.
127. Luxen, A.; Guillaume, M.; Melega, W. P.; Pike, V. W.; Solin, O.; Wagner, R. *Nucl. Med. Biol.* **1992**, *19*, 149.
128. Cumming, P.; Gjedde, A. *Synapse* **1998**, *29*, 37.
129. Solin, O.; Firnaeu, G.; Haaparanta, M.; Chirakal, R.; Sipila, H.; Garnett, E. S.; Nahmias, C. in: Proceedings of the Sixth International Symposium on Radiopharmaceutical Chemistry, Boston, MA, June 29 1986, Paper 36.
130. Cantacuzene, D.; Kirk, K. L.; McCulloh, D. H.; Creveling, C. R. *Science* **1979**, *204*, 1217.

131. Cumming, P.; Hausser, M.; Martin, W. R. W.; Grierson, J.; Adam, M. J.; Ruth, T. J.; McGeer, E.G. *Biochem. Pharm.* **1988**, *37*, 247.
132. Firnau, G.; Garnett, E. S.; Sourkes, T. L.; Missala, K. *Experientia* **1975**, *31*, 1254.
133. Creveling, C. R.; Kirk, K. L. *Biochem. Biophys. Res. Commun.* **1985**, *130*, 1123.
134. Wiese, C.; Cogoli-Greuter, M.; Weinreich, R.; Winterhalter, K. H. *J. Neurochem.* **1992**, *58*, 219.
135. Firnau, G.; Garnett, E. S.; Chan, P. K. H.; Belbeck, L. W. *J. Pharm. Pharmac.* **1976**, *28*, 584.
136. Garnett, E. S.; Firnau, G.; Chan, P. K. H.; Sood, S.; Belbeck, L. W. *Proc. Natl. Acad. Sci. USA.* **1978**, *75*, 464.
137. Oldendorf, W. H. *Am. J. Physiol.* **1973**, *224*, 967.
138. Garnett, E. S.; Nahmias, C.; Chirakal, R.; Firnau, G. Unpublished results.
139. Firnau, G.; Sood, S.; Pantel, R.; Garnett, S. *Mol. Pharmacol.* **1981** *19*, 130.
140. Wiese, C.; Cogoli-Greuter, M.; Argentini, M.; Mader, T.; Weinreich, R.; Winterhalter, K. H. *Biochem. Pharmacol.* **1992**, *44*, 99.
141. Wiese, C.; Cogoli-Greuter, M.; Weinreich, R.; Winterhalter, K. H. *Naunyn-Schmiedeberg's Arch. Pharmacol.* **1993**, *349*, 582.
142. Yee, R. E.; Huang, S-C.; Stout, D. B.; Irwin, I.; Shoghi-Jadid, K.; Togaski, D. M.; DeLanney, L. E.; Langston, J. W.; Satyamurthy, N.; Farahani, K. F.; Phelps, M. E.; Barrio, J.R. *J. Neurochem.* **2000**, *74*, 1147.
143. Barrio, J. R.; Huang, S. C.; Phelps, M. E. *Biochem. Pharmacol.* **1997**, *54*, 341.

144. Chiueh, C. C.; Zukowska-Grojec, Z.; Kirk, K. L.; Kopin, I. J. *J Pharmacol. Exp. Ther.* 1983, 225, 529.
145. Creveling, C. R.; McNeal, E. T.; Cantacuzene, D.; Kirk, K. L. *J. Med. Chem.* 1981, 24, 1395.
146. Firnau, G.; Garnett, E. S.; Chirakal, R.; Sood, S.; Nahmias, C.; Schrobilgen, G. *Appl. Radiat. Isot.* 1984, 37, 669.
147. DeJesus, O. T.; Mukherjee, J. *Biochem. Biophys. Res. Commun.* 1988, 150, 1027.
148. Nahmias, C.; Wahl, L.; Chirakal, R.; Firnau, G.; Garnett, E. S. *Mov. Disorders.* 1995, 10, 298.
149. Guldberg, H. C.; Marsden, C. A. *Pharmacol. Rev.* 1975, 27, 135.
150. Blaschko, H.; Chrusciel, T. L. *J. Physiol.* 1960, 151, 272.
151. DeJesus, O. T.; Endres, C. J.; Shelton, S. E.; Nickles, R. J.; Holden, J. E. *J. Nucl. Med.* 1997, 38, 630.
152. Barrio, J. R.; Huang, S.; Yu, D.; Melega, W. P.; Quintana, J.; Cherry, S. R.; Jacobson, A.; Namavari, M.; Satyamurthy, N.; Phelps, M. E. *J. Cereb. Blood Flow. Metab.* 1996, 16, 667.
153. Inoue, T.; Tomiyoshi, K.; Higuichi, T.; Ahmed, K.; Sarwar, M.; Aoyagi, K.; Amano, S. *J. Nucl. Med.* 1998, 39, 663.
154. Amano, S.; Inoue, T.; Tomiyoshi, K.; Ando, T.; Endo, K. *J. Nucl. Med.* 1998, 39, 1424.
155. Inoue, T.; Shibasaki, T.; Oriuchi, N.; Aoyagi, K.; Tomiyoshi, K.; Amano, S.;

- Mikuni, M.; Ida, I.; Aoki, J.; Endo, K. *J. Nucl. Med.* **1999**, *40*, 399.
156. Tomiyoshi, K.; Amed, K.; Muhammad, S.; Higuchi, T.; Inoue, T.; Endo, K.; Yang, D. *Nucl. Med. Commun.* **1997**, *18*, 169.
157. Stöcklin, G. L. *Eur. J. Nucl. Med.* **1998**, *25*, 1612.
158. Varagnolo, L.; Stokkel, M. P. M.; Mazzi, U.; Pauwels, E. K. *J. Nucl. Med. Biol.* **2000**, *27*, 103.
159. Kirk, K. L. *J. Org. Chem.* **1980**, *45*, 2015.
160. Günther, H. *NMR Spectroscopy: An Introduction*, John Wiley and Sons: Chichester, 1980; pp. 175-177.
161. Santry, D. P.; Mercier, H. P. A.; Schrobilgen, G. J. ISOTOPOMER: A Multi-NMR Simulation Program, Version 3.02NTF; Snowbird Software Inc.: Hamilton, ON, 2000.
162. Chirakal, R.; Vasdev, N., Schrobilgen, G. J.; Nahmias, C. *J. Fluorine Chem.* **1999**, *99*, 87.
163. Misaki, S. *J. Fluorine Chem.* **1981**, *17*, 159.
164. Kirk, K. L. *J. Org. Chem.* **1976**, *41*, 2373.
165. Hatano, K.; Ishiwata, K.; Yanagisawa, T. *Nucl. Med. Biol.* **1996**, *23*, 101.
166. Chambers, R. D.; Hutchinson, J.; Sparrowhawk, M. E.; Sandford, G.; Moilliet, J. S.; Thomson, J. *J. Fluorine Chem.* **2000**, *102*, 169.
167. Olah, G. A. Malhotra, R.; Narang, S. C. *Nitration: Methods and Mechanisms*, VCH Publishers, Inc.: New York, NY, 1989.

168. Hoggett, J. G.; Moodie, R. B.; Penton, J. R.; Schofield, K. *Nitration and Aromatic Reactivity*, University Press: Cambridge, UK., 1971.
169. Halliwell, B. *FEBS Lett.* **1997**, *411*, 157.
170. Hurst, J. K. *J. Clin. Invest.* **2002**, *109*, 1287.
171. Ischiropoulos, H. *Arch. Biochem. Biophys.* **1998**, *356*, 1.
172. Herce-Pagliai, C.; Kotescha, S.; Shuker, D. E. G. *Nitric Oxide* **1998**, *2*, 324.
173. Skawinski, W.; Flisak, J.; Chung, A. C.; Jordan, F.; Mendelsohn, R. *J. Labelled Compd. Radiopharm.* **1990**, *28*, 1179.
174. Skawinski, W. J.; Adebodun, F.; Cheng, J. T.; Jordan, F.; Mendelsohn, R. *Biochim. Biophys. Acta.*, **1993**, *1162*, 297.
175. Olah, G. A. Malhotra, R.; Narang, S. C. *Nitration: Methods and Mechanisms*, VCH Publishers, Inc.: New York, NY, 1989, pp. 9-83.
176. Chambers, R. D.; Skinner, C. J. *Brit. UK Pat. Appl.* **1996**, 8pp.
177. Olah, G. A. Malhotra, R.; Narang, S. C. *Nitration: Methods and Mechanisms*, VCH Publishers, Inc.: New York, NY, 1989, pp. 9-83.
178. Appelman, E. H. *Inorg. Chem.* **1967**, *6*, 1268.
179. Patrick, T. B.; Johri, K. K.; White, D. H.; Bertrand, W. S.; Mokhtar, R.; Kilbourn, M. R.; Welch, M. J. *Can. J. Chem.* **1986**, *64*, 138.
180. Christe, K. O.; Wilson, W. W. *J. Fluorine Chem.* **1990**, *47*, 117.
181. Dukat, W. W.; Holloway, J. H.; Hope, E. G.; Townson, P. J.; Powell, R. L. *J. Fluorine Chem.* **1993**, *62*, 293.

182. Gerken, M.; Schrobilgen, G. J. *Coord. Chem. Rev.* **2000**, *197*, 335.
183. The ^1H and ^{19}F chemical shifts of anhydrous HF in dry CH_2Cl_2 are 7.00 and -191.3 ppm, respectively, at 15 °C; this work.
184. Christe, K. O.; Wilson, W. W. *J. Fluorine Chem.* **1990**, *46*, 339
185. Clark, W. D.; Lin, T. Y.; Maleknia, S. D.; Lagow, R. J. *J. Org. Chem.* **1990**, *55*, 5933.
186. Chirakal, R.; McCarry, B.; Lonergan, M.; Firnau, G.; Garnett, S. *Appl. Radiat. Isot.* **1995**, *46*, 149.
187. Hudlický, M. *Organic Fluorine Chemistry*; Plenum Press: New York, NY, 1971; p 48.
188. Lazeretti, P.; Taddei, F. *Org. Magn. Reson.* **1971**, *3*, 113.
189. Fukui, K.; Kitano, N. *Japanese Pat.* **1957**, 7761.; *Chem Abs.* **1958**, *52*, 13773.
190. Verbeek, W.; Sundermeyer, W. *Angew. Chem., Int. Ed. Engl.* **1966**, *5*, 314; *Angew. Chem.* **1966**, *78*, 307.
191. Hindman, J. C.; Svirnickas, A. In *Noble Gas Compounds*; Hyman, H. H. Ed.; University of Chicago Press: Chicago, Ill, 1963; pp 251-262.
192. Brown, T. H.; Whipple, E. B.; Verdier, P. H. In *Noble Gas Compounds*; Hyman, H.H., Ed.; University of Chicago Press: Chicago, 1963; pp 263-274.
193. Bain, A. D. MEXICO: The McMaster Program for Exchange Lineshape Calculations: Hamilton, ON, 2001.
194. Ramsden, C. A.; Smith, R. G. *J. Am. Chem. Soc.* **1998**, *120*, 6842.

195. Schrobilgen, G. J. In *Synthetic Fluorine Chemistry*; Chambers, R. D., Olah, G. A., Prakash, G. K. S., Eds.; Wiley and Sons: New York, 1992; Chapter 1, pp. 1-30.
196. Selig, H.; Holloway, J. H. *Top. Curr. Chem.* **1984**, *124*, 33.
197. Lehmann, J. F.; Mercier, H. P. A.; Schrobilgen, G. J. *Coord. Chem. Rev.* **2002**, *233-234*, 1.
198. Shellhamer, D. F.; Chua Chiao, M.; Gallego, K. M.; Low, W. S. C.; Carter, B.; Heasley, V. L.; Chapman, R. D. *J. Fluorine Chem.* **1995**, *72*, 83.
199. Janzen, A. F. *Coord. Chem. Rev.* **1994**, *130*, 355
200. Beck, M. T.; Dózsa, L. *J. Am. Chem. Soc.* **1967**, *89*, 5713.
201. Gerken, M.; Boatz, J. A.; Kornath, A.; Haiges, R.; Schneider, S.; Schroer, T.; Christe, K. O. *J. Fluorine Chem.* **2002**, *116*, 49.
202. Lewis, R. J., Sr. *Hazardous Chemicals Desk Reference*, 4th Ed.; John Wiley and Sons: New York, NY, 1997; p. 267.
203. Peacock, R. D.; Selig, H.; Sheft, I. *Proc. Chem. Soc.* **1964**, 285.
204. Peacock, R. D.; Selig, H.; Sheft, I. *J. Inorg. Nucl. Chem.* **1966**, *28*, 2561.
205. Peterson, S. W.; Holloway, J. H.; Coyle, B. A.; Williams, J. M. *Science.* **1971**, 1238.
206. Ellern, A.; Mahjoub, A.; Seppelt, K. *Angew. Chem. Int. Ed. Engl.* **1996**, *35*, 1123.
207. Christe, K. O.; Wilson, W. W. *Inorg. Chem.* **1982**, *21*, 4113.
208. Ward, R. D. *J. Chem. Educ.* **1963**, *40*, 277.
209. Begun, G. M.; Compton, R. N. *Int. J. Mass Spectrom. Ion Phys.* **1979**, *30*, 379.

210. Studier, M. H.; Sloth, E. N. In *Noble Gas Compounds*; Hyman, H. H. Ed.; University of Chicago Press, Chicago, Ill., 1963, pp. 47-49.
211. Wilson, I. L. *J. Fluorine Chem.* **1975**, *5*, 13.
212. Liebman, J. F. *J. Fluorine Chem.* **1976**, *7*, 531.
213. Gillespie, R. J.; Hargittai, I. *The VSEPR Model of Molecular Geometry*; Allyn and Bacon: Boston, MA, 1991.
214. Andersson, S. *Acta Crystallogr. Sect. B.* **1979**, *35*, 1321.
215. Savin, A.; Nesper, R.; Wengert, S.; Fässler, T. F. *Angew. Chem.* **1997**, *109*, 1892; *Angew. Chem. Int. Ed. Engl.* **1997**, *36*, 1808.
216. Christe, K. O. *J. Fluorine Chem.* **1995**, *71*, 149.
217. Christe, K. O.; Dixon, D. A.; McLemore, D.; Wilson, W. W.; Sheehy, J. A.; Boatz, J. A. *J. Fluorine Chem.* **2000**, *101*, 151.
218. Bain, A. D.; Cramer, J. A. *J. Magn. Reson. A.* **1996**, *118*, 21.
219. Chambers, R. D.; Gray, W. W.; Sandford, G.; Vaughan, J. F. S. *J. Fluorine Chem.* **1999**, *94*, 213.